

Estimation of Latent Group Structures in Time-Varying Panel Data Models

Paul Haimerl^{*1}, Stephan Smeekes^{†2}, and Ines Wilms^{‡2}

¹Department of Economics and Business Economics, CoRE Center for Research in Energy:

Economics and Markets, Aarhus University, Universitetsbyen 51, 8000 Aarhus N, Denmark

²Department of Quantitative Economics, Maastricht University, Tongersestraat 53, 6211 ML
Maastricht, The Netherlands

November, 2025

Abstract. We consider panel data models where coefficients change smoothly over time and follow a latent group structure, being homogeneous within but heterogeneous across groups. To jointly estimate the group membership and group-specific coefficient trajectories, we propose *FUSE-TIME*, a pairwise adaptive group fused-Lasso estimator combined with polynomial spline sieves. We establish consistency, derive the asymptotic distributions of the penalized sieve estimator and its post-selection version, and show oracle efficiency. Monte Carlo experiments demonstrate strong finite-sample performance in terms of estimation accuracy and group identification. An application to the CO₂ intensity of GDP highlights the relevance of addressing both cross-sectional heterogeneity and time-variance in empirical exercises.

Keywords. Panel data model, time-varying coefficients, clustering, basis splines.

JEL classification. C22, C23, C38.

1 Introduction

In this paper, we study panel data models in which slope coefficients evolve smoothly over time and vary across an unobserved group structure, being homogeneous within groups but heterogeneous across groups. We propose a penalized sieve approach that leverages the pairwise adaptive group fused-Lasso (*PAGFL*; [Qian and Su, 2016a,b](#); [Mehrabani, 2023](#)) to simultaneously estimate the time-varying coefficients and the latent grouping. We term our resulting estimator *FUSE-TIME*–Fused

^{*}Correspondence to paul.haimerl@econ.au.dk

[†]s.smeekes@maastrichtuniversity.nl

[‡]i.wilms@maastrichtuniversity.nl

We are grateful to Phillip Heiler, Eric Hillebrand, Morten Ø. Nielsen, and Martin Schumann for valuable feedback. We also thank the participants of the National Econometrics Study Group (NESG 2024), the Econometric Models of Climate Change conference (EMCC VIII), the Aarhus Workshop in Econometrics (AWE V), the Workshop in Time Series Econometrics (WTSE XV_t), the ZeST seminar at Bielefeld University, and the department seminar at Aarhus University for insightful comments. We thank Ali Mehrabani and Xia Wang for providing helpful code. Ines Wilms is supported by a grant from the Dutch Research Council (NWO), research program Vidi under the grant number VI.Vidi.211.032.

Unobserved group Spline Estimation of TIME varying coefficients—and derive its asymptotic properties when the number of groups, the cross-sectional dimension, and the time dimension jointly diverge: establishing estimation consistency, clustering consistency, and deriving the asymptotic distribution.

This paper builds on and extends two strands of the literature. The first strand studies panel data models with latent group structures, where coefficients are homogeneous within groups but vary across groups. Prior studies recover the unobserved groupings either by applying clustering algorithms such as K -means to preliminary estimates or by directly embedding the grouping into the estimation procedure through penalization schemes (Bonhomme and Manresa, 2015; Ke et al., 2015; Su et al., 2016; Mehrabani, 2023; Lumsdaine et al., 2023; Mehrabani and Parsaeian, 2025). The second strand develops time-varying panel models, which describe temporal heterogeneity either through smoothly changing coefficients (Huang et al., 2004; Cai, 2007; Su and Jin, 2012; Robinson, 2012) or through discrete structural breaks (Bai, 2010; Qian and Su, 2016a).

We contribute to these strands by proposing a single convex optimization problem that jointly identifies the latent group structure and estimates the smooth group-specific coefficient trajectories. Our approach does not require any prior specification of the number of groups or group compositions. Instead, the number of groups and their compositions are determined automatically in a data-driven way through a penalized sieve estimation procedure that adds a *PAGFL* penalty (Qian and Su, 2016a; Mehrabani, 2023) to the objective function. The penalty collects all pairwise differences of individual coefficient vectors, shrinking them to zero if two units belong to the same group. Following Huang et al. (2004); Su et al. (2019), we approximate the time-varying coefficients using polynomial basis splines (B-splines), providing a flexible yet parsimonious representation of smooth temporal change. We propose a post-selection variant of our estimator, and introduce a consistent BIC-type information criterion (IC) to select the tuning parameter that regulates the number of groups and their compositions.

We provide primitive conditions for both the penalized sieve estimator and the post-selection variant of *FUSE-TIME* to achieve the oracle property, being asymptotically equivalent to an infeasible oracle estimator based on the true grouping. Our theoretical framework allows the number of groups, the cross-sectional dimension, and the time dimension to diverge jointly when deriving the asymptotic distributions of the estimators. *FUSE-TIME* thus provides a general framework for analyzing panels with both cross-sectional and temporal heterogeneity that is also robust to missing values and strikes a good balance between capturing heterogeneity and maintaining parsimony.

We also study the finite-sample performance of our estimator using both simulated and real

data. Overall, our proposed estimator performs well across a variety of simulation settings in terms of recovering the latent group structure and estimating the time-varying coefficients accurately. *FUSE-TIME* outperforms the method of [Su et al. \(2019\)](#), which employs the Classifier Lasso (*C-Lasso*; [Su et al., 2016](#)), while also being computationally more efficient. Additionally, we illustrate the merits of the *FUSE-TIME* estimator by analyzing trends in the carbon dioxide (CO₂) intensity of Gross Domestic Product (GDP), the amount of CO₂ emitted per unit of GDP produced. In a panel dataset of 92 countries spanning 1960 to 2023, the model identifies five groups, each with a unique trend of CO₂ intensity.

The plan for the remainder of this paper is as follows. Section 2 introduces the model along with our estimation procedure. The asymptotic theory is developed in Section 3. Section 4 investigates the finite-sample performance via a simulation study. Section 5 presents the empirical illustration. The [final section](#) concludes. We provide a software implementation in our companion R-package **PAGFL** ([Haimerl et al., 2025](#)). Replication files of the simulation study and empirical application are available at [GitHub](#).¹

Notation. Throughout, we denote vectors by boldface small letters and matrices by boldface capital letters. For a real matrix \mathbf{A} , the Frobenius norm is written as $\|\mathbf{A}\|_F = \sqrt{\text{tr}(\mathbf{A}\mathbf{A}')}$. $\mu_{\max}(\mathbf{A})$ and $\mu_{\min}(\mathbf{A})$ denote the largest and smallest eigenvalues, respectively. $\|\mathbf{A}\|_{\text{sp}} = \sqrt{\mu_{\max}(\mathbf{A}\mathbf{A}')}}$ gives the spectral norm. $\text{vec}(\mathbf{A})$ describes a column-wise vectorization of \mathbf{A} . $\|\mathbf{a}\|_2$ denotes the Euclidean norm for a real vector \mathbf{a} . The operators \xrightarrow{P} , \xrightarrow{D} , and plim signal convergence in probability, convergence in distribution, and the probability limit. \otimes represents the Kronecker product. The superscript zero, or index when appropriate, marks a true quantity. \mathbf{I}_a and $\mathbf{0}_a$ denote an $a \times a$ identity matrix and an $a \times 1$ vector of zeros. ‘With probability approaching one’ is abbreviated as w.p.a.1. For two sequences of positive (random) numbers a_n and b_n , $a_n \lesssim b_n$ indicates that a_n/b_n is (stochastically) bounded and $a_n \asymp b_n$ signals that both $a_n \lesssim b_n$ and $b_n \lesssim a_n$ hold.

2 Model and Estimation

In this section, we introduce the time-varying panel data model (Section 2.1) and our penalized sieve estimation procedure (Section 2.2).

¹R-Notebooks and a Dockerfile with replication material are published at github.com/Paul-Haimerl/replication-fuse-time.

2.1 The Model

Consider the time-varying panel data model

$$y_{it} = \gamma_i^0 + \beta_{it}^{0\prime} \mathbf{x}_{it} + \epsilon_{it}, \quad i = 1, \dots, N, \quad t = 1, \dots, T, \quad (2.1)$$

where y_{it} is the scalar response, \mathbf{x}_{it} is a $p \times 1$ vector of explanatory variables, the γ_i^0 's denote the unobserved individual fixed effects, and ϵ_{it} represents a zero-mean idiosyncratic error. The superscript 0 is used to denote a true parameter value. The fixed effects γ_i^0 may correlate with some elements of \mathbf{x}_{it} and are independently distributed across individuals. We assume that the p -dimensional vector of slope coefficients β_{it}^0 varies smoothly over time:

$$\beta_{it}^0 = \beta_i^0 \left(\frac{t}{T} \right). \quad (2.2)$$

Furthermore, we assume that the time-varying slope parameters adhere to the following unknown group structure

$$\beta_i^0 \left(\frac{t}{T} \right) = \sum_{k=1}^{K_0} \alpha_k^0 \left(\frac{t}{T} \right) \mathbf{1} \{i \in G_k^0\}, \quad (2.3)$$

where $\alpha_k^0(t/T)$ is a $p \times 1$ vector of group-specific time-varying functional coefficients and $\mathbf{1}\{\cdot\}$ denotes the indicator function. The latent group structure $\mathcal{G}_K^0 = \{G_1^0, \dots, G_{K_0}^0\}$ partitions the cross-sectional units into disjoint sets; $\cup_{k=1}^{K_0} G_k^0 = \{1, \dots, N\}$ and $G_j^0 \cap G_k^0 = \emptyset$ for any $j \neq k$. We denote the cardinality of group G_k^0 as N_k .

Remark 2.1. The group-specific coefficients $\alpha_k^0(\cdot)$ are smooth functions of t/T (see Assumption 1(vi), discussed in Section 3). As a consequence, the data generating process (DGP) in (2.1) captures smooth temporal variation rather than discrete structural breaks in the slope parameters. Furthermore, we assume discrete rather than continuous cross-sectional heterogeneity: unit-specific variation can be represented by a finite number of latent processes, namely the grouping in (2.3). We refer to [Bonhomme et al. \(2022\)](#) for a treatment of discrete groupings when cross-sectional heterogeneity is continuous. Our framework thus nests several previously studied models as special cases, including time-constant panel data models with latent group structures ([Su et al., 2016](#); [Sarafidis and Weber, 2015](#); [Wang et al., 2018](#)) and time-varying panel data models ([Cai, 2007](#); [Robinson, 2012](#); [Vogt and Linton, 2020](#)).

2.2 Penalized Sieve Estimation of Time-Varying Coefficients

Similarly to [Huang et al. \(2004\)](#); [Su et al. \(2019\)](#), we approximate the $p \times 1$ functional coefficient vector $\beta_i^0(t/T)$ using an M -dimensional vector $\mathbf{b}(t/T)$ of polynomial spline basis functions:

$$\beta_i^0\left(\frac{t}{T}\right) = \boldsymbol{\Pi}_i^{0'} \mathbf{b}\left(\frac{t}{T}\right) + \boldsymbol{\eta}_{it}, \quad (2.4)$$

where $\boldsymbol{\Pi}_i^0 = (\boldsymbol{\pi}_{i1}^0, \dots, \boldsymbol{\pi}_{ip}^0)$ denotes a $M \times p$ matrix of B-spline control points, and $\boldsymbol{\eta}_{it} = \beta_i^0(t/T) - \boldsymbol{\Pi}_i^{0'} \mathbf{b}(t/T)$ is a $p \times 1$ sieve approximation error. B-splines offer two decisive advantages over typically employed kernel estimators. First, spline functions are computationally efficient and numerically stable while maintaining good approximation properties. Second, B-splines can be expressed as linear combinations of the basis functions $\mathbf{b}(t/T)$. The possibility of separating time-varying basis functions $\mathbf{b}(t/T)$, which do not have to be estimated, from individual time-constant control points $\boldsymbol{\Pi}_i^0$, which are estimated, makes B-splines particularly convenient to use in conjunction with the *PAGFL* penalty.

Note that $\boldsymbol{\Pi}_i^{0'} \mathbf{b}(t/T)$ is a function in the sieve-space \mathbb{B}_M spanned by the M basis functions in $\mathbf{b}(t/T)$. By increasing the polynomial degree d (polynomial order $d+1$) and the number of interior knots M^* as T diverges, we extend $M = M^* + d + 1$ along with \mathbb{B}_M and obtain arbitrarily close approximations of $\beta_i^0(t/T)$. Appendix A contains full details on the spline basis functions.

Plugging (2.4) into model (2.1) yields

$$\begin{aligned} y_{it} &= \gamma_i^0 + \left[\boldsymbol{\Pi}_i^{0'} \mathbf{b}\left(\frac{t}{T}\right) + \boldsymbol{\eta}_{it} \right]' \mathbf{x}_{it} + \epsilon_{it} \\ y_{it} &= \gamma_i^0 + \boldsymbol{\pi}_i^{0'} \mathbf{z}_{it} + u_{it}, \end{aligned} \quad (2.5)$$

where $\boldsymbol{\pi}_i^0 = \text{vec}(\boldsymbol{\Pi}_i^0)$ is a $Mp \times 1$ coefficient vector, $\mathbf{z}_{it} = \mathbf{x}_{it} \otimes \mathbf{b}(t/T)$ is a $Mp \times 1$ vector of regressors, and u_{it} collects the idiosyncratic error ϵ_{it} and the sieve approximation error $\boldsymbol{\eta}_{it}' \mathbf{x}_{it}$. To obtain an estimate of the time-varying slope parameters $\beta_i^0(t/T)$ in model (2.1), we estimate the time-constant vector $\boldsymbol{\pi}_i^0$ in model (2.5) and take $\hat{\beta}_i(t/T) = \hat{\boldsymbol{\Pi}}_i' \mathbf{b}(t/T)$, where $\hat{\boldsymbol{\pi}}_i = \text{vec}(\hat{\boldsymbol{\Pi}}_i)$.

We jointly identify the latent group structure in (2.3) and the time-varying coefficients $\beta_i(t/T)$ through a *penalized* sieve technique, leveraging the *PAGFL* penalty ([Qian and Su, 2016a](#); [Mehrabani, 2023](#)). In what follows, we introduce this estimation procedure in the context of the time-varying panel data model (2.1). Beyond this baseline, our proposal can readily accommodate extensions, as discussed in Appendix D.

First, we concentrate out the individual fixed effects γ_i^0 in (2.5) using $\tilde{y}_{it} = y_{it} - T^{-1} \sum_{t=1}^T y_{it}$,

with $\tilde{\mathbf{z}}_{it}$ defined analogously. Let $\boldsymbol{\pi} = (\boldsymbol{\pi}'_1, \dots, \boldsymbol{\pi}'_N)'$ collect all individual parameters. We then take as objective function

$$\mathcal{F}_{NT}(\boldsymbol{\pi}, \lambda) = \frac{1}{T} \sum_{i=1}^N \sum_{t=1}^T (\tilde{y}_{it} - \boldsymbol{\pi}'_i \tilde{\mathbf{z}}_{it})^2 + \frac{\lambda}{N} \sum_{i=1}^{N-1} \sum_{j=i+1}^N \dot{\omega}_{ij} \|\boldsymbol{\pi}_i - \boldsymbol{\pi}_j\|_2, \quad (2.6)$$

where the first part is the usual sum of squared residuals and the second part is the *PAGFL* penalty term with tuning parameter $\lambda > 0$ and adaptive penalty weights $\dot{\omega}_{ij}$. The penalty encourages sparsity in the differences of all $N(N - 1)/2$ pairs of individual coefficient vectors. For large λ , some of these differences will be shrunken to exactly zero, implying that the corresponding cross-sectional units feature identical parameter estimates. The weights are set to $\dot{\omega}_{ij} = \|\dot{\boldsymbol{\pi}}_i - \dot{\boldsymbol{\pi}}_j\|_2^{-\kappa}$, where $\dot{\boldsymbol{\pi}}_i$ represents an initial consistent estimate $\dot{\boldsymbol{\pi}} = \arg \min_{\boldsymbol{\pi}} T^{-1} \sum_{i=1}^N \sum_{t=1}^T (\tilde{y}_{it} - \boldsymbol{\pi}'_i \tilde{\mathbf{z}}_{it})^2$ and κ is specified by the user; for simplicity and in line with the standard choice in the adaptive Lasso literature, we maintain $\kappa = 2$ throughout the paper.

Objective (2.6) generalizes the objective function in [Mehrabani \(2023, eq. 2.6\)](#) to our *FUSE-TIME* approach. The penalized sieve estimator (*PSE*) $\hat{\boldsymbol{\pi}}$ of *FUSE-TIME* is then obtained by minimizing (2.6), namely

$$\hat{\boldsymbol{\pi}}_\lambda = \arg \min_{\boldsymbol{\pi}} \mathcal{F}_{NT}(\boldsymbol{\pi}, \lambda).$$

Cross-sectional units with identical slope estimates are assigned to the same cluster by collecting all \hat{K} unique subvectors $\hat{\boldsymbol{\pi}}_i$ of $\hat{\boldsymbol{\pi}}_\lambda$ in the vector $\hat{\boldsymbol{\xi}} = (\hat{\boldsymbol{\xi}}'_1, \dots, \hat{\boldsymbol{\xi}}'_{\hat{K}})'$ and defining the set $\hat{G}_k = \{i : \hat{\boldsymbol{\pi}}_i = \hat{\boldsymbol{\xi}}_k, 1 \leq i \leq N\}$ for each $k = 1, \dots, \hat{K}$. Subsequently, the group-specific *PSE* coefficient function equals $\hat{\boldsymbol{\alpha}}_k(t/T) = \hat{\boldsymbol{\Xi}}'_k \mathbf{b}(t/T)$, where $\hat{\boldsymbol{\xi}}_k = \text{vec}(\hat{\boldsymbol{\Xi}}_k)$. As such, parameter estimation and identification of the latent group structure are performed simultaneously. The total number of clusters \hat{K} is determined by the tuning parameter λ . We propose to select λ using the consistent information criterion (IC) introduced in Section 3. In the following, unless required, we suppress the dependence of $\hat{\boldsymbol{\pi}}$ on λ to lighten the notation.

Remark 2.2. The penalty term in criterion (2.6) is time-invariant and, therefore, also the group structure. Nevertheless, cross-sectional units switching groups do not lead to inconsistent estimates of the time-varying coefficients but only to a larger number of groups \hat{K} , since each distinct combination of the time of the switch, origin group, and destination group implies one excess group. Alternatively, one can define the penalty in (2.6) over each of the M rows in $\boldsymbol{\Pi}_i$ individually, implying groupings specific to each basis function and thus allowing for time-varying group membership. Such an extension is further discussed in Appendix [D.1](#).

Objective function (2.6) is convex in $\boldsymbol{\pi}$. To solve for $\boldsymbol{\pi}$, we employ a computationally efficient Alternating Direction Method of Multipliers (ADMM) algorithm, adapted from [Mehrabani \(2023, sec. 5\)](#) and detailed in Appendix C. An open-source implementation of this algorithm is provided in our companion R-package PAGFL ([Haimerl et al., 2025](#)).

Remark 2.3. *FUSE-TIME* shows similarities with the proposal in [Su et al. \(2019\)](#). However, they use a different approach to identify the latent group structure, namely the *C-Lasso* of [Su et al. \(2016\)](#). The *C-Lasso* shrinks N individual coefficients towards K group-level coefficients and thus requires an additional tuning parameter to explicitly determine K . Additionally, the *C-Lasso* objective function is not convex, though decomposable into convex subproblems. Objective function (2.6), in contrast, is convex.

Finally, to mitigate the bias coming from the fusion penalty term in (2.6), we propose a post-selection fused-Lasso estimator of *FUSE-TIME*, labeled *post-Lasso* estimator for brevity, given the estimated group pattern $\hat{\mathcal{G}} = \{\hat{G}_1, \dots, \hat{G}_{\hat{K}}\}$:

$$\hat{\boldsymbol{\xi}}_{\hat{G}_k}^p = \left(\sum_{i \in \hat{G}_k} \sum_{t=1}^T \tilde{\mathbf{z}}_{it} \tilde{\mathbf{z}}'_{it} \right)^{-1} \sum_{i \in \hat{G}_k} \sum_{t=1}^T \tilde{\mathbf{z}}_{it} \tilde{y}_{it}, \quad k = 1, \dots, \hat{K}.$$

Subsequently, the final *post-Lasso* time-varying coefficient estimates follow as $\hat{\boldsymbol{\alpha}}_{\hat{G}_k}^p(t/T) = \hat{\boldsymbol{\Xi}}_{\hat{G}_k}^{p'} \mathbf{b}(t/T)$, using $\hat{\boldsymbol{\xi}}_{\hat{G}_k}^p = \text{vec}(\hat{\boldsymbol{\Xi}}_{\hat{G}_k}^p)$.

3 Asymptotic Properties

In this section, we study the consistency of the coefficient estimates and the clustering procedure (Sections 3.1 and 3.2). Furthermore, we establish the limiting distribution of the *PSE* and the *post-Lasso* estimator (Section 3.3), and we propose a consistent BIC criterion to select the tuning parameter (Section 3.4). Formal proofs appear in Appendix B.

3.1 Preliminary Convergence Rates

Let $\mathbb{C}^\theta[0, 1]$ denote the space of functions that are θ -times continuously differentiable on the unit interval. Moreover, let $\mathbf{x}_{it}^{(2)} = \mathbf{x}_{it}$ if no intercept is included in \mathbf{x}_{it} and $\mathbf{x}_{it} = (1, \mathbf{x}_{it}^{(2) \prime})'$ otherwise.

Assumption 1.

(i) There exists a positive constant $c_{\epsilon\epsilon} < \infty$ such that $N^{-1} \sum_{i=1}^N \sum_{j=1}^N |\max_t E(\epsilon_{it}\epsilon_{jt})| \leq c_{\epsilon\epsilon}$.²

²We abbreviate $\max_{1 \leq i \leq N}$, $\max_{1 \leq t \leq T}$, and $\max_{1 \leq i \leq N, 1 \leq t \leq T}$ with \max_i , \max_t , and $\max_{i,t}$, respectively. \min_i , \min_t , and $\min_{i,t}$ are defined likewise.

- (ii) $\left\{(\mathbf{x}_{it}^{(2)}, \epsilon_{it}), t = 1, \dots, T\right\}$ is a strong mixing process with geometric decay such that the mixing coefficient $\phi(j)$ satisfies $\phi(j) \leq c_\phi \varphi^j$ for some $c_\phi < \infty$, $0 \leq \varphi < 1$, and each $i = 1, \dots, N$.
- (iii) There exist two positive constants $c_x < \infty$ and $c_\epsilon < \infty$ such that $\max_{i,t} E\|\mathbf{x}_{it}\|_2^q \leq c_x$ and $\max_{i,t} E|\epsilon_{it}|^q \leq c_\epsilon$ for some $q \geq 6$, when $\mathbf{x}_{it} \neq 1$.
- (iv) There exist a lower and upper bound $0 < \underline{c}_{xx} \leq \bar{c}_{xx} < \infty$ such that $\underline{c}_{xx} \leq \min_{i,t} \mu_{\min} \left(\text{Var}(\mathbf{x}_{it}^{(2)}) \right) \leq \max_{i,t} \mu_{\max} \left(E(\mathbf{x}_{it}^{(2)} \mathbf{x}_{it}^{(2)\prime}) \right) \leq \bar{c}_{xx}$.
- (v) $\lim_{N \rightarrow \infty} N_k/N \in [0, 1]$ for each $k = 1, \dots, K_0$ and $N_k > 1$ for all $k \in \{k : \lim_{N \rightarrow \infty} N_k/N = 0, 1 \leq k \leq K_0\}$.
- (vi) $\boldsymbol{\alpha}_k^0(t/T) \in \mathbb{C}^\theta[0, 1]$ for each $k = 1, \dots, K_0$ and some $1 < \theta \leq d + 2$.

Assumption 1(i) is standard in the factor model literature and limits cross-sectional dependence (cf. [Bai and Ng, 2002](#)). This condition is trivially satisfied if the idiosyncratic errors are independently distributed, an assumption frequently made for similar panel data models with latent group structures (cf. [Su et al., 2016](#); [Qian and Su, 2016a](#); [Su et al., 2019](#)).

Assumption 1(ii)-(iv) loosely follows [Su et al. \(2019, Assumption 1\(ii\)-\(iv\)\)](#). Assumption 1(ii) imposes a strong mixing process, which nests popular and extensively studied time series processes with geometrically decaying innovations, such as common ARMA, GARCH, Markov-switching, or threshold autoregressive models. Serial correlation as well as conditional heteroscedasticity in the error process are allowed. As [Su et al. \(2019\)](#) point out, in dynamic panels Assumption 1(ii) implies the fixed effects γ_i to be nonrandom. If the fixed effects are treated as random variables, the strong mixing condition in Assumption 1(ii) must hold conditional on each realized γ_i , with the distribution of γ_i being bounded uniformly in i (cf. [Hahn and Kuersteiner, 2011](#), Condition 3).

Assumptions 1(i)-(ii) can also be replaced by similar primitive ([Bonhomme and Manresa, 2015](#), Assumption 1(d)-(f)) or higher-level assumptions ([Mehrabani, 2023](#), Assumption A.1(i)-(iii)) that limit the degree of dependence across time and the cross-section such that a central limit theorem can be applied.

Assumptions 1(iii)-(iv) place common moment conditions on the regressors and innovations. The conditions on the regressors in Assumptions 1(iii)-(iv) are redundant if \mathbf{x}_{it} is deterministic. Assumption 1(v) allows group sizes to remain constant or to diverge at a speed slower than N . Assumption 1(vi) imposes smoothness on the true functional coefficients and ensures that they can be well approximated by splines of polynomial degree d .

Let J_{\min} denote the minimum group separability in the sieve-space \mathbb{B}_M , $J_{\min} = \min_{i \in G_k^0, j \notin G_k^0} \|\boldsymbol{\pi}_i^0 - \boldsymbol{\pi}_j^0\|_2$.

Assumption 2.

- (i) $\lim_{T \rightarrow \infty} MT^{-1/2} = 0$.
- (ii) $\lim_{T \rightarrow \infty} (MT^{-1/2} + M^{-\theta+1/2})^{-1} J_{\min} = \infty$.
- (iii) $\text{plim}_{T \rightarrow \infty} (T^{-1/2} + M^{-\theta-1/2})^{-1} \lambda J_{\min}^{-\kappa} = c_\lambda$ for some constant $c_\lambda > 0$.
- (iv) $\text{plim}_{(N,T) \rightarrow \infty} (MT^{-1/2} + M^{-\theta+1/2})^{-\kappa-1} M^{1/2} \lambda N_k / N = \infty$ for each $k = 1, \dots, K_0$.

Assumption 2(i) controls the size of the spline basis system. Assumption 2(ii) determines the rate at which the minimum group separability in \mathbb{B}_M may shrink to zero. Assumption 2(iii) governs the speed at which the tuning parameter λ must shrink to zero. Assumption 2(iv) places conditions on the relative rates of the number of coefficients to be estimated, coefficient convergence, and λ so that group-specific trajectories can still be consistently estimated. In sum, N , T , M , and K_0 diverge to infinity, whereas λ and J_{\min} tend to zero in the limit.

Theorem 3.1. *Given that Assumptions 1 and 2(i)-(iii) are satisfied, for $i = 1, \dots, N$, we have*

- (i) $\|\hat{\boldsymbol{\pi}}_i - \boldsymbol{\pi}_i^0\|_2 = O_p(MT^{-1/2} + M^{-\theta+1/2})$,
- (ii) $N^{-1} \sum_{i=1}^N \|\hat{\boldsymbol{\pi}}_i - \boldsymbol{\pi}_i^0\|_2^2 = O_p(M^2 T^{-1} + M^{-2\theta+1})$.

Theorem 3.1 establishes pointwise and mean-square convergence of $\hat{\boldsymbol{\pi}}_i$. The first term in the rates of Theorem 3.1 reflects the stochastic error. The second term corresponds to the asymptotic bias of the sieve technique. Increasing the complexity of the spline system M involves a bias-variance trade-off. On the one hand, the larger M , the slower the convergence due to the increased size of the coefficient vector.³ On the other, increasing M reduces the asymptotic sieve bias. Moreover, the greater the order of continuous differentiability of the true coefficient functions θ , the faster the sieve bias shrinks in M .

Corollary 3.2. *Given that Assumptions 1 and 2(i)-(iii) are satisfied, for $i = 1, \dots, N$, we have*

$$(i) \sup_{v \in [0,1]} \|\hat{\boldsymbol{\beta}}_i(v) - \boldsymbol{\beta}_i^0(v)\|_2 = O_p(MT^{-1/2} + M^{-\theta+1/2}),$$

$$(ii) \int_0^1 \|\hat{\boldsymbol{\beta}}_i(v) - \boldsymbol{\beta}_i^0(v)\|_2^2 dv = O_p(MT^{-1} + M^{-2\theta}).$$

³Note that $O_p(MT^{-1/2} + M^{-\theta+1/2}) = o_p(1)$ by Assumptions 1(vi) and 2(i).

Corollary 3.2 relates the results of Theorem 3.1 to the actual functional coefficients. Note that the true coefficient functions are time-continuous. As a consequence, we report the supremum and integral over the unit interval. Interestingly, the pointwise rates of $\hat{\pi}_i$ and $\hat{\beta}_i(v)$ match, whereas the L_2 rate of $\hat{\beta}_i(v)$ is faster in M . This result is due to the boundedness of the B-splines (see Lemma A.1(ii)).

3.2 Clustering Consistency

This subsection establishes clustering consistency.

Theorem 3.3. *Given that Assumptions 1 and 2 are satisfied, $\Pr(\|\hat{\pi}_i - \hat{\pi}_j\|_2 = 0 \forall i, j \in G_k^0, 1 \leq k \leq K_0) \rightarrow 1$, as $(N, T) \rightarrow \infty$.*

Theorem 3.3 establishes that, in the limit, all cross-sectional units belonging to the same group G_k^0 are jointly assigned to the same group; no other units are assigned to this group.

Corollary 3.4. *Given that Assumptions 1 and 2 are satisfied,*

- (i) $\lim_{(N, T) \rightarrow \infty} \Pr(\hat{K} = K_0) = 1$,
- (ii) $\lim_{(N, T) \rightarrow \infty} \Pr(\hat{\mathcal{G}}_{K_0} = \mathcal{G}_{K_0}^0) = 1$.

Based on Theorem 3.3, Corollary 3.4 shows that the correct number of groups and group structure will be derived asymptotically. This result is intuitive since, given Theorem 3.3, $\hat{\pi}$ can only hold K_0 distinct individual subvectors and all homogeneous individuals are assigned to the same group as $(N, T) \rightarrow \infty$. Since the latent grouping will be identified w.p.a.1, Corollary 3.4 motivates the oracle property of the procedure. This implies that the estimation procedure is asymptotically equivalent to an infeasible oracle estimator based on the true grouping.

3.3 Limiting Distribution of the *PSE* and *Post-Lasso* Estimators

In the following, we derive the asymptotic distribution of the *PSE* and the *post-Lasso*.

Assumption 3. $\lim_{(N, T) \rightarrow \infty} (N_k T M)^{1/2} \lambda J_{\min}^{-\kappa} = 0$ for each $k = 1, \dots, K_0$.

The penalty term in (2.6) grows quadratically in N . Hence, Assumption 3 strengthens Assumption 2(iii) and imposes conditions for the penalty term to vanish asymptotically, resulting in coinciding limiting distributions for the *PSE* and the *post-Lasso*. To this end, Assumption 3 specifies a larger group separation or a faster rate at which λ converges to zero. Assumption 3 is only relevant for the *PSE* and need not hold for the asymptotic properties of the *post-Lasso*.

Let $\epsilon_i = (\epsilon_{i1}, \dots, \epsilon_{iT})'$.

Assumption 4.

- (i) There exists a positive constant $\bar{c}_{\epsilon\epsilon} < \infty$ such that $\lim_{(N,T) \rightarrow \infty} \max_{i \in G_k^0} \mu_{\max}(E(\epsilon_i \epsilon_i')) \leq \bar{c}_{\epsilon\epsilon}$ for each $k = 1, \dots, K_0$.
- (ii) $\lim_{(N,T) \rightarrow \infty} NTM^{-2\theta} = 0$.

Assumption 4(i) imposes a mild restriction on the error process, enabling the use of the Lindeberg condition to derive the limiting distribution in Theorem 3.5. Assumption 4(ii) provides an additional regularity condition that precludes the sieve approximation error from dominating the limiting distributions of the *PSE* and the *post-Lasso*. Let $\hat{\mathbf{Q}}_{G_k^0, \tilde{z}\tilde{z}} = \sum_{i \in G_k^0} \hat{\mathbf{Q}}_{i, \tilde{z}\tilde{z}}$ with $\hat{\mathbf{Q}}_{i, \tilde{z}\tilde{z}} = T^{-1} \sum_{t=1}^T \tilde{z}_{it} \tilde{z}_{it}'$ and $\tilde{\mathbf{Z}}_i = (\tilde{z}_{i1}, \dots, \tilde{z}_{iT})$. Furthermore, define the variance-covariance matrix $\hat{\Omega}_{G_k^0} = \hat{\nu}'_{G_k^0} \hat{\mathbf{E}}_{G_k^0} \hat{\nu}_{G_k^0}$ with

$$\hat{\nu}_{G_k^0} = \left(MN_k^{-1} \hat{\mathbf{Q}}_{G_k^0, \tilde{z}\tilde{z}} \right)^{-1} (\mathbf{I}_p \otimes \mathbf{b}(v)),$$

$$\hat{\mathbf{E}}_{G_k^0} = \frac{M}{N_k T} \sum_{i \in G_k^0} \tilde{\mathbf{Z}}_i' E(\epsilon_i \epsilon_i') \tilde{\mathbf{Z}}_i,$$

and $\mathbf{q}_{G_k^0} = \sqrt{M/(N_k T)} \sum_{i \in G_k^0} \sum_{t=1}^T E(\tilde{z}_{it} \tilde{\epsilon}_{it})$.

Theorem 3.5. *Given that Assumptions 1-4 are satisfied,*

- (i) $\sqrt{N_k T / M} \hat{\Omega}_{G_k^0}^{-1/2} (\hat{\alpha}_k(t/T) - \alpha_k^0(t/T)) - \hat{\mathbf{E}}_{G_k^0}^{-1/2} \mathbf{q}_{G_k^0} \xrightarrow{D} N(0, \mathbf{I}_p)$,
- (ii) $\sqrt{N_k T / M} \hat{\Omega}_{G_k^0}^{-1/2} (\hat{\alpha}_{\hat{G}_k}^p(t/T) - \alpha_k^0(t/T)) - \hat{\mathbf{E}}_{G_k^0}^{-1/2} \mathbf{q}_{G_k^0} \xrightarrow{D} N(0, \mathbf{I}_p)$.

$\mathbf{q}_{G_k^0}$ equals zero in the case of strictly exogenous regressors. However, commonly referred to as the Nickell bias, $\mathbf{q}_{G_k^0}$ is nonzero and of order $O(\sqrt{N_k/T})$ for dynamic panel data models (Nickell, 1981; Phillips and Sul, 2007). The bias emerges when T remains fixed or grows slower than N_k . The within-transformation nets out the fixed effect γ_i but simultaneously induces a contemporaneous correlation between the error term and the autoregressive regressor, thus biasing the coefficient estimate if T does not grow fast enough relative to the number of individuals that feed into the group-specific autoregressive coefficient function (Nickell, 1981; Kiviet, 1995; Hahn and Kuersteiner, 2011; Su et al., 2016).

The *PSE* and the *post-Lasso* estimators are asymptotically equivalent to the infeasible oracle estimator with true grouping structure, hence both achieve oracle efficiency. Additionally, the B-splines yield arbitrarily close approximation of the true coefficient functions $\alpha_k^0(t/T)$. Given Assumption 3, both estimators feature the same asymptotic distribution. Nevertheless, despite their equivalence in the limit, we recommend using the *post-Lasso* in finite-sample applications.

The penalty term of the *PSE* can lead to non-negligible bias, particularly in small samples. The simulation study in Section 4 corroborates this finding.

Given a consistent estimator $\hat{\mathcal{E}}_{\hat{G}_k}$ and exploiting the oracle property in Corollary 3.4, the variance of the limiting distribution can be estimated consistently. Potential techniques to derive $\hat{\mathcal{E}}_{\hat{G}_k}$ are numerous. We follow the literature on heteroscedasticity and autocorrelation robust estimation of covariance matrices and take

$$\hat{\mathcal{E}}_{\hat{G}_k} = \hat{\mathcal{E}}_{\hat{G}_k}^{(0)} + \sum_{h=1}^{H_T} w(h, H_T) \left(\hat{\mathcal{E}}_{\hat{G}_k}^{(h)} + \hat{\mathcal{E}}_{\hat{G}_k}^{(h)\prime} \right),$$

where H_T is the window size, $\hat{\mathcal{E}}_{\hat{G}_k}^{(h)} = N_k^{-1} \sum_{i \in \hat{G}_k} T^{-1} \sum_{t=h+1}^T \tilde{z}_{it} \tilde{z}'_{it-1} \hat{\epsilon}_{it} \hat{\epsilon}_{it-1}$, and $\hat{\epsilon}_{it} = \tilde{y}_{it} - \hat{\alpha}_{\hat{G}_k}^{p'}(t/T) \tilde{x}_{it}$ (Newey and West, 1987; Hahn and Kuersteiner, 2002; Pesaran, 2006; Müller, 2014). $w(h, H_T)$ denotes a weighting function subject to $\sup_h |w(h, H_T)| < \infty$ and $\lim_{T \rightarrow \infty} w(h, H_T) = 1$. It is common to specify $w(h, H_T) = 1 - h/(H_T + 1) \mathbf{1}\{h \leq H_T\}$ (Newey and West, 1987). A rigorous derivation of the consistency of $\hat{\mathcal{E}}_{\hat{G}_k}$ and required primitive conditions are beyond the scope of this paper and are left for future work (see, e.g., Su and Jin, 2012, Theorem 4.3 for further reference).

Remark 3.1. It is important to highlight that the limiting distributions in Theorem 3.5 hold conditional on the true group structure, rather than uniformly for all possible groupings. This limitation is ubiquitous in the literature on latent-class panel data models that involve a model selection step (Leeb and Pötscher, 2008).

3.4 Selecting the Tuning Parameter λ

In the remainder of this section, we make the dependence of \hat{K}_λ and $\hat{G}_{k,\lambda}$ on λ explicit. We choose the tuning parameter λ that minimizes the following BIC-type criterion

$$IC(\lambda) = \ln \left(\hat{\sigma}_{\hat{G}_{k,\lambda}}^2 \right) + \rho_{NT} p M \hat{K}_\lambda, \quad (3.1)$$

where $\hat{\sigma}_{\hat{G}_{k,\lambda}}^2 = (NT)^{-1} \sum_{k=1}^{\hat{K}_\lambda} \sum_{i \in \hat{G}_{k,\lambda}} \sum_{t=1}^T \left(\tilde{y}_{it} - \hat{\alpha}_{\hat{G}_{k,\lambda}}^{p'}(t/T) \tilde{x}_{it} \right)^2$ and ρ_{NT} represents a tuning parameter (see Qian and Su, 2016a; Su et al., 2019; Mehrabani, 2023, for similar approaches). Define the set $\Lambda = [0, \lambda_{\max}]$ for some sufficiently large $\lambda_{\max} < \infty$ and partition Λ into $\Lambda_{0,NT}$, $\Lambda_{-,NT}$, and $\Lambda_{+,NT}$, such that $\Lambda_{0,NT} = \{\lambda \in \Lambda : \hat{K}_\lambda = K_0\}$, $\Lambda_{-,NT} = \{\lambda \in \Lambda : \hat{K}_\lambda < K_0\}$, and $\Lambda_{+,NT} = \{\lambda \in \Lambda : \hat{K}_\lambda > K_0\}$.⁴ In addition, assume that all $\lambda \in \Lambda_0$ comply with the regularity

⁴We index the three subsets of Λ with NT to make it apparent that \hat{K} is obtained from a random sample of dimension (N, T) .

conditions stated in Assumptions 2-3. Denote the set of all K -partitions of $\{1, \dots, N\}$ as \mathbb{G} .

Assumption 5. $\text{plim}_{(N,T) \rightarrow \infty} \min_{1 \leq K < K_0} \inf_{\mathcal{G}_K \in \mathbb{G}} \hat{\sigma}_{\mathcal{G}_K}^2 = \underline{\sigma}^2 > \sigma_0^2$.

Assumption 5 is standard in the literature and implies that the mean squared error (*MSE*) of an underfitted model is asymptotically larger than σ_0^2 , the *MSE* of the true model.

Assumption 6.

(i) $\lim_{(N,T) \rightarrow \infty} \rho_{NT} MK_0 = 0$.

(ii) $\lim_{(N,T) \rightarrow \infty} T \rho_{NT} = \infty$.

Assumption 6 collects conditions such that the penalty term in (3.1) either dominates the *MSE* or vanishes in the limit, depending on whether $\hat{K} > K_0$ or $\hat{K} \leq K_0$, respectively.

Theorem 3.6. *Given that Assumptions 1-6 are satisfied,*

$$\Pr \left(\inf_{\lambda \in \Lambda_{-,NT} \cup \Lambda_{+,NT}} IC(\lambda) > \sup_{\lambda \in \Lambda_{0,NT}} IC(\lambda) \right) \rightarrow 1 \text{ as } (N,T) \rightarrow \infty.$$

From Theorem 3.6 follows that neither an underfitted nor an overfitted model maximizes the IC as N and T diverge to infinity. Consequently, the IC in (3.1) uncovers the true model asymptotically.

When applying the IC, a practitioner must select ρ_{NT} . After some preliminary experiments and in line with previous literature, we recommend specifying $\rho_{NT} = c_\lambda \log(NT)(NT)^{-1/2}$ with $c_\lambda = 0.04$ (cf. Mehrabani, 2023, sec. 6).

4 Monte Carlo Simulation Study

This section examines the finite-sample properties of *FUSE-TIME* using several Monte Carlo simulation studies. Section 4.1 describes the DGPs, followed by implementation details and evaluation metrics in Section 4.2. In Section 4.3, we present the results.

4.1 The Data Generating Processes

We consider three DGPs for all (N, T) combinations of $N = \{50, 100\}$ and $T = \{50, 100\}$. The cross-sectional individuals are sampled from $K_0 = 3$ groups with the proportions 0.3, 0.3, and 0.4. Throughout the simulation study, we draw the individual fixed effects γ_i^0 and the idiosyncratic innovations ϵ_{it} from mutually independent standard normal distributions. Following Su et al. (2019, sec. 6), the DGPs are constructed as follows:

DGP 1: Trending panel data model

$$y_{it} = \gamma_i^0 + \beta_{i,0}^0 \left(\frac{t}{T} \right) + \epsilon_{it},$$

with the coefficient functions

$$\beta_{i,0}^0(v) = \begin{cases} \alpha_{1,0}^0(v) = 6F(v; 0.5, 0.1) & \text{if } i \in G_1^0 \\ \alpha_{2,0}^0(v) = 6[2v - 6v^2 + 4v^3 + F(v; 0.7, 0.05)] & \text{if } i \in G_2^0 \\ \alpha_{3,0}^0(v) = 6[4v - 8v^2 + 4v^3 + F(v; 0.6, 0.05)] & \text{if } i \in G_3^0. \end{cases}$$

$F(v; a, b) = [1 + \exp(-(v - a)/b)]^{-1}$ denotes a cumulative logistic function.

DGP 2: Trending panel with an exogenous regressor

$$y_{it} = \gamma_i^0 + \beta_{i,1}^0 \left(\frac{t}{T} \right) + \beta_{i,2}^0 \left(\frac{t}{T} \right) x_{it} + \epsilon_{it},$$

that augments DGP 1 with a scalar exogenous explanatory variable x_{it} which is generated from a standard normal distribution. Let $\beta_{i,1}^0(t/T) = 0.5\beta_{i,0}^0(t/T)$ (and hence $\alpha_{i,1}^0(t/T) = 0.5\alpha_{i,0}^0(t/T)$), where $\beta_{i,0}^0$ and $\alpha_{i,0}^0$ are as defined in DGP 1, and

$$\beta_{i,2}^0(v) = \begin{cases} \alpha_{1,2}^0(v) = 3[2v - 4v^2 + 2v^3 + F(v; 0.6, 0.1)] & \text{if } i \in G_1^0 \\ \alpha_{2,2}^0(v) = 3[v - 3v^2 + 2v^3 + F(v; 0.7, 0.04)] & \text{if } i \in G_2^0 \\ \alpha_{3,2}^0(v) = 3[0.5v - 0.5v^2 + F(v; 0.4, 0.07)] & \text{if } i \in G_3^0. \end{cases}$$

DGP 3: Dynamic panel data model

$$y_{it} = \gamma_i^0 + \beta_{i,3}^0 \left(\frac{t}{T} \right) y_{it-1} + \epsilon_{it},$$

featuring a time-varying autoregressive functional relationship. In order to comply with the strong mixing condition in Assumption A.1(ii), $\sup_{v \in [0,1]} |\alpha_{k,3}^0(v)| < 1$ for all $k = 1, \dots, K_0$, the autoregressive coefficient is taken as

$$\beta_{i,3}^0(v) = \begin{cases} \alpha_{1,3}^0(v) = 1.5[-0.5 + 2v - 5v^2 + 2v^3 + F(v; 0.6, 0.03)] & \text{if } i \in G_1^0 \\ \alpha_{2,3}^0(v) = 1.5[-0.5 + v - 3v^2 + 2v^3 + F(v; 0.2, 0.04)] & \text{if } i \in G_2^0 \\ \alpha_{3,3}^0(v) = 1.5[-0.5 + 0.5v - 0.5v^2 + F(v; 0.8, 0.07)] & \text{if } i \in G_3^0. \end{cases}$$

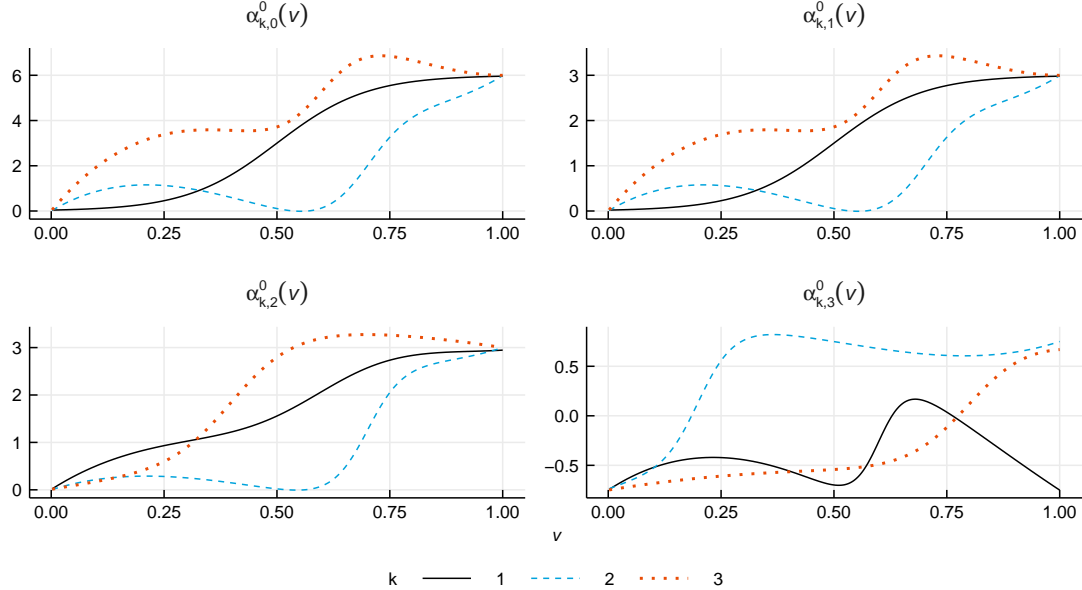


Figure 1: Simulated group-specific coefficient functions for DGP 1 (top left), DGP 2 (top right and bottom left) and DGP 3 (bottom right)

Figure 1 presents the sample paths of the simulated coefficient functions across the three DGPs.

4.2 Implementation and Evaluation

The *FUSE-TIME* estimator is obtained as described in Section 2.2. We select the number of interior knots M^* of the spline system $\mathbf{b}(t/T)$ by taking $M^* = \max \{ \lfloor (NT)^{1/7} - \log(p) \rfloor, 1 \}$, where $\lfloor \cdot \rfloor$ rounds to the lower integer. When T is small, large M^* tend to overfit the individual time-varying coefficients and pollute the grouping. Conversely, a small M^* caps the flexibility of the time-varying coefficients and may complicate the group differentiation in large panels with many latent groups. Furthermore, we set $d = 3$ since cubic splines offer a good trade-off between flexibility and parsimony. This gives a $M^* + d + 1 = M$ -dimensional vector of spline basis functions.

We compute the *FUSE-TIME* estimator for a grid of λ values; the grids are specified in Table E.1 of Appendix E for the three DGPs. The IC in equation (3.1) selects the λ tuning parameter. We hereby set $\rho_{NT} = c_\lambda \log(NT)(NT)^{-1/2}$ with $c_\lambda = 0.04$ as described in Section 3.4. In large samples, the results do not vary substantially in c_λ .

To evaluate performance, we inspect grouping and estimation accuracy. The clustering performance is evaluated across n_{sim} Monte Carlo experiments according to the following criteria:

- (i) Frequency of $\hat{K} = K_0$, $n_{\text{sim}}^{-1} \sum_{j=1}^{n_{\text{sim}}} \mathbf{1}\{\hat{K}_j = K_0\}$.
- (ii) Frequency of $\hat{\mathcal{G}}_{\hat{K}} = \mathcal{G}^0$, $n_{\text{sim}}^{-1} \sum_{j=1}^{n_{\text{sim}}} \mathbf{1}\{\hat{\mathcal{G}}_{\hat{K},j} = \mathcal{G}_j^0\}$.

- (iii) Adjusted Rand Index (*ARI*). The *ARI* ranges from minus one to one and measures the similarity between two groupings; one signals total agreement, minus one total disagreement, and zero reflects random assignment. We report the average *ARI* over all Monte Carlo iterations $ARI = n_{\text{sim}}^{-1} \sum_{j=1}^{n_{\text{sim}}} ARI_j(\hat{\mathcal{G}}_{\hat{K},j}, \mathcal{G}_j^0)$.
- (iv) Average \hat{K} , $\bar{K} = n_{\text{sim}}^{-1} \sum_{j=1}^{n_{\text{sim}}} \hat{K}_j$.

The root mean square error (*RMSE*) quantifies the estimation accuracy of the time-varying coefficient functions and is computed as

$$RMSE(\hat{\alpha}_l) = \frac{1}{N} \sum_{i=1}^N \sqrt{\frac{1}{T} \sum_{t=1}^T \left[\hat{\alpha}_{i,l} \left(\frac{t}{T} \right) - \alpha_{i,l}^0 \left(\frac{t}{T} \right) \right]^2},$$

where $\hat{\alpha}_{i,l}(t/T) = \hat{\alpha}_{k,l}(t/T)$ if $i \in \hat{G}_k$ and $\alpha_{i,l}^0(t/T) = \alpha_{j,l}^0(t/T)$ if $i \in G_j^0$, for $l = \{0, 1, 2, 3\}$.

When reporting results on estimation accuracy, note that we explicitly distinguish between the proposed *PSE* and the *post-Lasso* estimator as defined in Section 2.2; whereas throughout the rest of the paper we refer to the latter as the *FUSE-TIME* estimator. Their performance is compared with two benchmarks. The first is the infeasible oracle estimator that is based on the true latent grouping \mathcal{G}_0 , averaged across all n_{sim} experiments. The second is the *time-varying C-Lasso* by Su et al. (2019). Appendix E.3 lists details on the implementation of the *time-varying C-Lasso* and Appendix E.4 benchmarks the computational cost of the *FUSE-TIME* and *C-Lasso* software implementations; the computational gains of the former are sizable.

4.3 Simulation Study Results

We simulate all DGPs $n_{\text{sim}} = 300$ times and apply *FUSE-TIME* as well as the *time-varying C-Lasso* procedures. Table 1 reports metrics on the grouping performance; note that there is no distinction between *PSE* and *post-Lasso* in terms of grouping performance, hence we report the results of our proposal under *FUSE-TIME* in Table 1.

FUSE-TIME convincingly outperforms the *C-Lasso* benchmark, particularly in smaller samples and DGPs 2 and 3. *FUSE-TIME*'s clustering accuracy improves quickly with increasing T , but not with N . This is intuitive since the clustering routine is driven by the estimated individual control points $\hat{\pi}_i$, which are not consistent with respect to the cross-sectional dimension (see Theorem 3.1). Accordingly, when T is small, the estimation of individual coefficient functions is highly noisy, complicating correct group assignment. This property is particularly evident when comparing DGP 1 and DGP 2. The latter involves estimating a second regression curve, which introduces addi-

Table 1: Clustering accuracy

	N	T	Freq. $\hat{K} = K_0$		Freq. $\hat{\mathcal{G}}_{\hat{K}} = \mathcal{G}_{K_0}^0$		ARI		\bar{K}	
			FT	C-Lasso	FT	C-Lasso	FT	C-Lasso	FT	C-Lasso
DGP 1	50	50	1.000	0.947	0.960	0.867	0.997	0.974	3.000	2.980
	50	100	1.000	1.000	1.000	1.000	1.000	1.000	3.000	3.000
	100	50	1.000	0.900	0.943	0.667	0.998	0.940	3.000	2.900
	100	100	1.000	1.000	1.000	1.000	1.000	1.000	3.000	3.000
DGP 2	50	50	0.937	0.430	0.623	0.140	0.949	0.691	2.957	2.430
	50	100	1.000	0.357	0.983	0.320	0.999	0.725	3.000	2.357
	100	50	0.943	0.523	0.487	0.023	0.951	0.618	2.957	2.523
	100	100	1.000	0.973	0.977	0.540	0.999	0.960	3.000	2.973
DGP 3	50	50	0.713	0.000	0.120	0.000	0.838	0.503	3.280	2.000
	50	100	0.937	0.000	0.677	0.000	0.974	0.541	3.063	2.000
	100	50	0.750	0.000	0.047	0.000	0.829	0.485	2.810	2.000
	100	100	0.993	0.000	0.633	0.000	0.983	0.542	2.993	2.000

Notes: Frequency of obtaining the correct number of groups $\hat{K} = K_0$ and the correct grouping $\hat{\mathcal{G}}_{\hat{K}} = \mathcal{G}_{K_0}^0$, the ARI, and the average estimated number of total groups \bar{K} based on a Monte Carlo study with 300 replications. *FT-FUSE-TIME*—denotes our proposed methodology. *C-Lasso* refers to the benchmark model by [Su et al. \(2019\)](#).

tional uncertainty and subsequently does not lead to the near-perfect clustering observed in DGP 1. Nevertheless, *FUSE-TIME* still shows strong clustering performance for DGP 2. In contrast, the results for the dynamic panel data model of DGP 3 are markedly worse than for the other DGPs, especially when $T = 50$. Similar estimation devices have previously reported decreased performance for dynamic panel data models (see [Mehrabani, 2023](#)). Nevertheless, as indicated by the *ARI* measure, even when individual cross-sectional units are misclassified, the estimated grouping remains a close approximation of the true unobserved group structure, with *FUSE-TIME* substantially outperforming the C-Lasso: ARIs in the range of 0.83-0.98 for *FUSE-TIME* versus 0.49-0.54 for C-Lasso.

Table 2 reports the *RMSE* for each time-varying coefficient, and split among *PSE* and *post-Lasso* estimators. Figure 2 provides the estimated sample paths of the functional coefficients for each DGP and $N, T = 50$. The *RMSE* results largely align with the clustering performance. This also holds for the comparison with the *time-varying C-Lasso*, which returns considerably poorer results regarding the *RMSE* as well. Unlike clustering accuracy, the *post-Lasso RMSE* also improves with N due to the larger number of cross-sectional units available for pooling when estimating group-specific trajectories. Notably, the *post-Lasso* performs well relative to the oracle estimator, even in cases, such as DGP 3, where the clustering results may suggest a poor fit. This finding is likely because misclassified units tend to feature sample paths that are particularly similar to other groups, leading to a minor impact on the *RMSE* compared to the oracle estimation. Precise

Table 2: *RMSE* of coefficient estimates

	N	T	<i>PSE</i>		<i>post-Lasso</i>		oracle
			<i>FUSE-TIME</i>	<i>C-Lasso</i>	<i>FUSE-TIME</i>	<i>C-Lasso</i>	
DGP 1	$\hat{\alpha}_0(t/T)$	50	0.274	0.915	0.160	0.311	0.159
		50	0.197	1.037	0.146	0.277	0.146
		100	0.274	1.034	0.146	0.299	0.146
		100	0.190	1.095	0.139	0.271	0.139
DGP 2	$\hat{\alpha}_1(t/T)$	50	0.263	0.432	0.154	0.231	0.130
		50	0.189	0.453	0.140	0.209	0.117
		100	0.275	0.433	0.146	0.226	0.117
		100	0.189	0.529	0.134	0.153	0.079
DGP 3	$\hat{\alpha}_2(t/T)$	50	0.306	0.655	0.153	0.231	0.135
		50	0.207	0.698	0.127	0.186	0.116
		100	0.321	0.662	0.139	0.220	0.119
		100	0.206	0.836	0.121	0.075	0.085
	$\hat{\alpha}_3(t/T)$	50	0.217	0.422	0.145	0.418	0.074
		50	0.168	0.457	0.119	0.423	0.059
		100	0.243	0.413	0.147	0.416	0.060
		100	0.153	0.422	0.052	0.412	0.050

Notes: *RMSE* of the *PSE*, the *post-Lasso*, and an infeasible oracle estimator based on a Monte Carlo study with 300 replications. *FUSE-TIME* denotes our proposed methodology. *C-Lasso* refers to the benchmark model by [Su et al. \(2019\)](#). The index in $\hat{\alpha}_l(t/T)$ does not refer to the group structure but to the coefficients $l = \{0, 1, 2, 3\}$ used in DGPs 1-3 (see. Section 4.1).

identification of group-specific coefficients despite several misclassifications has been previously reported by [Bonhomme and Manresa \(2015\)](#). Table 2 further highlights that the shrinkage penalty leads to a sizeable finite-sample bias in the *PSE*, even though the *PSE* and the *post-Lasso* share the same asymptotic distribution (see Theorem 3.5). This motivates our usage of the *post-Lasso* for empirical applications. Finally, Figure 2 corroborates the previous findings: while minor deviations occur, partly due to misclassified units, the estimated trajectories closely follow the true underlying function.

Additionally, we also simulate the three DGPs with either idiosyncratic errors following an *AR*(1) process with lag polynomial $a(L) = 1 - 0.3L$ or unbalanced panels with missing data, where we generate sample paths that randomly discard 30% of the observations. Detailed results are available in Appendix E. For unbalanced panels with missing data (see Appendix E.2), the simulation results largely mirror the ones presented here. Discarding part of the sample has a similar effect to decreasing T in a balanced panel. However, when the innovations follow an *AR*(1) process (see Appendix E.1), the performance decreases markedly, particularly when T is small. Introducing autocorrelation to the errors increases the estimation uncertainty and thus contaminates the clustering mechanism. However, even when the grouping is correctly estimated, the coefficient trajectories offer a significantly poorer fit than the baseline case.

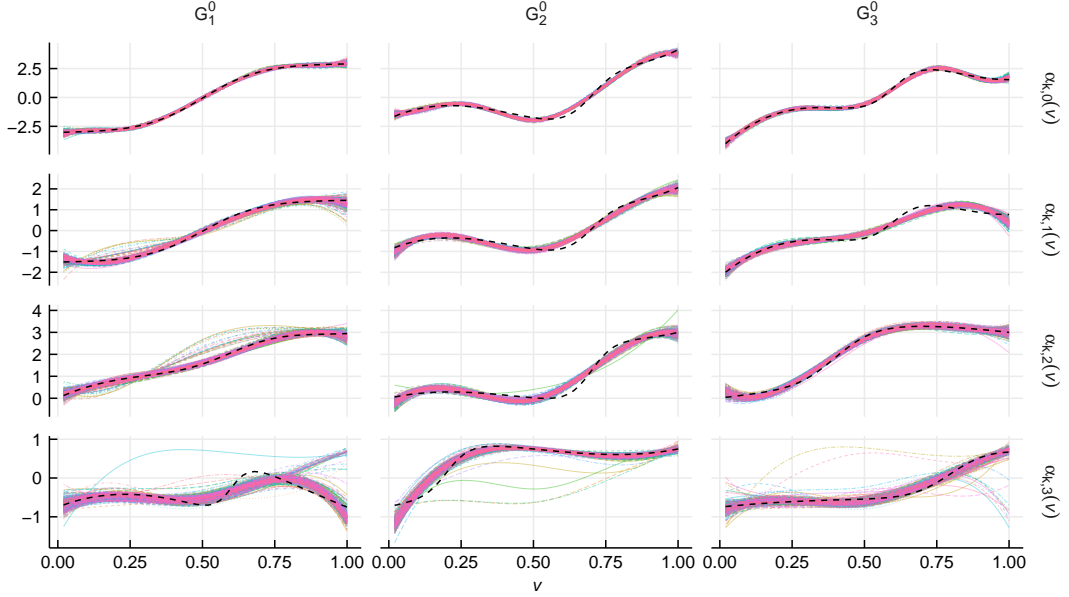


Figure 2: Estimated *FUSE-TIME* post-Lasso functional coefficients when $N, T = 50$ and $n_{\text{sim}} = 300$. The true coefficient functions are shown in black (dashed).

5 Empirical Illustration

Many major economies pledge to reduce the emission of harmful greenhouse gases, a key driver of global warming. Achieving this objective without impeding economic growth requires emissions per unit of GDP to decrease. CO₂ accounts for approximately 66% of the anthropogenic contribution to global warming and is a ubiquitous by-product of economic activity and energy production (Bennedsen et al., 2023). Consequently, understanding the relationship between CO₂ pollution and economic growth is crucial for effective policy and climate action. We contribute by applying our *FUSE-TIME* procedure to identify trends in the CO₂ emission intensity of GDP, the CO₂ emitted per unit of GDP produced.

The CO₂ intensity of GDP is determined by the structural composition of an economy and the “greenness” of its energy production (Bella et al., 2014). For instance, transitioning from a production-based to a service-oriented economy reduces energy consumption and direct emissions from high-pollution industries. Likewise, shifting from emission-intensive solid fuels, such as coal or biomass, to cleaner carriers like natural gas or renewables, lowers the elasticity between energy demand and associated pollution. The combined effects of economic restructuring and energy source optimization are often credited with driving the decoupling of GDP growth from production-based emissions in high-income countries (Jakob et al., 2012; Wang et al., 2017). This decoupling pattern has inspired an extensive literature on the inverted U-shaped environmental Kuznets curve, which posits a positive elasticity between income and emissions during the early stages of economic devel-

opment, turning negative as technological progress and greater prosperity take hold (see Grossman and Krueger, 1995; Wagner, 2015; Bennedsen et al., 2023, among other). However, as (log) GDP, an integrated process, clearly does not satisfy the regularity conditions in Assumption 1, we instead study the relationship between emissions and income by estimating trends in CO₂ intensity. Trend functions capture the long-term behavior of CO₂ intensity by smoothing over short-run fluctuations such as business cycles, fuel price volatility, or temporary energy supply disruptions. Moreover, it is well-established that economies exhibit considerable heterogeneity in their developmental trajectories (Kose et al., 2003; Azomahou et al., 2006). Consequently, assuming a common CO₂ intensity trend across many countries is implausible. Nevertheless, much of the existing empirical literature imposes cross-sectional homogeneity or homogeneity conditional on an exogenous grouping (Awaworyi Churchill et al., 2018; Bennedsen et al., 2023). We relax this condition. Using our *FUSE-TIME* procedure, different economies only share a common trend if the consistent grouping mechanism identifies homogeneous coefficients, enabling us to exploit the cross-sectional dimension without imposing restrictive homogeneity assumptions. In addition, given the small number of group-specific trend functions relative to the cross-sectional dimension, it becomes feasible to interpret the long-term behavior of CO₂ intensity for a large number of economies.

To estimate trends in the CO₂ intensity of GDP, we employ production-based CO₂ emissions data from the Global Carbon Project (Friedlingstein et al., 2024).⁵ GDP series are obtained from the World Bank Development Indicators database.⁶ Both datasets are in annual frequency and span the time period from 1960 to 2023 for 92 countries. Details on the countries included in the sample and descriptive statistics are provided in Appendix F. Using this data, we compute the CO₂ intensity and construct an unbalanced panel where the individual series range from 29 to 64 years in length.

Let $y_{it} = \text{CO}_{2it}/\text{GDP}_{it}$, with CO₂ measured in million tonnes and GDP in billion 2024 U.S. dollar. We formulate the time-varying panel data model subject to a latent grouping

$$y_{it} = \gamma_i + \beta_i \left(\frac{t}{T} \right) + \epsilon_{it},$$

where $\beta_i(t/T)$ denotes the trend function of interest (time-varying intercept).

Searching over a dense grid of d , M^* , and λ values, $d = 2$, $M^* = 4$, and $\lambda = 0.72$ yields the lowest IC, implying five latent groups; the entire grid is provided in Appendix F. Figure 3 presents

⁵Dataset *National fossil carbon emissions v2024*, available at globalcarbonbudgetdata.org. Accessed November 14

⁶Series *NY.GDP.MKTP.CD*, available at data.worldbank.org/indicator/NY.GDP.MKTP.CD. Accessed November 12, 2024.

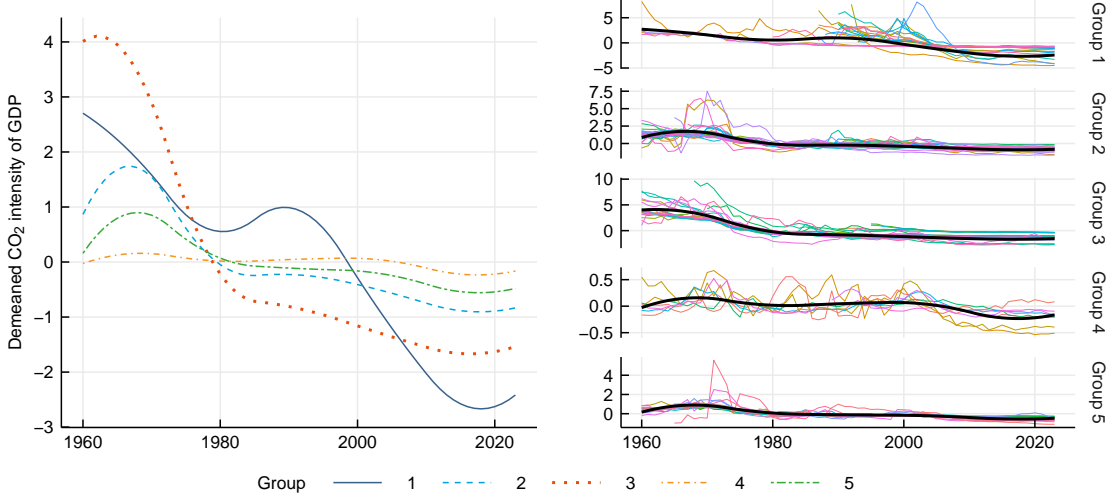


Figure 3: The left panel displays the group-specific *FUSE-TIME post-Lasso* trend functions. The right panel contrasts the estimated trend functions (black, thick) with the demeaned data of CO₂ intensity (colored, thin).

the estimated group-specific trend functions $\hat{\alpha}_{\hat{G}_k}^p(t/T)$. Figure 4 sketches the spatial pattern in the group structure. Table F.2 in Appendix F provides a detailed record of which countries are assigned to which group.

Group 1 predominantly comprises middle- and high-income economies in Eastern Europe and Asia, which have exhibited a substantial and ongoing decline in CO₂ emission intensity since the 1990s. Structural changes and rapid technological advances following the fall of the USSR and the economic liberalization of China may drive this trend. Group 2 largely includes low-to-middle-income economies, with outliers such as Switzerland, Hong Kong, and Singapore. The trend of Group 2 features a much more gradual decrease compared to the first group due to more moderate growth in both income and emissions. Group 3 primarily consists of high-income countries that experienced a sharp decline in emission intensity pre-1980, followed by a continued but more dampened decline thereafter. This pattern reflects a stark reduction in emissions until the 1980s, accompanied by consistent GDP growth throughout the entire sample period, aligning with a transition to service-based economies and the offshoring of emission- and energy-intensive sectors to low-income countries. Group 4 contains low-income and developing economies, characterized by the absence of a trend. In these economies, technological progress has yet to reduce emission intensity significantly or, as in the case of Brazil, income growth is largely driven by the exploitation of natural resources. Group 5, consisting of low-income economies, exhibits a similar but slightly more attenuated trend compared to Group 2.

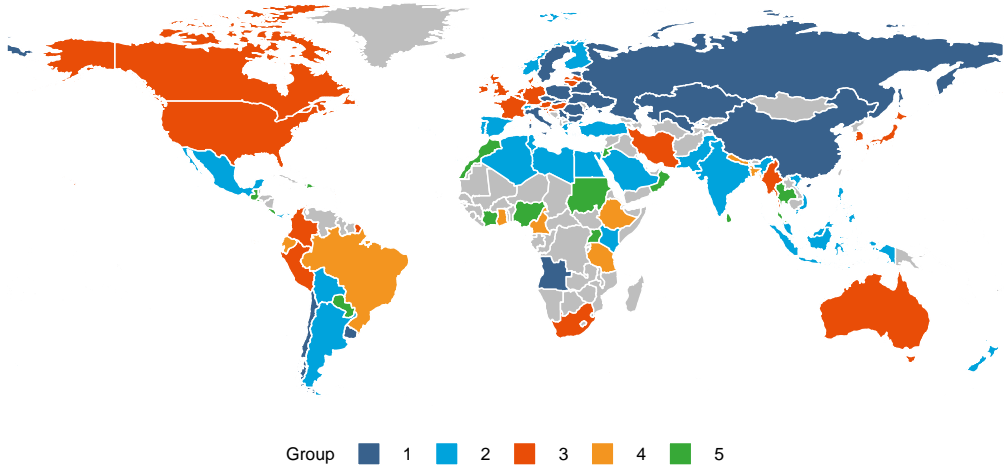


Figure 4: Estimated group structure in the trends of CO₂ intensity.

6 Conclusion

This article introduces a novel penalized sieve estimation technique—*FUSE-TIME*—to estimate panel data models with smoothly time-varying coefficients that are subject to an unobserved group structure. Our approach simultaneously identifies the functional coefficients, the number of latent groups, and group compositions. In addition, we propose a consistent BIC-type criterion to determine the penalty tuning parameter, introduce a *post-Lasso* estimator, and prove oracle-efficiency. Monte Carlo simulation studies confirm strong finite-sample performance in recovering the latent group structure and accurately estimating the time-varying coefficients across a wide range of scenarios. We apply our method to analyze trends in the CO₂ emission intensity of GDP.

An important yet largely unexplored extension regards inference methods for (time-varying) panel data models with a latent group pattern. The estimated grouping is an inherently noisy representation of the true unobserved structure. Subsequently, the clustering introduces uncertainty to the slope coefficients, analogous to the well-established problem of non-uniform convergence of post-selection estimation (see [Greenshtein and Ritov, 2004](#); [Leeb and Pötscher, 2008](#); [Adamek et al., 2023](#)). To the best of our knowledge, [Dzemski and Okui \(2024\)](#) provide the only approach to creating confidence sets of the grouping by inverting poolability tests to date. Consequently, the development of inference methods for penalized panel data models that admit a latent grouping, including confidence sets for the group structure, as well as tests for coefficient poolability and constancy akin to [Friedrich and Lin \(2024\)](#), remains an important direction for future research.

References

Adamek, R., Smeeches, S., and Wilms, I. (2023). Lasso inference for high-dimensional time series. *Journal of Econometrics*, 235(2):1114–1143.

Ando, T. and Bai, J. (2016). Panel data models with grouped factor structure under unknown group membership. *Journal of Applied Econometrics*, 31(1):163–191.

Awaworyi Churchill, S., Inekwe, J., Ivanovski, K., and Smyth, R. (2018). The environmental kuznets curve in the oecd: 1870–2014. *Energy Economics*, 75:389–399.

Azomahou, T., Laisney, F., and Nguyen Van, P. (2006). Economic development and co2 emissions: A nonparametric panel approach. *Journal of Public Economics*, 90(6):1347–1363.

Bai, J. (2010). Common breaks in means and variances for panel data. *Journal of Econometrics*, 157(1):78–92. Nonlinear and Nonparametric Methods in Econometrics.

Bai, J. and Ng, S. (2002). Determining the number of factors in approximate factor models. *Econometrica*, 70(1):191–221.

Bella, G., Massidda, C., and Mattana, P. (2014). The relationship among co2 emissions, electricity power consumption and gdp in oecd countries. *Journal of Policy Modeling*, 36(6):970–985.

Bennedsen, M., Hillebrand, E., and Jensen, S. (2023). A neural network approach to the environmental kuznets curve. *Energy Economics*, 126:106985.

Bernstein, D. S. (2009). *Matrix Mathematics, Theory, Facts, and Formulas with Application to Linear Systems Theory*. Princeton University Press.

Bonhomme, S., Lamadon, T., and Manresa, E. (2022). Discretizing unobserved heterogeneity. *Econometrica*, 90(2):625–643.

Bonhomme, S. and Manresa, E. (2015). Grouped patterns of heterogeneity in panel data. *Econometrica*, 83(3):1147–1184.

Cai, Z. (2007). Trending time-varying coefficient time series models with serially correlated errors. *Journal of Econometrics*, 136(1):163–188.

Cashin, P., Mohaddes, K., Raissi, M., and Raissi, M. (2014). The differential effects of oil demand and supply shocks on the global economy. *Energy Economics*, 44:113–134.

De Boor, C. (2001). *A practical guide to splines*. Springer-Verlag New York.

Diebold, F. X., Li, C., and Yue, V. Z. (2008). Global yield curve dynamics and interactions: A dynamic nelson–siegel approach. *Journal of Econometrics*, 146(2):351–363. Honoring the research contributions of Charles R. Nelson.

Dung, V. T. and Tjahjowidodo, T. (2017). A direct method to solve optimal knots of B-spline curves: An application for non-uniform B-spline curves fitting. *PloS one*, 12(3):e0173857.

Dzemski, A. and Okui, R. (2024). Confidence set for group membership. *Quantitative Economics*, 15(2):245–277.

Freyaldenhoven, S. (2022). Factor models with local factors — determining the number of relevant factors. *Journal of Econometrics*, 229(1):80–102.

Friedlingstein, P., O’Sullivan, M., Jones, M. W., Andrew, R. M., Hauck, J., Landschützer, P., Le Quéré, C., Li, H., Luijkx, I. T., Olsen, A., Peters, G. P., Peters, W., Pongratz, J., Schwingshakel, C., Sitch, S., Canadell, J. G., Ciais, P., Jackson, R. B., Alin, S. R., Arneth, A., Arora, V., Bates, N. R., Becker, M., Bellouin, N., Berghoff, C. F., Bittig, H. C., Bopp, L., Cadule, P., Campbell, K., Chamberlain, M. A., Chandra, N., Chevallier, F., Chini, L. P., Colligan, T., Decayeux, J., Djeutchouang, L., Dou, X., Duran Rojas, C., Enyo, K., Evans, W., Fay, A., Feely, R. A., Ford, D. J., Foster, A., Gasser, T., Gehlen, M., Gkritzalis, T., Grassi, G., Gregor, L., Gruber, N., Gürses, O., Harris, I., Hefner, M., Heinke, J., Hurtt, G. C., Iida, Y., Ilyina, T., Jacobson, A. R., Jain, A., Jarníková, T., Jersild, A., Jiang, F., Jin, Z., Kato, E., Keeling, R. F., Klein Goldewijk, K., Knauer, J., Korsbakken, J. I., Lauvset, S. K., Lefevre, N., Liu, Z., Liu, J., Ma, L., Maksyutov, S., Marland, G., Mayot, N., McGuire, P., Metzl, N., Monacci, N. M.,

Morgan, E. J., Nakao, S.-I., Neill, C., Niwa, Y., Nützel, T., Olivier, L., Ono, T., Palmer, P. I., Pierrot, D., Qin, Z., Resplandy, L., Roobaert, A., Rosan, T. M., Rödenbeck, C., Schwinger, J., Smallman, T. L., Smith, S., Sospedra-Alfonso, R., Steinhoff, T., Sun, Q., Sutton, A. J., Séférian, R., Takao, S., Tatebe, H., Tian, H., Tilbrook, B., Torres, O., Tourigny, E., Tsujino, H., Tubiello, F., van der Werf, G., Wanninkhof, R., Wang, X., Yang, D., Yang, X., Yu, Z., Yuan, W., Yue, X., Zaehle, S., Zeng, N., and Zeng, J. (2024). Supplemental data of global carbon budget 2024. *Earth System Science Data Discussions*, 2024:1–133.

Friedrich, M. and Lin, Y. (2024). Sieve bootstrap inference for linear time-varying coefficient models. *Journal of Econometrics*, 239(1):105345. Climate Econometrics.

Greenshtein, E. and Ritov, Y. (2004). Persistence in high-dimensional linear predictor selection and the virtue of overparametrization. *Bernoulli*, 10(6):971–988.

Grossman, G. M. and Krueger, A. B. (1995). Economic growth and the environment. *The Quarterly Journal of Economics*, 110(2):353–377.

Hahn, J. and Kuersteiner, G. (2002). Asymptotically unbiased inference for a dynamic panel model with fixed effects when both n and t are large. *Econometrica*, 70(4):1639–1657.

Hahn, J. and Kuersteiner, G. (2011). Bias reduction for dynamic nonlinear panel models with fixed effects. *Econometric Theory*, 27(6):1152–1191.

Haimerl, P., Smeekes, S., Wilms, I., and Mehrabani, A. (2025). *PAGFL: Joint Estimation of Latent Groups and Group-Specific Coefficients in Panel Data Models*. R-package version 1.1.3.

Hansen, M. H. and Kooperberg, C. (2002). Spline Adaptation in Extended Linear Models (with comments and a rejoinder by the authors. *Statistical Science*, 17(1):2 – 51.

Huang, J. Z., Wu, C. O., and Zhou, L. (2004). Polynomial spline estimation and inference for varying coefficient models with longitudinal data. *Statistica Sinica*, 14(3):763–788.

Jakob, M., Haller, M., and Marschinski, R. (2012). Will history repeat itself? economic convergence and convergence in energy use patterns. *Energy Economics*, 34(1):95–104.

Ke, Z. T., Fan, J., and Wu, Y. (2015). Homogeneity pursuit. *Journal of the American Statistical Association*, 110(509):175–194. PMID: 26085701.

Kiviet, J. F. (1995). On bias, inconsistency, and efficiency of various estimators in dynamic panel data models. *Journal of Econometrics*, 68(1):53–78.

Kose, M. A., Otrok, C., and Whiteman, C. H. (2003). International business cycles: World, region, and country-specific factors. *American Economic Review*, 93(4):1216–1239.

Leeb, H. and Pötscher, B. M. (2008). Sparse estimators and the oracle property, or the return of hedges' estimator. *Journal of Econometrics*, 142(1):201–211.

Lumsdaine, R. L., Okui, R., and Wang, W. (2023). Estimation of panel group structure models with structural breaks in group memberships and coefficients. *Journal of Econometrics*, 233(1):45–65.

Ma, S. and Huang, J. (2017). A concave pairwise fusion approach to subgroup analysis. *Journal of the American Statistical Association*, 112(517):410–423.

Mehrabani, A. (2023). Estimation and identification of latent group structures in panel data. *Journal of Econometrics*, 235(2):1464–1482.

Mehrabani, A. and Parsaeian, S. (2025). Shrinkage estimation and identification of latent group structures in panel data with interactive fixed effects. *Journal of Business & Economic Statistics*. In press.

Müller, U. K. (2014). HAC corrections for strongly autocorrelated time series. *Journal of Business & Economic Statistics*, 32(3):311–322.

Newey, W. K. and West, K. D. (1987). A simple, positive semi-definite, heteroskedasticity and autocorrelation consistent covariance matrix. *Econometrica*, 55(3):703–708.

Nickell, S. (1981). Biases in dynamic models with fixed effects. *Econometrica*, 49(6):1417–1426.

Pesaran, M. H. (2006). Estimation and inference in large heterogeneous panels with a multifactor error structure. *Econometrica*, 74(4):967–1012.

Phillips, P. C. and Sul, D. (2007). Bias in dynamic panel estimation with fixed effects, incidental trends and cross section dependence. *Journal of Econometrics*, 137(1):162–188.

Qian, J. and Su, L. (2016a). Shrinkage estimation of common breaks in panel data models via adaptive group fused lasso. *Journal of Econometrics*, 191(1):86–109.

Qian, J. and Su, L. (2016b). Shrinkage estimation of regression models with multiple structural changes. *Econometric Theory*, 32(6):1376–1433.

Robinson, P. M. (2012). Nonparametric trending regression with cross-sectional dependence. *Journal of Econometrics*, 169(1):4–14. Recent Advances in Panel Data, Nonlinear and Nonparametric Models: A Festschrift in Honor of Peter C.B. Phillips.

Sarafidis, V. and Weber, N. (2015). A partially heterogeneous framework for analyzing panel data. *Oxford Bulletin of Economics and Statistics*, 77(2):274–296.

Scarpiniti, M., Comminiello, D., Parisi, R., and Uncini, A. (2013). Nonlinear spline adaptive filtering. *Signal Processing*, 93(4):772–783.

Su, L. and Jin, S. (2012). Sieve estimation of panel data models with cross section dependence. *Journal of Econometrics*, 169(1):34–47. Recent Advances in Panel Data, Nonlinear and Nonparametric Models: A Festschrift in Honor of Peter C.B. Phillips.

Su, L., Shi, Z., and Phillips, P. C. B. (2016). Identifying latent structures in panel data. *Econometrica*, 84(6):2215–2264.

Su, L., Wang, X., and Jin, S. (2019). Sieve estimation of time-varying panel data models with latent structures. *Journal of Business & Economic Statistics*, 37(2):334–349.

Vogt, M. and Linton, O. (2020). Multiscale clustering of nonparametric regression curves. *Journal of Econometrics*, 216(1):305–325. Annals Issue in honor of George Tiao: Statistical Learning for Dependent Data.

Wagner, M. (2015). The environmental kuznets curve, cointegration and nonlinearity. *Journal of Applied Econometrics*, 30(6):948–967.

Wang, H., Ang, B., and Su, B. (2017). A multi-region structural decomposition analysis of global co2 emission intensity. *Ecological Economics*, 142:163–176.

Wang, W., Phillips, P. C. B., and Su, L. (2018). Homogeneity pursuit in panel data models: Theory and application. *Journal of Applied Econometrics*, 33(6):797–815.

A Details on the Sieve Estimation of Time-varying Coefficient Functions

Consider a B-spline with $M^* > 0$ interior knots that is piece-wise polynomial of degree $d \geq 1$ (polynomial order $d + 1$) on the unit interval. The $M \times 1$ vector $\mathbf{b}(v)$ holds the common time-varying basis functions $\mathbf{b}(v) = (b_{-d}(v), \dots, b_{M^*}(v))'$, with $M = M^* + d + 1$ and $v \in [0, 1]$. Let \mathbb{V}_{int} represent an increasing sequence $0 < v_1 < \dots < v_{M^*} < 1$, such that \mathbb{V}_{int} gives M^* equidistant interior knots of the B-spline, which divide the unit interval into $M^* + 1$ partitions.⁷ The total set of knots \mathbb{V} extends \mathbb{V}_{int} to $0 = v_{-d} = \dots = v_0 < v_1 < \dots < v_{M^*} < v_{M^*+1} = \dots = v_M = 1$. The boundary knots $\{v_m\}_{m=-d}^0 \cup \{v_m\}_{m=M^*+1}^M$ coincide at either zero or one and force the final B-spline to pass through the start and end points exactly using the *de Boor recurrence relation*:

$$b_{m,j}(v) = a_{m,j}(v)b_{m,j-1}(v) + [1 - a_{m+1,j}(v)]b_{m+1,j-1}(v),$$

with $a_{m,j}(v) = [(v - v_m)/(v_{m+j} - v_m)]\mathbf{1}\{v_{m+j} \neq v_m\}$, $b_{m,0}(v) = \mathbf{1}\{v_m \leq v < v_{m+1}\}$, and $b_{m,d}(v) = b_m(v)$ (De Boor, 2001, ch. 9, eq. 14). Hence, each basis function $b_m(v)$, $m = -d, \dots, M^*$, defined on the knots $\{v_m\}_{m=-d}^M$, is a convex combination of two lower-order basis functions and vanishes outside the interval $\{V_m\}_{m=-d}^{M^*}$ with

$$V_m = \begin{cases} [v_m, v_{m+d+1}), & \text{for } m = -d, \dots, M^* - d - 1 \\ [v_m, v_{m+d+1}], & \text{for } m = M^* - d, \dots, M^*. \end{cases} \quad (\text{A.1})$$

The space generated by these M polynomial basis functions is denoted as \mathbb{B}_M and each function in \mathbb{B}_M is a B-spline that is piece-wise polynomial of degree d on each sub-interval $\{V_m\}_{m=-d}^{M^*}$ and globally $d - 1$ times continuously differentiable for $d \geq 1$. We refer to De Boor (2001) for a textbook treatment of spline functions.

The $M \times 1$ vector of control points $\boldsymbol{\pi}_{il}^0$ weights each basis function in $\mathbf{b}(v)$ and, in turn, constructs a linear combination, the B-spline, that approximates a scalar square-integrable coefficient function $\beta_{il}^0(v)$

$$\beta_{il}^0(v) = \boldsymbol{\pi}_{il}^0 \mathbf{b}(v) + \eta_{il}, \quad l = 1, \dots, p. \quad (\text{A.2})$$

⁷We conjecture that the basic results of this paper also hold for free-knot spline functions, where the distance between interior knots may deviate from $1/(M^* + 1)$. However, altering the theory in this respect and introducing a data-driven knot placement routine is very involved (see Hansen and Kooperberg, 2002; Scarpiniti et al., 2013; Dung and Tjahjowidodo, 2017). A rigorous extension of the theory to free-knot splines is beyond the scope of this paper.

⁸A B-spline can be equivalently expressed as convex combinations of control points, with $B_{m,0}$ acting as indicators. In this case, recursively constructed convex combinations of control points yield the M^* polynomial functions, which continuously tie together at the interior knots (see De Boor, 2001, pp. 99).

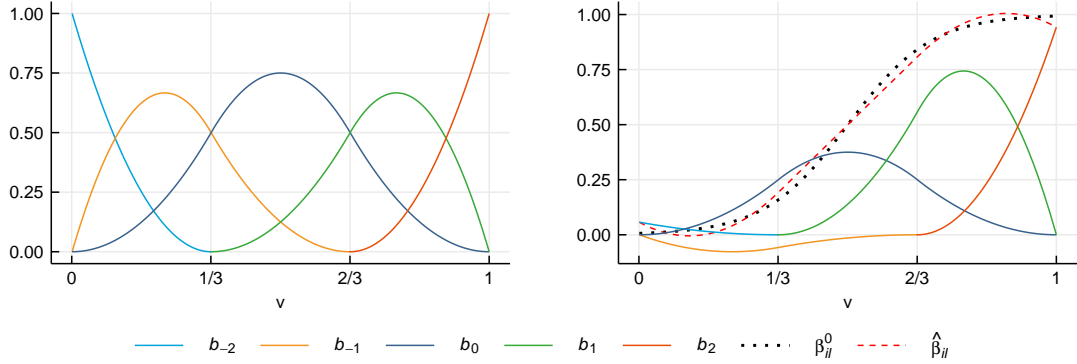


Figure A.1: The left panel sketches five polynomial basis functions $b_m(v)$, $m = -d, \dots, M^*$ for $d = 2$ and $M^* = 2$. The right panel displays the weighted basis functions (solid) and the resulting B-spline (red, dashed), approximating a logistic CDF $\beta_{il}^0(v)$ (black, dotted).

The sieve approximation error $\eta_{il}(v) = \beta_{il}^0(v) - \pi_{il}^0 \mathbf{b}(v)$ is zero if $\beta_{il}^0(v) \in \mathbb{B}_M$ and M is known. However, since $\beta_{il}^0(v)$ may generally not belong to the linear space \mathbb{B}_M , we allow M to increase with the sample size and obtain ever closer approximations of the true underlying coefficient function. \mathbb{B}_M acts as a tractable sieve space, where increasing M is akin to moving to an ever denser sieve. Throughout the paper, we assume the generalizing case $\beta_{il}^0(v) \notin \mathbb{B}_M$.

Figure A.1 illustrates the approximation of a logistic cumulative distribution function (CDF) using a B-spline with $M^* = 2$ interior knots and polynomial degree $d = 2$, resulting in a system of $M = M^* + d + 1 = 5$ basis functions. The vector of control points π_{il}^0 is estimated by regressing realizations of the function of interest, in this example, a logistic CDF, on $\mathbf{b}(v)$, using least squares (Huang et al., 2004, sec. 2).

This technique readily extends to a p -dimensional functional vector $\beta_i^0(v)$. Instead of a $M \times 1$ vector of control points π_{il}^0 , we now require a $M \times p$ matrix Π_i^0 , where each column of Π_i^0 corresponds to one of the p scalar functions in $\beta_i^0(v)$. Subsequently,

$$\beta_i^0(v) = \Pi_i^0 \mathbf{b}(v) + \eta_i,$$

as in (2.4).

B Proof of the Results in Section 3

B.1 Technical Lemmas

Lemma B.1. *Let $b_m(v) > 0$, $m = -d, \dots, M^*$, denote a basis function of degree $d > 0$ (order $d + 1$), defined on the sequence of knots \mathbb{V} as introduced in Appendix A.*

(i) Then $\|\mathbf{b}(v)\|_2 = \left[\sum_{j=-d}^{M^*} b_m(v)^2 \right]^{1/2} \leq \left[\sum_{j=-d}^{M^*} b_m(v) \right]^{1/2} = 1$.

(ii) $\int_0^1 b_m(v) dv = O(M^{-1})$ and $\int_0^1 \|\mathbf{b}(v)\|_2 dv = \int_0^1 \left[\sum_{j=-d}^{M^*} b_m(v)^2 \right]^{1/2} dv \leq \int_0^1 \left[\sum_{j=-d}^{M^*} b_m(v) \right]^{1/2} dv = 1$.

(iii) There exist two constants $0 < \underline{c}_b \leq \bar{c}_b < \infty$ such that

$$\underline{c}_b \leq \mu_{\min} \left(M \int_0^1 \mathbf{b}(v) \mathbf{b}(v)' dv \right) \leq \mu_{\max} \left(M \int_0^1 \mathbf{b}(v) \mathbf{b}(v)' dv \right) \leq \bar{c}_b.$$

(iv) Given Assumption 1(vi) and $\beta_i^0(v) \notin \mathbb{B}_{V,M}$, there exists a coefficient matrix $\Pi_i^0 \in \mathbb{R}^{M \times p}$ such that $\sup_{v \in [0,1]} \|\beta_i^0(v) - \Pi_i^0 \mathbf{b}(v)\|_2 = O(M^{-\theta})$, where $\theta \geq 1$.

Lemma B.2. Define $\hat{\mathbf{Q}}_{i,\tilde{z}\tilde{z}} = T^{-1} \sum_{t=1}^T \tilde{z}_{it} \tilde{z}'_{it}$ and $\hat{\mathbf{Q}}_{i,\tilde{z}\tilde{z}} = \sum_{i \in G_k^0} T^{-1} \sum_{t=1}^T \tilde{z}_{it} \tilde{z}'_{it}$. Given Assumptions 1(i)-(ii), 1(iv), and 1(vi), there exist two constants $0 < \underline{c}_{\tilde{z}\tilde{z}} \leq \bar{c}_{\tilde{z}\tilde{z}} < \infty$ such that

(i) $\Pr \left(\underline{c}_{\tilde{z}\tilde{z}} \leq \min_i \mu_{\min}(M \hat{\mathbf{Q}}_{i,\tilde{z}\tilde{z}}) \leq \max_i \mu_{\max}(M \hat{\mathbf{Q}}_{i,\tilde{z}\tilde{z}}) \leq \bar{c}_{\tilde{z}\tilde{z}} \right) = 1 - o(N^{-1})$,

(ii) $\Pr \left(\underline{c}_{\tilde{z}\tilde{z}} \leq \min_i \mu_{\min}(N_k^{-1} M \hat{\mathbf{Q}}_{i,\tilde{z}\tilde{z}}) \leq \max_i \mu_{\max}(N_k^{-1} M \hat{\mathbf{Q}}_{i,\tilde{z}\tilde{z}}) \leq \bar{c}_{\tilde{z}\tilde{z}} \right) = 1 - o(N^{-1})$.

Lemma B.3. Define $\hat{\mathbf{q}}_{i,\tilde{z}\tilde{u}} = T^{-1} \sum_{t=1}^T \tilde{z}_{it} \tilde{u}_{it}$, with the composite error $\tilde{u}_{it} = \tilde{\epsilon}_{it} + \tilde{\varrho}_{it}$, $\varrho_{it} = \boldsymbol{\eta}'_{it} \mathbf{x}_{it}$. Given Assumption 1,

(i) $\|\hat{\mathbf{q}}_{i,\tilde{z}\tilde{u}}\|_2 = O_p(T^{-1/2} M^{-\theta-1/2})$,

(ii) $N^{-1} \sum_{i=1}^N \|\hat{\mathbf{q}}_{i,\tilde{z}\tilde{u}}\|_2^2 = O_p(T^{-1} + M^{-2\theta-1})$.

Lemma B.4. Recall the preliminary estimate $\dot{\boldsymbol{\pi}} = \arg \min_{\boldsymbol{\pi}} T^{-1} \sum_{i=1}^N \sum_{t=1}^T (\tilde{y}_{it} - \boldsymbol{\pi}'_i \tilde{z}_{it})^2$. Given Assumptions 1 and 2(i), $\|\dot{\boldsymbol{\pi}}_i - \boldsymbol{\pi}_i^0\|_2 = O_p(MT^{-1/2} + M^{-\theta-1/2})$.

Lemma B.5. Suppose that Assumptions 1 and 2(i)-(ii) hold. Then

(i) $\min_{i,j \in G_k^0} \dot{\omega}_{ij} = \|\dot{\boldsymbol{\pi}}_i - \dot{\boldsymbol{\pi}}_j\|_2^{-\kappa} = O_p((MT^{-1/2} + M^{-\theta+1/2})^{-\kappa})$,

(ii) $\max_{i \in G_k^0, j \notin G_k^0} \dot{\omega}_{ij} = O_p(J_{\min}^{-\kappa})$.

Lemma B.6. Suppose that Assumption 1 is satisfied. Let $\mathbf{b}_c = \mathbf{c} \otimes \mathbf{b}(v)$ for some nonrandom $p \times 1$ vector \mathbf{c} with $\|\mathbf{c}\|_2 = 1$.

(i) $\|\mathbf{b}_c\|_2 = 1$.

(ii) $s_{c,\hat{G}_k} = O_p(1)$, with

$s_{c,\hat{G}_k}^2 = M(N_k T)^{-1} \mathbf{b}'_c \left(M N_k^{-1} \hat{\mathbf{Q}}_{G_k^0, \tilde{z}\tilde{z}} \right)^{-1} \sum_{i \in G_k^0} \left(\tilde{\mathbf{Z}}'_i E(\boldsymbol{\epsilon}_i \boldsymbol{\epsilon}'_i) \tilde{\mathbf{Z}}_i \right) \left(M N_k^{-1} \hat{\mathbf{Q}}_{G_k^0, \tilde{z}\tilde{z}} \right)^{-1} \mathbf{b}_c$, and the individual terms as defined in the proof of Theorem 3.5.

Lemma B.7. Suppose that Assumptions 1-4 hold. Let $\bar{\mathbb{G}}_K = \{\bar{\mathcal{G}}_K = \{\bar{\mathcal{G}}_k\}_{k=1}^K : \nexists i, j \in \bar{\mathcal{G}}_K \text{ where } i \in G_l^0, j \notin G_l^0, 1 \leq l \leq K_0\}$ with $K_0 < K \leq K_{\max} \leq N$.⁹ Then, $\max_{K_0 < K \leq K_{\max}} \sup_{\bar{\mathcal{G}}_K \in \bar{\mathbb{G}}_K} |\hat{\sigma}_{\bar{\mathcal{G}}_K}^2 - \hat{\sigma}_{\mathcal{G}^0}^2| = O_p(T^{-1}M)$. The MSE $\sigma_{\bar{\mathcal{G}}_K}^2$ is defined as in Theorem 3.6.

B.2 Proofs of Theorems, Corollaries, and Lemmas

Proof of Theorem 3.1. Define $\mathbf{a}_i = \boldsymbol{\pi}_i - \boldsymbol{\pi}_i^0$. Recall the unit-specific criterion function $\mathcal{F}_{NT,i}^*(\boldsymbol{\pi}_i) = T^{-1} \sum_{t=1}^T [\tilde{y}_{it} - \boldsymbol{\pi}_i' \tilde{\mathbf{z}}_{it}]^2$ and $\mathcal{F}_{NT,i}(\boldsymbol{\pi}_i, \lambda) = \mathcal{F}_{NT,i}^*(\boldsymbol{\pi}_i) + \lambda N^{-1} \sum_{j=1, j \neq i}^N \dot{\omega}_{ij} \|\boldsymbol{\pi}_i - \boldsymbol{\pi}_j\|_2$ following (2.6).

Part (i): Recognize that

$$\begin{aligned} \mathcal{F}_{NT,i}^*(\boldsymbol{\pi}_i) - \mathcal{F}_{NT,i}^*(\boldsymbol{\pi}_i^0) &= \frac{1}{T} \sum_{t=1}^T [\tilde{y}_{it} - \boldsymbol{\pi}_i' \tilde{\mathbf{z}}_{it}]^2 - \frac{1}{T} \sum_{t=1}^T [\tilde{y}_{it} - \boldsymbol{\pi}_i^0' \tilde{\mathbf{z}}_{it}]^2 \\ &= \frac{1}{T} \sum_{t=1}^T [\tilde{y}_{it} - (\mathbf{a}_i + \boldsymbol{\pi}_i^0)' \tilde{\mathbf{z}}_{it}]^2 - \frac{1}{T} \sum_{t=1}^T \tilde{u}_{it}^2 = \frac{1}{T} \sum_{t=1}^T [\tilde{u}_{it} - \mathbf{a}_i' \tilde{\mathbf{z}}_{it}]^2 - \frac{1}{T} \sum_{t=1}^T \tilde{u}_{it}^2 \\ &= \frac{1}{T} \sum_{t=1}^T \tilde{u}_{it}^2 - \frac{1}{T} \sum_{t=1}^T [2\tilde{u}_{it} \mathbf{a}_i' \tilde{\mathbf{z}}_{it}] + \frac{1}{T} \sum_{t=1}^T [\mathbf{a}_i' \tilde{\mathbf{z}}_{it}]^2 - \frac{1}{T} \sum_{t=1}^T \tilde{u}_{it}^2 \\ &= -2\mathbf{a}_i' \frac{1}{T} \sum_{t=1}^T (\tilde{\mathbf{z}}_{it} \tilde{u}_{it}) + \mathbf{a}_i' \frac{1}{T} \sum_{t=1}^T (\tilde{\mathbf{z}}_{it} \tilde{\mathbf{z}}_{it}') \mathbf{a}_i \\ &= -2\mathbf{a}_i' \hat{\mathbf{q}}_{i, \tilde{z}\tilde{u}} + \mathbf{a}_i' \hat{\mathbf{Q}}_{i, \tilde{z}\tilde{z}} \mathbf{a}_i. \end{aligned} \tag{B.1}$$

Notice that $\mathcal{F}_{NT,i}(\hat{\boldsymbol{\pi}}_i, \lambda) \leq \mathcal{F}_{NT,i}(\boldsymbol{\pi}_i^0, \lambda)$ holds trivially since $\hat{\boldsymbol{\pi}}_i$ estimates $\boldsymbol{\pi}_i^0$ by minimizing $\mathcal{F}_{NT,i}(\boldsymbol{\pi}_i, \lambda)$.

Using the above decomposition (B.1),

$$\begin{aligned} 0 &\geq \mathcal{F}_{NT,i}(\hat{\boldsymbol{\pi}}_i, \lambda) - \mathcal{F}_{NT,i}(\boldsymbol{\pi}_i^0, \lambda) \\ &= -2\hat{\mathbf{a}}_i' \hat{\mathbf{q}}_{i, \tilde{z}\tilde{u}} + \hat{\mathbf{a}}_i' \hat{\mathbf{Q}}_{i, \tilde{z}\tilde{z}} \hat{\mathbf{a}}_i + \frac{\lambda}{N} \sum_{j=1, j \neq i}^N \dot{\omega}_{ij} (\|\hat{\boldsymbol{\pi}}_i - \hat{\boldsymbol{\pi}}_j\|_2 - \|\boldsymbol{\pi}_i^0 - \boldsymbol{\pi}_j^0\|_2). \end{aligned} \tag{B.2}$$

Let $i \in G_k^0$. Focusing on the penalty term in (B.2),

$$\begin{aligned} &\frac{\lambda}{N} \sum_{j=1, j \neq i}^N \dot{\omega}_{ij} (\|\hat{\boldsymbol{\pi}}_i - \hat{\boldsymbol{\pi}}_j\|_2 - \|\boldsymbol{\pi}_i^0 - \boldsymbol{\pi}_j^0\|_2) \\ &\geq \frac{\lambda}{N} \sum_{j=1, j \neq i}^N \dot{\omega}_{ij} \|\hat{\boldsymbol{\pi}}_i - \hat{\boldsymbol{\pi}}_j - \boldsymbol{\pi}_i^0 + \boldsymbol{\pi}_j^0\|_2 \\ &\geq \frac{\lambda}{N} \sum_{j \notin G_k^0} \dot{\omega}_{ij} \|\hat{\mathbf{a}}_i - \hat{\mathbf{a}}_j\|_2. \end{aligned}$$

⁹ $\bar{\mathbb{G}}_K$ denotes the set of all $K > K_0$ partitions over N such that there exists excess groups, where no two heterogeneous individuals are pooled together. Subsequently, \mathcal{G}^0 can be retrieved just by merging certain groups of each $\bar{\mathcal{G}}_K \in \bar{\mathbb{G}}_K$.

The first inequality holds due to the triangle inequality and the second inequality since all other individuals of group k are discarded. Multiplying with -1 and employing the triangle inequality again gives

$$\frac{\lambda}{N} \sum_{j \notin G_k^0} \dot{\omega}_{ij} \|\hat{\mathbf{a}}_i - \hat{\mathbf{a}}_j\|_2 \geq -\frac{\lambda}{N} \sum_{j \notin G_k^0} \dot{\omega}_{ij} \|\hat{\mathbf{a}}_i + \hat{\mathbf{a}}_j\|_2 \geq -\frac{\lambda}{N} \sum_{j \notin G_k^0} \dot{\omega}_{ij} (\|\hat{\mathbf{a}}_i\|_2 + \|\hat{\mathbf{a}}_j\|_2). \quad (\text{B.3})$$

Plugging (B.3) back into (B.2) and averaging across all individuals results in

$$\begin{aligned} 0 &\geq \frac{1}{N} \sum_{i=1}^N \left[-2\hat{\mathbf{a}}_i' \hat{\mathbf{q}}_{i,\tilde{z}\tilde{u}} \right] + \frac{1}{N} \sum_{i=1}^N \left[\hat{\mathbf{a}}_i' \hat{\mathbf{Q}}_{i,\tilde{z}\tilde{z}} \hat{\mathbf{a}}_i \right] \\ &\quad - \frac{\lambda}{N^2} \sum_{k=1}^{K_0} \sum_{i \in G_k^0} \sum_{j \notin G_k^0} [\dot{\omega}_{ij} (\|\hat{\mathbf{a}}_i\|_2 + \|\hat{\mathbf{a}}_j\|_2)] \\ &\geq \frac{1}{N} \sum_{i=1}^N \left[-2\hat{\mathbf{a}}_i' \hat{\mathbf{q}}_{i,\tilde{z}\tilde{u}} \right] + \frac{1}{N} \sum_{i=1}^N \left[\hat{\mathbf{a}}_i' \hat{\mathbf{Q}}_{i,\tilde{z}\tilde{z}} \hat{\mathbf{a}}_i \right] \\ &\quad - \frac{\lambda}{N^2} \left(\max_{i \in G_k^0, j \notin G_k^0} \dot{\omega}_{ij} \right) \sum_{k=1}^{K_0} \sum_{i \in G_k^0} \sum_{j \notin G_k^0} [\|\hat{\mathbf{a}}_i\|_2 + \|\hat{\mathbf{a}}_j\|_2] \\ &\geq \frac{1}{N} \sum_{i=1}^N \left[-2\hat{\mathbf{a}}_i' \hat{\mathbf{q}}_{i,\tilde{z}\tilde{u}} \right] + \frac{1}{N} \sum_{i=1}^N \left[\hat{\mathbf{a}}_i' \hat{\mathbf{Q}}_{i,\tilde{z}\tilde{z}} \hat{\mathbf{a}}_i \right] - \frac{2\lambda}{N} \left(\max_{i \in G_k^0, j \notin G_k^0} \dot{\omega}_{ij} \right) \sum_{i=1}^N \\ &\quad \|\hat{\mathbf{a}}_i\|_2. \end{aligned} \quad (\text{B.4})$$

The second inequality in (B.4) holds by taking the maximum adaptive penalty. In the following, we show the derivation of the third inequality in (B.4) explicitly. Focusing on the third term of the second inequality in (B.4),

$$\begin{aligned} &\frac{\lambda}{N^2} \left(\max_{i \in G_k^0, j \notin G_k^0} \dot{\omega}_{ij} \right) \sum_{k=1}^{K_0} \sum_{i \in G_k^0} \sum_{j \notin G_k^0} (\|\hat{\mathbf{a}}_i\|_2 + \|\hat{\mathbf{a}}_j\|_2) \\ &= \frac{\lambda}{N^2} \left(\max_{i \in G_k^0, j \notin G_k^0} \dot{\omega}_{ij} \right) \left[\sum_{k=1}^{K_0} \sum_{i \in G_k^0} \sum_{j \notin G_k^0} (\|\hat{\mathbf{a}}_i\|_2) + \sum_{k=1}^{K_0} \sum_{i \in G_k^0} \sum_{j \notin G_k^0} (\|\hat{\mathbf{a}}_j\|_2) \right] \\ &\leq \frac{\lambda}{N^2} \left(\max_{i \in G_k^0, j \notin G_k^0} \dot{\omega}_{ij} \right) \left[\sum_{i=1}^N (\|\hat{\mathbf{a}}_i\|_2 (N-1)) + \sum_{j=1}^N (\|\hat{\mathbf{a}}_j\|_2 (N-1)) \right] \\ &= \frac{\lambda}{N^2} \left(\max_{i \in G_k^0, j \notin G_k^0} \dot{\omega}_{ij} \right) 2(N-1) \sum_{i=1}^N \|\hat{\mathbf{a}}_i\|_2 \\ &\leq \frac{2\lambda}{N} \left(\max_{i \in G_k^0, j \notin G_k^0} \dot{\omega}_{ij} \right) \sum_{i=1}^N \|\hat{\mathbf{a}}_i\|_2, \end{aligned}$$

where one is the smallest possible group cardinality, which gives a maximum of $N-1$ summands

in the third sum of $\sum_{k=1}^{K_0} \sum_{i \in G_k^0} \sum_{j \notin G_k^0}$.

Returning to (B.4),

$$\begin{aligned} 0 &\geq \frac{1}{N} \sum_{i=1}^N [-2\hat{\mathbf{a}}'_i \hat{\mathbf{q}}_{i,\tilde{z}\tilde{u}}] + \frac{1}{N} \sum_{i=1}^N [\hat{\mathbf{a}}'_i \hat{\mathbf{Q}}_{i,\tilde{z}\tilde{z}} \hat{\mathbf{a}}_i] - \frac{2\lambda}{N} \left(\max_{i \in G_k^0, j \notin G_k^0} \dot{\omega}_{ij} \right) \sum_{i=1}^N \|\hat{\mathbf{a}}_i\|_2 \\ &\geq \frac{1}{N} \sum_{i=1}^N \left[-2\|\hat{\mathbf{a}}_i\|_2 \|\hat{\mathbf{q}}_{i,\tilde{z}\tilde{u}}\|_2 + \|\hat{\mathbf{a}}_i\|_2^2 \frac{\underline{c}_{\tilde{z}\tilde{z}}}{M} - 2\lambda \left(\max_{i \in G_k^0, j \notin G_k^0} \dot{\omega}_{ij} \right) \|\hat{\mathbf{a}}_i\|_2 \right] \\ &= \frac{1}{N} \sum_{i=1}^N \left[\|\hat{\mathbf{a}}_i\|_2^2 - \|\hat{\mathbf{a}}_i\|_2 \frac{2M}{\underline{c}_{\tilde{z}\tilde{z}}} \left(\|\hat{\mathbf{q}}_{i,\tilde{z}\tilde{u}}\|_2 + \lambda \left(\max_{i \in G_k^0, j \notin G_k^0} \dot{\omega}_{ij} \right) \right) \right]. \end{aligned} \quad (\text{B.5})$$

The inequality in (B.5) holds due to the sub-multiplicative property regarding the first summand, and using Lemma B.2(i) to substitute $M\hat{\mathbf{Q}}_{i,\tilde{z}\tilde{z}}$ with $\underline{c}_{\tilde{z}\tilde{z}}$ in the second summand.

Recognize that $\max_{i \in G_k^0, j \notin G_k^0} \dot{\omega}_{ij} = O_p(J_{\min}^{-\kappa})$ as provided by Lemma B.5(ii), with $\lambda O_p(J_{\min}^{-\kappa}) = O_p(T^{-1/2} + M^{-\theta-1/2})$ by Assumption 2(iii). Furthermore, Lemma B.3(i) yields $\|\hat{\mathbf{q}}_{i,\tilde{z}\tilde{u}}\|_2 = O_p(T^{-1/2} + M^{-\theta-1/2})$. Plugging these rates into (B.5) we obtain

$$\begin{aligned} 0 &\geq \frac{1}{N} \sum_{i=1}^N \left[\|\hat{\mathbf{a}}_i\|_2^2 - \|\hat{\mathbf{a}}_i\|_2 \frac{4M}{\underline{c}_{\tilde{z}\tilde{z}}} O_p(T^{-1/2} + M^{-\theta-1/2}) \right] \\ &= \frac{1}{N} \sum_{i=1}^N \left[O_p(MT^{-1/2} + M^{-\theta+1/2})^{-2} \|\hat{\mathbf{a}}_i\|_2^2 - \frac{4}{\underline{c}_{\tilde{z}\tilde{z}}} \|\hat{\mathbf{a}}_i\|_2 O_p(MT^{-1/2} + M^{-\theta+1/2})^{-1} \right], \end{aligned} \quad (\text{B.6})$$

where the second equality is expanded with $(MT^{-1/2} + M^{-\theta+1/2})^{-2}$. For a sufficiently large $\|\hat{\mathbf{a}}_i\|_2$, $\|\hat{\mathbf{a}}_i\|_2 \ll \|\hat{\mathbf{a}}_i\|_2^2$, in which case $\mathcal{F}_{NT,i}(\hat{\boldsymbol{\pi}}_i, \lambda)$ dominates $\mathcal{F}_{NT,i}(\boldsymbol{\pi}_i^0, \lambda)$ and the inequality (B.6) cannot hold. Since $\mathcal{F}_{NT,i}(\boldsymbol{\pi}_i^0, \lambda)$ cannot be minimized and $\mathcal{F}_{NT,i}(\hat{\boldsymbol{\pi}}_i, \lambda) \leq \mathcal{F}_{NT,i}(\boldsymbol{\pi}_i^0, \lambda)$ must hold, $(MT^{-1/2} + M^{-\theta+1/2})^{-1} \|\hat{\mathbf{a}}_i\|_2$ is stochastically bounded and $\|\hat{\mathbf{a}}_i\|_2 = \|\hat{\boldsymbol{\pi}}_i - \boldsymbol{\pi}_i^0\|_2 = O_p(MT^{-1/2} + M^{-\theta+1/2})$. Assumption 2(i) ensures that $MT^{-1/2}$ is not explosive and $-\theta + 1/2 < 0$ holds by Assumption 1(vi). This concludes the proof of Theorem 3.1(i).

Part (ii): Expanding upon the intermediary result in (B.4) gives

$$\begin{aligned} 0 &\geq \mathcal{F}_{NT,i}(\hat{\boldsymbol{\pi}}_i, \lambda) - \mathcal{F}_{NT,i}(\boldsymbol{\pi}_i^0, \lambda) \\ &\geq \frac{1}{N} \sum_{i=1}^N [-2\hat{\mathbf{a}}'_i \hat{\mathbf{q}}_{i,\tilde{z}\tilde{u}}] + \frac{1}{N} \sum_{i=1}^N [\hat{\mathbf{a}}'_i \hat{\mathbf{Q}}_{i,\tilde{z}\tilde{z}} \hat{\mathbf{a}}_i] - \frac{2\lambda}{N} \left(\max_{i \in G_k^0, j \notin G_k^0} \dot{\omega}_{ij} \right) \sum_{i=1}^N \|\hat{\mathbf{a}}_i\|_2 \\ &\geq -2 \left[\frac{1}{N} \sum_{i=1}^N \|\hat{\mathbf{a}}_i\|_2^2 \right]^{1/2} \left[\frac{1}{N} \sum_{i=1}^N \|\hat{\mathbf{q}}_{i,\tilde{z}\tilde{u}}\|_2^2 \right]^{1/2} + \frac{\underline{c}_{\tilde{z}\tilde{z}}}{M} \frac{1}{N} \sum_{i=1}^N \|\hat{\mathbf{a}}_i\|_2^2 - \frac{2}{\sqrt{N}} \lambda \left(\max_{i \in G_k^0, j \notin G_k^0} \dot{\omega}_{ij} \right) \left[\frac{1}{N} \sum_{i=1}^N \|\hat{\mathbf{a}}_i\|_2^2 \right]^{1/2}, \end{aligned}$$

where the last inequality holds because of (i) the Cauchy-Schwarz inequality in the first summand, (ii) by employing the lower bound $\underline{c}_{\tilde{z}\tilde{z}}$ of the minimum eigenvalue of the predictor variance-covariance matrix in the second summand according to Lemma B.2(i), and (iii) by the Cauchy-Schwarz inequality for vector spaces in the third summand.

Isolating $1/N \sum_{i=1}^N \|\hat{\mathbf{a}}_i\|_2^2$ and rearranging yields

$$\frac{M}{\underline{c}_{\tilde{z}\tilde{z}}} \left[2 \left[\frac{1}{N} \sum_{i=1}^N \|\hat{\mathbf{q}}_{i,\tilde{z}\tilde{u}}\|_2^2 \right]^{1/2} + \frac{2}{\sqrt{N}} \lambda \left(\max_{i \in G_k^0, j \notin G_k^0} \dot{\omega}_{ij} \right) \right] \left[\frac{1}{N} \sum_{i=1}^N \|\hat{\mathbf{a}}_i\|_2^2 \right]^{1/2} \geq \frac{1}{N} \sum_{i=1}^N \|\hat{\mathbf{a}}_i\|_2^2$$

Again, recognize that $\lambda(\max_{i \in G_k^0, j \notin G_k^0} \dot{\omega}_{ij}) = O_p(T^{-1/2} + M^{-\theta-1/2})$ by Lemma B.5(ii) and Assumption 2(iii). Furthermore, $N^{-1} \sum_{i=1}^N \|\hat{\mathbf{q}}_{i,\tilde{z}\tilde{u}}\|_2^2 = O_p(T^{-1} + M^{-2\theta-1})$ by Lemma B.3(ii). Putting these pieces together and collecting terms,

$$\begin{aligned} \frac{2M}{\underline{c}_{\tilde{z}\tilde{z}}} \left[\left[O_p(T^{-1} + M^{-2\theta-1}) \right]^{1/2} + \frac{1}{\sqrt{N}} O_p(T^{-1/2} + M^{-\theta-1/2}) \right] \left[\frac{1}{N} \sum_{i=1}^N \|\hat{\mathbf{a}}_i\|_2^2 \right]^{1/2} &\geq \frac{1}{N} \sum_{i=1}^N \|\hat{\mathbf{a}}_i\|_2^2 \\ \frac{2}{\underline{c}_{\tilde{z}\tilde{z}}} \left[O_p(M^2 T^{-1} + M^{-2\theta+1}) \frac{1}{N} \sum_{i=1}^N \|\hat{\mathbf{a}}_i\|_2^2 \right]^{1/2} &\geq \frac{1}{N} \sum_{i=1}^N \|\hat{\mathbf{a}}_i\|_2^2, \end{aligned}$$

where by the same argument as in the proof of Theorem 3.1(i), $N^{-1} \sum_{i=1}^N \|\hat{\mathbf{a}}_i\|_2^2 = N^{-1} \sum_{i=1}^N \|\hat{\boldsymbol{\pi}}_i - \boldsymbol{\pi}_i^0\|_2^2 = O_p(M^2 T^{-1} + M^{-2\theta+1})$ holds to warrant $\mathcal{F}_{NT,i}(\hat{\boldsymbol{\pi}}_i, \lambda) \leq \mathcal{F}_{NT,i}(\boldsymbol{\pi}_i^0, \lambda)$. \square

Proof of Theorem 3.2. Following Su et al. (2019, Corollary 4.1), recall that $\hat{\boldsymbol{\beta}}_i(v) = \hat{\boldsymbol{\Pi}}_i' \mathbf{b}(v) = (\hat{\boldsymbol{\Pi}}_i - \boldsymbol{\Pi}_i^0)' \mathbf{b}(v) + \boldsymbol{\Pi}_i^0' \mathbf{b}(v)$. Using this decomposition,

$$\begin{aligned} \|\hat{\boldsymbol{\beta}}_i(v) - \boldsymbol{\beta}_i^0(v)\|_2 &= \|(\hat{\boldsymbol{\Pi}}_i - \boldsymbol{\Pi}_i^0)' \mathbf{b}(v) + \boldsymbol{\Pi}_i^0' \mathbf{b}(v) - \boldsymbol{\beta}_i^0(v)\|_2 \\ &\leq \|(\hat{\boldsymbol{\Pi}}_i - \boldsymbol{\Pi}_i^0)' \mathbf{b}(v)\|_2 + \|\boldsymbol{\Pi}_i^0' \mathbf{b}(v) - \boldsymbol{\beta}_i^0(v)\|_2 = \|\mathbf{d}_{1i}\|_2 + \|\mathbf{d}_{2i}\|_2, \end{aligned} \tag{B.7}$$

where the inequality holds because of the triangle property.

Part (i): Focusing on the first summand in (B.7) and taking the supremum over the unit interval results in

$$\sup_{v \in [0,1]} \|\mathbf{d}_{1i}\|_2 = \sup_{v \in [0,1]} \|(\hat{\boldsymbol{\Pi}}_i - \boldsymbol{\Pi}_i^0)' \mathbf{b}(v)\|_2 \leq \|\hat{\boldsymbol{\Pi}}_i - \boldsymbol{\Pi}_i^0\|_F \sup_{v \in [0,1]} \|\mathbf{b}(v)\|_2 \leq \|\hat{\boldsymbol{\Pi}}_i - \boldsymbol{\Pi}_i^0\|_F,$$

where the first inequality holds because of the Cauchy-Schwarz inequality and the second inequality since $\|\mathbf{b}(v)\|_2 \leq 1$ as shown in Lemma B.1(i). Moreover, $\|\hat{\boldsymbol{\Pi}}_i - \boldsymbol{\Pi}_i^0\|_F = \|\hat{\boldsymbol{\pi}}_i - \boldsymbol{\pi}_i^0\|_2 = O_p(MT^{-1/2} + M^{-\theta+1/2})$ by Theorem 3.1(i) and $\sup_{v \in [0,1]} \|\mathbf{d}_{2i}\|_2 = \sup_{v \in [0,1]} \|\boldsymbol{\Pi}_i^0' \mathbf{b}(v) - \boldsymbol{\beta}_i^0(v)\|_2 = O(M^{-\theta})$ ac-

cording to Lemma B.1(iv). As a consequence, $\sup_{v \in [0,1]} \left\| \hat{\beta}_i(v) - \beta_i^0(v) \right\|_2 = O_p(MT^{-1/2} + M^{-\theta+1/2}) + O(M^{-\theta}) = O_p(MT^{-1/2} + M^{-\theta+1/2})$.

Part (ii): We employ the same decomposition as in (B.7), $\int_0^1 \|\hat{\beta}_i(v) - \beta_i^0(v)\|_2^2 dv = \int_0^1 \|\mathbf{d}_{1i} + \mathbf{d}_{2i}\|_2^2 dv$. By the parallelogram law $\int_0^1 \|\mathbf{d}_{1i} + \mathbf{d}_{2i}\|_2^2 dv \leq 2 \int_0^1 \|\mathbf{d}_{1i}\|_2^2 dv + 2 \int_0^1 \|\mathbf{d}_{2i}\|_2^2 dv$.

Again, analyzing both summands on their own,

$$\begin{aligned} \int_0^1 \|\mathbf{d}_{1i}\|_2^2 dv &= \int_0^1 \left\| (\hat{\Pi}_i - \Pi_i^0)' \mathbf{b}(v) \right\|_2^2 dv = \text{tr} \left[(\hat{\Pi}_i - \Pi_i^0)' \int_0^1 \mathbf{b}(v) \mathbf{b}(v)' dv (\hat{\Pi}_i - \Pi_i^0) \right] \\ &= O(M^{-1}) \left\| \hat{\Pi}_i - \Pi_i^0 \right\|_F^2 = O(M^{-1}) O_p(M^2 T^{-1} + M^{-2\theta+1}) = O_p(MT^{-1} + M^{-2\theta}), \end{aligned}$$

since $\int_0^1 \mathbf{b}(v) \mathbf{b}(v)' dv = O(M^{-1})$ by Lemma B.1(iii) and $\|\hat{\pi}_i - \pi_i^0\|_2 = O_p(MT^{-1/2} + M^{-\theta+1/2})$ by Theorem 3.1(i).

Following Lemma B.1(iv), $\int_0^1 \|\mathbf{d}_{2i}\|_2^2 dv \leq \int_0^1 \sup_{v \in [0,1]} \left\| \Pi_i^0' \mathbf{b}(v) - \beta_i^0(v) \right\|_2^2 dv = O(M^{-2\theta})$. Subsequently, $\int_0^1 \left\| \hat{\beta}_i(v) - \beta_i^0(v) \right\|_2^2 dv \leq O_p(MT^{-1} + M^{-2\theta}) + O(M^{-2\theta}) = O_p(MT^{-1} + M^{-2\theta})$. \square

Proof of Theorem 3.3. Following Mehrabani (2023, Theorem 3.2), define the $Mp \times 1$ vector $\mathbf{a}_{ij} = \boldsymbol{\pi}_i - \boldsymbol{\pi}_j = (a_{ij,1}, \dots, a_{ij,Mp})'$ and suppose there exists an $i \in G_k^0$ such that $\|a_{ij}\|_2 \neq 0$ for any $j \in G_k^0$. Let $|a_{ij,r}| = \max_{l=1, \dots, Mp} |a_{ij,l}|$ and reorder \mathbf{a}_{ij} such that $r = Mp$. As a consequence, each $|a_{ij,l}| \in [0, |a_{ij,Mp}|]$, $l = 1, \dots, Mp$. Hence $\|\mathbf{a}_{ij}\|_2 = \left[\sum_{l=1}^{Mp} a_{ij,l}^2 \right]^{1/2} \leq \left[Mp a_{ij,Mp}^2 \right]^{1/2} = (Mp)^{1/2} |a_{ij,Mp}|$ and $(Mp)^{-1/2} \leq |a_{ij,Mp}| / \|\mathbf{a}_{ij}\|_2 \leq 1$.

Recall the criterion function

$$\begin{aligned} \mathcal{F}_{NT,i}(\boldsymbol{\pi}_i, \lambda) &= \frac{1}{T} \sum_{t=1}^T (\tilde{y}_{it} - \boldsymbol{\pi}_i' \tilde{\mathbf{z}}_{it})^2 + \frac{\lambda}{N} \sum_{j=1, j \neq i}^N \dot{\omega}_{ij} \|\boldsymbol{\pi}_i - \boldsymbol{\pi}_j\|_2 \\ &= \frac{1}{T} \sum_{t=1}^T (\tilde{y}_{it}^2 - 2\tilde{y}_{it} \boldsymbol{\pi}_i' \tilde{\mathbf{z}}_{it} + \tilde{\mathbf{z}}_{it}' \boldsymbol{\pi}_i \boldsymbol{\pi}_i' \tilde{\mathbf{z}}_{it}) \\ &\quad + \frac{\lambda}{N} \sum_{j=1, j \neq i}^N \dot{\omega}_{ij} \left[\sum_{l=1}^{Mp} (\pi_{il}^2 - 2\pi_{il}\pi_{jl} + \pi_{jl}^2) \right]^{1/2}. \end{aligned} \tag{B.8}$$

Differentiating (B.8) with respect to the scalar $\pi_{i,Mp}$ yields the first order condition (FOC)

$$\begin{aligned}
\frac{\partial \mathcal{F}_{NT,i}}{\partial \pi_{i,Mp}} &\stackrel{!}{=} 0 \\
&= -\frac{2}{T} \sum_{t=1}^T \tilde{y}_{it} \tilde{z}_{it,Mp} + \frac{2}{T} \sum_{t=1}^T \hat{\pi}'_i \tilde{z}_{it} \tilde{z}_{it,Mp} \\
&\quad + \frac{\lambda}{N} \sum_{j=1, j \neq i}^N \dot{\omega}_{ij} \left\{ \frac{1}{2} \left[\sum_{l=1}^{Mp} (\hat{\pi}_{il}^2 - 2\hat{\pi}_{il}\hat{\pi}_{jl} + \hat{\pi}_{jl}^2)^2 \right]^{-1/2} (2\hat{\pi}_{i,Mp} - 2\hat{\pi}_{j,Mp}) \right\} \quad (\text{B.9}) \\
&= -\frac{2}{T} \sum_{t=1}^T \tilde{z}_{it,Mp} (\tilde{y}_{it} - \hat{\pi}'_i \tilde{z}_{it}) + \frac{\lambda}{N} \sum_{j=1, j \neq i}^N \dot{\omega}_{ij} \frac{\hat{\pi}_{i,Mp} - \hat{\pi}_{j,Mp}}{\|\pi_i - \pi_j\|_2}.
\end{aligned}$$

Now, (i) expand (B.9) with $(T^{-1/2} + M^{-\theta-1/2})^{-1}$, (ii) recognize $\hat{\pi}_i = \pi_i^0 + (\hat{\pi}_i - \pi_i^0)$, (iii) rewrite the penalty term to discriminate between $j \in G_k^0$ and $j \notin G_k^0$, and (iv) define $e_{ij,Mp} = (\hat{\pi}_{i,Mp} - \hat{\pi}_{j,Mp})/\|\hat{\pi}_i - \hat{\pi}_j\|_2$. This results in

$$\begin{aligned}
0 &= -2(T^{-1/2} + M^{-\theta-1/2})^{-1} \frac{1}{T} \sum_{t=1}^T \tilde{z}_{it,Mp} (\tilde{y}_{it} - \pi_i^0 \tilde{z}_{it} - (\hat{\pi}_i - \pi_i^0)' \tilde{z}_{it}) \\
&\quad + (T^{-1/2} + M^{-\theta-1/2})^{-1} \frac{\lambda}{N} \sum_{j \in G_k^0, j \neq i} \dot{\omega}_{ij} e_{ij,Mp} + (T^{-1/2} + M^{-\theta-1/2})^{-1} \frac{\lambda}{N} \sum_{j \notin G_k^0, j \neq i} \dot{\omega}_{ij} e_{ij,Mp} \\
&= -2(T^{-1/2} + M^{-\theta-1/2})^{-1} \frac{1}{T} \sum_{t=1}^T \tilde{z}_{it,Mp} \tilde{u}_{it} + 2(T^{-1/2} + M^{-\theta-1/2})^{-1} \frac{1}{T} \sum_{t=1}^T \tilde{z}_{it,Mp} (\hat{\pi}_i - \pi_i^0)' \tilde{z}_{it} \\
&\quad + (T^{-1/2} + M^{-\theta-1/2})^{-1} \frac{\lambda}{N} \sum_{j \in G_k^0, j \neq i} \dot{\omega}_{ij} e_{ij,Mp} + (T^{-1/2} + M^{-\theta-1/2})^{-1} \frac{\lambda}{N} \sum_{j \notin G_k^0} \dot{\omega}_{ij} e_{ij,Mp}, \quad (\text{B.10})
\end{aligned}$$

(B.10) is made up of four terms, say $0 = d_{1i} + d_{2i} + d_{3i} + d_{4i}$. Studying each summand in isolation,

- $d_{1i} = -2(T^{-1/2} + M^{-\theta-1/2})^{-1} T^{-1} \sum_{t=1}^T \tilde{z}_{it,Mp} \tilde{u}_{it}$. Note that $\|\hat{\mathbf{q}}_{i,\tilde{z}\tilde{u}}\|_2 = O_p(T^{-1/2} + M^{-\theta-1/2})$ by Lemma B.2(i). Therefore, it is straightforward to see that d_{1i} is $O_p(1)$.
- $d_{2i} = 2(T^{-1/2} + M^{-\theta-1/2})^{-1} T^{-1} \sum_{t=1}^T \tilde{z}_{it,Mp} (\hat{\pi}_i - \pi_i^0)' \tilde{z}_{it}$. Since $\|\hat{\mathbf{q}}_{i,\tilde{z}_{Mp}\tilde{z}}(\hat{\pi}_i - \pi_i^0)\|_2 \leq \|\hat{\mathbf{q}}_{i,\tilde{z}_{Mp}\tilde{z}}\|_2 \|\hat{\pi}_i - \pi_i^0\|_2 = O_p(M^{-1}) O_p(MT^{-1/2} + M^{-\theta+1/2}) = O_p(T^{-1/2} + M^{-\theta-1/2})$ by Lemma B.3(i) and Theorem 3.1(i), where $T^{-1} \sum_{t=1}^T \tilde{z}_{it,Mp} \tilde{z}'_{it} = \hat{\mathbf{q}}_{i,\tilde{z}_{Mp}\tilde{z}}$, the rate of d_{2i} follows as $O_p(1)$.
- $d_{3i} = (T^{-1/2} + M^{-\theta-1/2})^{-1} \lambda N^{-1} \sum_{j \in G_k^0, j \neq i} \dot{\omega}_{ij} e_{ij,Mp}$. The lower bound $(Mp)^{-1/2} \leq |e_{ij,Mp}|$ gives the inequality $|d_{3i}| \geq (T^{-1/2} + M^{-\theta-1/2})^{-1} \lambda N^{-1} (Mp)^{-1/2} \sum_{j \in G_k^0, j \neq i} \dot{\omega}_{ij}$. Moreover, recall that Lemma B.5(i) states $\min_{i,j \in G_k^0} \dot{\omega}_{ij} = O_p((MT^{-1/2} + M^{-\theta+1/2})^{-\kappa})$ and that $\sum_{j \in G_k^0, j \neq i}$ sums over $N_k - 1$ elements. As a consequence, $\sum_{j \in G_k^0, j \neq i} \dot{\omega}_{ij} \geq (N_k - 1) \min_{i,j \in G_k^0} \dot{\omega}_{ij} =$

$(N_k - 1)O_p((MT^{-1/2} + M^{-\theta+1/2})^{-\kappa})$. Combining all these elements yields $p^{1/2}|d_{3i}| \geq (T^{-1/2} + M^{-\theta-1/2})^{-1}\lambda N^{-1}M^{-1/2}(N_k - 1)O_p((MT^{-1/2} + M^{-\theta+1/2})^{-\kappa})$. Note that by Assumption 1(v), $(N_k - 1)N^{-1} = \tau_k - 1/N \geq 0$, where $\tau_k = N_k/N$. Rearranging and using the bound on τ_k yields $p^{1/2}|d_{3i}| \geq O_p((MT^{-1/2} + M^{-\theta+1/2})^{-\kappa-1}M^{1/2}\lambda\tau_k)$, which, under Assumption 2(iv), diverges to infinity in the limit.

- $d_{4i} = (T^{-1/2} + M^{-\theta-1/2})^{-1}\lambda N^{-1} \sum_{j \notin G_k^0} \dot{\omega}_{ij} e_{ij, Mp}$. Recall that by Lemma B.5(ii), $\max_{i \in G_k^0} \dot{\omega}_{ij} = O_p(J_{\min}^{-\kappa})$. Furthermore, as shown above, $1 \geq |a_{ij, Mp}|/\|\mathbf{a}_{ij}\|_2 = |e_{ij, p}|$ and subsequently $\sum_{j \notin G_k^0} |e_{ij, Mp}| \leq N - N_k$ since $\sum_{j \notin G_k^0}$ sums over $N - N_k$ elements. Lastly, $|d_{4i}| \leq (T^{-1/2} + M^{-\theta-1/2})^{-1}\lambda O_p(J_{\min}^{-\kappa})N^{-1}(N - N_k) = O_p(1)$ by Assumptions 1(iv) and 2(iii).

Since $|d_{3i}| \gg |d_{1i} + d_{2i} + d_{3i}|$ cannot hold for large (N, T) , $\|\hat{\pi}_i - \pi_i^0\|_2$ must not be differentiable w.p.a.1 for all $i, j \in G_k^0$ for $k = 1, \dots, K_0$ and $(T^{-1/2} + M^{-\theta-1/2})^{-1}\lambda \dot{\omega}_{ij} e_{ij} = O_p(1)$ in (B.10). This translates to $\Pr(\|\hat{\pi}_i - \hat{\pi}_j\|_2 = 0) \rightarrow 1 \forall i, j \in G_k^0$ as $(N, T) \rightarrow \infty$. \square

Proof of Theorem 3.4.

Part (i): Theorem 3.3 gives $\Pr(\|\hat{\pi}_i - \pi_i^0\|_2 = 0) \rightarrow 1 \forall i, j \in G_k^0$ as $(N, T) \rightarrow \infty$. As a consequence, it also holds that $\lim_{(N, T) \rightarrow \infty} \Pr(\hat{K} = K_0) = 1$ since \hat{K} is the number of unique subvectors of $\hat{\pi} = (\hat{\pi}_1', \dots, \hat{\pi}_N')'$.

Part (ii): Suppose there exist two heterogeneous units $i \in G_k^0, j \notin G_k^0$ that nonetheless exhibit $\|\hat{\pi}_i - \hat{\pi}_j\|_2 = 0$. Expanding $\hat{\pi}_i - \hat{\pi}_j$ by $\pm \pi_i^0$ and recognizing $\|\hat{\pi}_i - \pi_i^0\|_2 = O_p(MT^{-1/2} + M^{-\theta+1/2})$ following Theorem 3.1(i), we obtain

$$0 = \hat{\pi}_i - \hat{\pi}_j = (\pi_i^0 + (\hat{\pi}_i - \pi_i^0)) - (\pi_j^0 + (\hat{\pi}_j - \pi_j^0)) = \pi_i^0 - \pi_j^0 + O_p(MT^{-1/2} + M^{-\theta+1/2}). \quad (\text{B.11})$$

(B.11) makes it easy to see that if $\|\hat{\pi}_i - \hat{\pi}_j\|_2 = 0$, then $\|\pi_i^0 - \pi_j^0\|_2 = O_p(MT^{-1/2} + M^{-\theta+1/2})$. Recall that $\|\pi_i^0 - \pi_j^0\|_2 \geq J_{\min}$ by construction. However, Assumption 2(ii) states that $(MT^{-1/2} + M^{-\theta+1/2})^{-1}J_{\min} \rightarrow \infty$, in which case (B.11) cannot hold. In consequence, $\|\hat{\pi}_i - \hat{\pi}_j\|_2 \neq 0$ for all $i \in G_k^0, j \notin G_k^0$ and $\lim_{(N, T) \rightarrow \infty} \Pr(\hat{\mathcal{G}}_{K_0} = \mathcal{G}_{K_0}^0) = 1$. \square

Proof of Theorem 3.5.

Part (i): Note the decomposition $\|\hat{\alpha}_k(v) - \hat{\alpha}_{\hat{G}_k}^p(v)\|_2 = \left\| (\hat{\Xi}_k - \hat{\Xi}_{\hat{G}_k}^p)' \mathbf{b}(v) \right\|_2 \leq \left\| \hat{\Xi}_k - \hat{\Xi}_{\hat{G}_k}^p \right\|_F \|\mathbf{b}(v)\|_2$. Since $\|\mathbf{b}(v)\|_2 = 1$ by Lemma B.1(i), it suffices to show that $(N_k T)^{1/2} M^{-1/2} \left\| \hat{\Xi}_k - \hat{\Xi}_{\hat{G}_k}^p \right\|_F = o_p(1)$

in order to prove that the *PSE* and *post-Lasso* feature an identical limiting distribution.¹⁰

Recall the FOC from the proof of Theorem 3.3, (B.9)

$$\frac{\partial \mathcal{F}_{NT,i}}{\partial \boldsymbol{\pi}_i} = 0 = -\frac{2}{T} \sum_{t=1}^T \tilde{\mathbf{z}}_{it} (\tilde{y}_{it} - \hat{\boldsymbol{\pi}}_i' \tilde{\mathbf{z}}_{it}) + \frac{\lambda}{N} \sum_{j=1, j \neq i}^N \dot{\omega}_{ij} (\hat{\boldsymbol{\pi}}_i - \hat{\boldsymbol{\pi}}_j) \|\hat{\boldsymbol{\pi}}_i - \hat{\boldsymbol{\pi}}_j\|_2^{-1}.$$

Write $\hat{\boldsymbol{\pi}}_i = \hat{\boldsymbol{\xi}}_k$ for any $i \in \hat{G}_k$ and sum over all $i \in \hat{G}_k$ to obtain

$$\begin{aligned} 0 &= -\frac{2}{T} \sum_{i \in \hat{G}_k} \sum_{t=1}^T \tilde{\mathbf{z}}_{it} \left[\tilde{y}_{it} - \hat{\boldsymbol{\xi}}_k' \tilde{\mathbf{z}}_{it} \right] + \frac{\lambda}{N} \sum_{i \in \hat{G}_k} \sum_{j=1, j \neq i}^N \dot{\omega}_{ij} (\hat{\boldsymbol{\pi}}_i - \hat{\boldsymbol{\pi}}_j) \|\hat{\boldsymbol{\pi}}_i - \hat{\boldsymbol{\pi}}_j\|_2^{-1} \\ &= -\frac{2}{T} \sum_{i \in \hat{G}_k} \sum_{t=1}^T \left[\tilde{\mathbf{z}}_{it} \tilde{y}_{it} - \tilde{\mathbf{z}}_{it} \hat{\boldsymbol{\xi}}_k' \tilde{\mathbf{z}}_{it} \right] + \hat{\mathbf{r}}_{\hat{G}_k} \\ &= -2 \left[\hat{\mathbf{q}}_{\hat{G}_k, \tilde{z}\tilde{y}} - \hat{\mathbf{Q}}_{\hat{G}_k, \tilde{z}\tilde{z}} \hat{\boldsymbol{\xi}}_k \right] + \hat{\mathbf{r}}_{\hat{G}_k}, \end{aligned} \tag{B.12}$$

where $\hat{\mathbf{r}}_{\hat{G}_k} = \lambda N^{-1} \sum_{i \in \hat{G}_k} \sum_{j=1, j \neq i}^N \dot{\omega}_{ij} \hat{\mathbf{e}}_{ij}$, $\hat{\mathbf{e}}_{ij} = (\hat{\boldsymbol{\pi}}_i - \hat{\boldsymbol{\pi}}_j) \|\hat{\boldsymbol{\pi}}_i - \hat{\boldsymbol{\pi}}_j\|_2^{-1}$, $\hat{\mathbf{q}}_{\hat{G}_k, \tilde{z}\tilde{y}} = \sum_{i \in \hat{G}_k} T^{-1} \sum_{t=1}^T \tilde{\mathbf{z}}_{it} \tilde{y}_{it}$, and $\hat{\mathbf{Q}}_{\hat{G}_k, \tilde{z}\tilde{z}} = \sum_{i \in \hat{G}_k} T^{-1} \sum_{t=1}^T \tilde{\mathbf{z}}_{it} \tilde{\mathbf{z}}_{it}'$.

Solving (B.12) for $\hat{\boldsymbol{\xi}}_k$ gives

$$\hat{\boldsymbol{\xi}}_k = \hat{\mathbf{Q}}_{\hat{G}_k, \tilde{z}\tilde{z}}^{-1} \hat{\mathbf{q}}_{\hat{G}_k, \tilde{z}\tilde{y}} - 1/2 \hat{\mathbf{Q}}_{\hat{G}_k, \tilde{z}\tilde{z}}^{-1} \hat{\mathbf{r}}_{\hat{G}_k} = \hat{\boldsymbol{\xi}}_{\hat{G}_k}^p - 1/2 \hat{\mathbf{Q}}_{\hat{G}_k, \tilde{z}\tilde{z}}^{-1} \hat{\mathbf{r}}_{\hat{G}_k}.$$

It is straightforward to see that the *PSE* estimator $\hat{\boldsymbol{\xi}}_k$ and the *post-Lasso* $\hat{\boldsymbol{\xi}}_{\hat{G}_k}^p$ are asymptotically equivalent if $\hat{\mathbf{Q}}_{\hat{G}_k, \tilde{z}\tilde{z}}^{-1} \hat{\mathbf{r}}_{\hat{G}_k} = o_p(1)$. We employ Theorem 3.4 and make use of the oracle property to demonstrate this result. Subsequently, one can infer the limiting behavior of $\hat{\mathbf{Q}}_{\hat{G}_k, \tilde{z}\tilde{z}}^{-1} \hat{\mathbf{r}}_{\hat{G}_k}$ by studying $\hat{\mathbf{Q}}_{G_k^0, \tilde{z}\tilde{z}}^{-1} \hat{\mathbf{r}}_{G_k^0}$. Scaling by $\sqrt{N_k T / M}$ and taking the squared L_2 norm yields

$$\begin{aligned} \left\| \sqrt{\frac{N_k T}{M}} \hat{\mathbf{Q}}_{G_k^0, \tilde{z}\tilde{z}}^{-1} \hat{\mathbf{r}}_{G_k^0} \right\|_2^2 &= \left\| \left(\frac{M}{N_k} \hat{\mathbf{Q}}_{G_k^0, \tilde{z}\tilde{z}} \right)^{-1} \sqrt{\frac{TM}{N_k}} \hat{\mathbf{r}}_{G_k^0} \right\|_2^2 \\ &\leq \left[\mu_{\min} \left(\frac{M}{N_k} \hat{\mathbf{Q}}_{G_k^0, \tilde{z}\tilde{z}} \right) \right]^{-2} \left\| \sqrt{\frac{TM}{N_k}} \hat{\mathbf{r}}_{G_k^0} \right\|_2^2, \end{aligned} \tag{B.13}$$

¹⁰The $\sqrt{N_k T / M}$ scaling is required for the *post-Lasso* estimator to converge in distribution. See the proof of Theorem 3.5(ii).

where $c_{\tilde{z}\tilde{z}} \leq \mu_{\min} \left(MN_k^{-1} \hat{\mathcal{Q}}_{G_k^0, \tilde{z}\tilde{z}} \right)$ by Lemma B.2(ii). Focusing on the norm in (B.13),

$$\begin{aligned}
\left\| \sqrt{\frac{TM}{N_k}} \hat{\mathbf{r}}_{G_k^0} \right\|_2^2 &= \frac{TM}{N_k} \frac{\lambda^2}{N^2} \left\| \sum_{i \in G_k^0} \sum_{j \notin G_k^0} \dot{\omega}_{ij} \hat{\mathbf{e}}_{ij} \right\|_2^2 \\
&\leq \frac{TM}{N_k} \frac{\lambda^2}{N^2} \left(\sum_{i \in G_k^0} \sum_{j \notin G_k^0} |\dot{\omega}_{ij}| \|\hat{\mathbf{e}}_{ij}\|_2 \right)^2 \\
&\leq \frac{TM}{N_k} \frac{\lambda^2}{N^2} \left(\max_{i \in G_k^0, j \notin G_k^0} |\dot{\omega}_{ij}| \right)^2 \left(\sum_{i \in G_k^0} \sum_{j \notin G_k^0} \|\hat{\mathbf{e}}_{ij}\|_2 \right)^2 \\
&\leq TM \lambda^2 \left(\max_{i \in G_k^0, j \notin G_k^0} |\dot{\omega}_{ij}| \right)^2 \frac{N_k^2 (N - N_k)^2}{N^2 N_k} \\
&\leq TM \lambda^2 \left(\max_{i \in G_k^0, j \notin G_k^0} |\dot{\omega}_{ij}| \right)^2 N_k,
\end{aligned} \tag{B.14}$$

where the first inequality by the Cauchy-Schwarz inequality; the second inequality holds by taking the maximum adaptive weight; the third inequality holds by recognizing that $\|\hat{\mathbf{e}}_{ij}\|_2 \leq 1$ by the Triangle inequality; the fourth inequality holds by taking $N^{-2} N_k (N - N_k)^2 = N_k (1 - 2\tau_k + \tau_k^2) \leq N_k$ using Assumption 1(v), where $\tau_k = N_k/N$. Furthermore, note that $\max_{i \in G_k^0, j \in G_k^0} (|\dot{\omega}_{ij}|^2) = O_p(J_{\min}^{-2\kappa})$ by Lemma B.5(ii). Plugging these pieces into (B.14), it becomes apparent that

$$\left\| \sqrt{\frac{TM}{N_k}} \hat{\mathbf{r}}_{G_k^0} \right\|_2^2 \leq TM \lambda^2 O_p(J_{\min}^{-2\kappa}) N_k = O_p(\sqrt{N_k TM} \lambda J_{\min}^{-\kappa})^2.$$

Assumption 3 gives $O_p(\sqrt{N_k TM} \lambda J_{\min}^{-\kappa}) = o_p(1)$. In consequence, the whole term (B.13) becomes negligible in the limit and $\|\hat{\boldsymbol{\alpha}}_k(v) - \hat{\boldsymbol{\alpha}}_{\hat{G}_k}^p(v)\|_2 = o_p(1)$.

Part (ii): We make use of the decomposition

$$\begin{aligned}
\sqrt{\frac{N_k T}{M}} \left[\hat{\boldsymbol{\alpha}}_{\hat{G}_k}^p(v) - \boldsymbol{\alpha}_k^0(v) \right] &= \sqrt{\frac{N_k T}{M}} (\hat{\boldsymbol{\Xi}}_{\hat{G}_k}^p - \boldsymbol{\Xi}_k^0)' \mathbf{b}(v) + \sqrt{\frac{N_k T}{M}} (\boldsymbol{\Xi}_k^{0\prime} \mathbf{b}(v) - \boldsymbol{\alpha}_k^0(v)) \\
&= \mathbf{d}_{1, \hat{G}_k} + \mathbf{d}_{2, \hat{G}_k},
\end{aligned} \tag{B.15}$$

where $\boldsymbol{\alpha}_k^0(v) = \boldsymbol{\Xi}_k^{0\prime} \mathbf{b}(v) + (\boldsymbol{\alpha}_k^0(v) - \boldsymbol{\Xi}_k^{0\prime} \mathbf{b}(v))$.

It is easy to show that $\mathbf{d}_{2, \hat{G}_k} / s_{c, \hat{G}_k} = \sqrt{N_k T / M} O(M^{-\theta}) O_p(1) = o_p(1)$, since $\|\boldsymbol{\alpha}_k^0(v) - \boldsymbol{\Xi}_k^{0\prime} \mathbf{b}(v)\|_2 = O(M^{-\theta})$ by Lemma B.1(iv), $\sqrt{N_k T / M^{2\theta}} = o_p(1)$ according to Assumption 4(ii), and $s_{c, \hat{G}_k} = O_p(1)$

by Lemma B.6(ii).¹¹ As a result, the second summand is negligible for the remainder of the proof and it is sufficient to study \mathbf{d}_{1,\hat{G}_k} only.

Regarding \mathbf{d}_{1,\hat{G}_k} , consider $\mathbf{d}'_{1,\hat{G}_k} \mathbf{c}$ for some nonrandom $p \times 1$ vector \mathbf{c} with $\|\mathbf{c}\|_2 = 1$. Define $\mathbf{b}_c = \mathbf{c} \otimes \mathbf{b}(v)$. Recognize that $\text{vec}(\mathbf{b}'(v)(\hat{\Xi}_{\hat{G}_k}^p - \Xi_k^0)\mathbf{c}) = (\mathbf{c}' \otimes \mathbf{b}(v))\text{vec}(\hat{\Xi}_{\hat{G}_k}^p - \Xi_k^0)$ (see Bernstein, 2009, p. 249). In addition, let $\hat{\mathbf{q}}_{\hat{G}_k,\tilde{z}a} = \sum_{i \in \hat{G}_k} T^{-1} \sum_{t=1}^T \tilde{\mathbf{z}}_{it} a_{it}$ for $a = \{\tilde{y}, \tilde{u}, \tilde{\epsilon}\}$. Recall that the error term \tilde{u}_{it} can be decomposed into an idiosyncratic and a sieve component $\tilde{u}_{it} = \tilde{\varrho}_{it} + \tilde{\epsilon}_{it}$ where $\varrho_{it} = \boldsymbol{\eta}'_{it} \mathbf{x}_{it}$ (see, e.g., (2.5)). Then,

$$\begin{aligned}
\mathbf{d}'_{1,\hat{G}_k} \mathbf{c} &= \sqrt{\frac{N_k T}{M}} \mathbf{b}'(v)(\hat{\Xi}_{\hat{G}_k}^p - \Xi_k^0)\mathbf{c} = \sqrt{\frac{N_k T}{M}} \mathbf{b}'_c (\hat{\xi}_{\hat{G}_k}^p - \xi_k^0) = \sqrt{\frac{N_k T}{M}} \mathbf{b}'_c [\hat{\mathbf{Q}}_{\hat{G}_k,\tilde{z}\tilde{z}}^{-1} \hat{\mathbf{q}}_{\hat{G}_k,\tilde{z}\tilde{y}} - \xi_k^0] \\
&= \sqrt{\frac{N_k T}{M}} \mathbf{b}'_c \hat{\mathbf{Q}}_{\hat{G}_k,\tilde{z}\tilde{z}}^{-1} [\hat{\mathbf{q}}_{\hat{G}_k,\tilde{z}\tilde{y}} - \hat{\mathbf{Q}}_{\hat{G}_k,\tilde{z}\tilde{z}} \xi_k^0] \\
&= \sqrt{\frac{N_k T}{M}} \mathbf{b}'_c \hat{\mathbf{Q}}_{\hat{G}_k,\tilde{z}\tilde{z}}^{-1} \left[\hat{\mathbf{q}}_{\hat{G}_k,\tilde{z}\tilde{u}} + \sum_{i \in \hat{G}_k} \frac{1}{T} \sum_{t=1}^T \mathbf{z}_{it} \mathbf{z}'_{it} (\boldsymbol{\pi}_i^0 - \xi_k^0) \right] \\
&= \sqrt{\frac{N_k T}{M}} \mathbf{b}'_c \hat{\mathbf{Q}}_{\hat{G}_k,\tilde{z}\tilde{z}}^{-1} \hat{\mathbf{q}}_{\hat{G}_k,\tilde{z}\tilde{\epsilon}} + \sqrt{\frac{N_k T}{M}} \mathbf{b}'_c \hat{\mathbf{Q}}_{\hat{G}_k,\tilde{z}\tilde{z}}^{-1} \hat{\mathbf{q}}_{\hat{G}_k,\tilde{z}\tilde{\varrho}} \\
&\quad + \sqrt{\frac{N_k}{TM}} \mathbf{b}'_c \hat{\mathbf{Q}}_{\hat{G}_k,\tilde{z}\tilde{z}}^{-1} \sum_{i \in \hat{G}_k} \sum_{t=1}^T \mathbf{z}_{it} \mathbf{z}'_{it} (\boldsymbol{\pi}_i^0 - \xi_k^0).
\end{aligned} \tag{B.16}$$

Exploiting the oracle property by Theorem 3.4, we study \mathbf{d}_{1,\hat{G}_k} by analyzing \mathbf{d}_{1,G_k^0} . Subsequently,

$$\begin{aligned}
\mathbf{d}'_{1,G_k^0} \mathbf{c} &= \sqrt{\frac{N_k T}{M}} \mathbf{b}'_c \hat{\mathbf{Q}}_{G_k^0,\tilde{z}\tilde{z}}^{-1} \hat{\mathbf{q}}_{G_k^0,\tilde{z}\tilde{\epsilon}} + \sqrt{\frac{N_k T}{M}} \mathbf{b}'_c \hat{\mathbf{Q}}_{G_k^0,\tilde{z}\tilde{z}}^{-1} \hat{\mathbf{q}}_{\hat{G}_k,\tilde{z}\tilde{\varrho}} \\
&= d_{11,G_k^0} + d_{12,G_k^0},
\end{aligned} \tag{B.17}$$

where the last summand in (B.16) equals zero since $\boldsymbol{\pi}_i^0 = \xi_k^0$ for $i \in G_k^0$.

We show that d_{12,G_k^0} vanishes in the limit before studying the asymptotic behavior of d_{11,G_k^0} . But first, note two preliminary results that are used later.

$$\begin{aligned}
\frac{1}{N_k T} \sum_{i \in G_k^0} \sum_{t=1}^T \tilde{\varrho}_{it}^2 &= \frac{1}{N_k T} \sum_{i \in G_k^0} \sum_{t=1}^T \left(\left[\boldsymbol{\beta}_i^0 \left(\frac{t}{T} \right) - \boldsymbol{\Pi}_i^0 \mathbf{b} \left(\frac{t}{T} \right) \right]' \tilde{\mathbf{x}}_{it} \right)^2 \\
&\leq \left[\sup_{v \in [0,1]} \left\| \boldsymbol{\alpha}_k^0(v) - \boldsymbol{\Xi}_k^{0\prime} \mathbf{b}(v) \right\|_2 \right]^2 \frac{1}{N_k T} \sum_{i \in G_k^0} \sum_{t=1}^T \tilde{\mathbf{x}}_{it} \tilde{\mathbf{x}}'_{it} \\
&\leq O_p(M^{-\theta})^2 \bar{c}_{xx} (1 + o_p(1)) = O_p(M^{-2\theta}),
\end{aligned} \tag{B.18}$$

¹¹ s_{c,G_k^0} is a scaling factor that is introduced at a later stage.

where the rates are given by Lemma B.1(iv) and Assumption 1(iv). In addition,

$$\begin{aligned}
& \frac{M}{N_k T} \sum_{i \in G_k^0} \sum_{t=1}^T \left[\mathbf{b}'_c \left(M N_k^{-1} \hat{\mathbf{Q}}_{G_k^0, \tilde{z}\tilde{z}} \right)^{-1} \tilde{z}_{it} \right]^2 \\
&= \frac{M}{N_k T} \sum_{i \in G_k^0} \sum_{t=1}^T \left[\mathbf{b}'_c \left(M N_k^{-1} \hat{\mathbf{Q}}_{G_k^0, \tilde{z}\tilde{z}} \right)^{-1} \tilde{z}_{it} \tilde{z}'_{it} \left(M N_k^{-1} \hat{\mathbf{Q}}_{G_k^0, \tilde{z}\tilde{z}} \right)^{-1} \mathbf{b}_c \right] \\
&= \frac{M}{N_k T} \sum_{i \in G_k^0} \sum_{t=1}^T [\boldsymbol{\varpi}' \tilde{z}_{it} \tilde{z}'_{it} \boldsymbol{\varpi}] \\
&= \frac{M}{N_k T} \sum_{i \in G_k^0} \sum_{t=1}^T \left[\mathbf{g}'_{\boldsymbol{\varpi}} \left(\frac{t}{T} \right) \tilde{\mathbf{x}}_{it} \tilde{\mathbf{x}}'_{it} \mathbf{g}_{\boldsymbol{\varpi}} \left(\frac{t}{T} \right) \right], \tag{B.19}
\end{aligned}$$

where $\mathbf{g}_{\boldsymbol{\varpi}}(v)$ is a $p \times 1$ vector of spline functions $\mathbf{g}_{\boldsymbol{\varpi}}(v) = (g_1(v, \boldsymbol{\varpi}_1), \dots, g_p(v, \boldsymbol{\varpi}_p))'$, with $g_l(v, \boldsymbol{\varpi}_l) = \boldsymbol{\varpi}'_l \mathbf{b}(v)$, and $\boldsymbol{\varpi}_l = (\varpi_{l1}, \dots, \varpi_{lM})'$. The $M \times p$ matrix \mathbf{W} is defined as $\boldsymbol{\varpi} = \text{vec}(\mathbf{W}) = \mathbf{b}'_c \left(M N_k^{-1} \hat{\mathbf{Q}}_{G_k^0, \tilde{z}\tilde{z}} \right)^{-1}$ with $\mathbf{W} = (\boldsymbol{\varpi}_1, \dots, \boldsymbol{\varpi}_p)$. Additionally, $\mathbf{g}_{\boldsymbol{\varpi}}(v) = \mathbf{W}' \mathbf{b}(v)$. The last inequality in (B.19) holds due to the decomposition $\boldsymbol{\varpi}' \tilde{z}_{it} = \boldsymbol{\varpi}' (\tilde{\mathbf{x}}_{it} \otimes \mathbf{b}(t/T)) = \mathbf{b}(t/T)' \mathbf{W} \tilde{\mathbf{x}}_{it} = \mathbf{g}'_{\boldsymbol{\varpi}}(t/T) \tilde{\mathbf{x}}_{it}$.

We rewrite (B.19) as

$$\begin{aligned}
& \frac{M}{N_k T} \sum_{i \in G_k^0} \sum_{t=1}^T \mathbf{g}'_{\boldsymbol{\varpi}} \left(\frac{t}{T} \right) \tilde{\mathbf{x}}_{it} \tilde{\mathbf{x}}'_{it} \mathbf{g}_{\boldsymbol{\varpi}} \left(\frac{t}{T} \right) \\
&= \frac{M}{N_k T} \sum_{i \in G_k^0} \sum_{t=1}^T \mathbf{g}'_{\boldsymbol{\varpi}} \left(\frac{t}{T} \right) E(\tilde{\mathbf{x}}_{it} \tilde{\mathbf{x}}'_{it}) \mathbf{g}_{\boldsymbol{\varpi}} \left(\frac{t}{T} \right) (1 + o_p(1)) \\
&\leq \frac{M \bar{c}_{\tilde{x}\tilde{x}}}{T} \sum_{t=1}^T \mathbf{g}'_{\boldsymbol{\varpi}} \left(\frac{t}{T} \right) \mathbf{g}_{\boldsymbol{\varpi}} \left(\frac{t}{T} \right) = \frac{M \bar{c}_{\tilde{x}\tilde{x}}}{T} \sum_{t=1}^T \boldsymbol{\varpi}' \mathbf{b} \left(\frac{t}{T} \right) \mathbf{b} \left(\frac{t}{T} \right)' \boldsymbol{\varpi} \\
&= \bar{c}_{\tilde{x}\tilde{x}} \|\boldsymbol{\varpi}\|_2^2 \frac{1}{T} \sum_{t=1}^T M \mathbf{b} \left(\frac{t}{T} \right) \mathbf{b} \left(\frac{t}{T} \right)'.
\end{aligned} \tag{B.20}$$

The first equality holds since $T^{-1} \sum_{t=1}^T \tilde{\mathbf{x}}_{it} \tilde{\mathbf{x}}'_{it} = T^{-1} \sum_{t=1}^T E(\tilde{\mathbf{x}}_{it} \tilde{\mathbf{x}}'_{it}) (1 + o_p(1))$ by Huang et al. (2004, Lemma A.2). The first inequality uses the fact that $E(\tilde{\mathbf{x}}_{it} \tilde{\mathbf{x}}'_{it}) = E(\mathbf{x}_{it} \mathbf{x}'_{it}) - E(\mathbf{x}_{it}) E(\mathbf{x}'_{it}) \leq E(\mathbf{x}_{it} \mathbf{x}'_{it}) \leq \bar{c}_{\tilde{x}\tilde{x}}$ by Assumption 1(iv) and consequently $(N_k T)^{-1} \sum_{i \in G_k^0} \sum_{t=1}^T E(\tilde{\mathbf{x}}_{it} \tilde{\mathbf{x}}'_{it}) \leq \bar{c}_{\tilde{x}\tilde{x}}$. Recall that by property of the Riemann sum and Lemma B.1(iii), $\lim_{T \rightarrow \infty} T^{-1} \sum_{t=1}^T M \mathbf{b}(t/T) \mathbf{b}(t/T)' = \int_0^1 M \mathbf{b}(v) \mathbf{b}(v)' dv = O(1)$. Moreover, $\|\mathbf{W}\|_F = O_p(1)$ since $\text{vec}(\mathbf{W}) = \mathbf{b}'_c \left(M N_k^{-1} \hat{\mathbf{Q}}_{G_k^0, \tilde{z}\tilde{z}} \right)^{-1}$, with $\|M N_k^{-1} \hat{\mathbf{Q}}_{G_k^0, \tilde{z}\tilde{z}}\|_F = O_p(1)$ following Lemma B.2(ii) and $\|\mathbf{b}_c\|_2 = O_p(1)$ following Lemma B.6(i). Plugging these results into (B.20), the rate of (B.20) and therefore of (B.19) becomes apparent as $\bar{c}_{\tilde{x}\tilde{x}} \text{vec}(\boldsymbol{\varpi})' \text{vec}(\boldsymbol{\varpi}) T^{-1} \sum_{t=1}^T M \mathbf{b}(t/T) \mathbf{b}(t/T)' = O_p(1)$.

Turning to d_{12,G_k^0} ,

$$\begin{aligned}
|d_{12,G_k^0}| &= \left| \sqrt{\frac{N_k T}{M}} \mathbf{b}'_c \hat{\mathbf{Q}}_{G_k^0, \tilde{z}\tilde{z}}^{-1} \hat{\mathbf{q}}_{\hat{G}_k, \tilde{z}\tilde{\varrho}} \right| = \left| (N_k T)^{-1/2} M^{1/2} \frac{1}{T} \sum_{i \in G_k^0} \sum_{t=1}^T \mathbf{b}'_c (M N_k^{-1} \hat{\mathbf{Q}}_{G_k^0, \tilde{z}\tilde{z}})^{-1} \tilde{z}_{it} \tilde{\varrho}_{it} \right| \\
&\leq (N_k T)^{-1/2} M^{1/2} \frac{1}{T} \sum_{i \in G_k^0} \sum_{t=1}^T \left| \mathbf{b}'_c (M N_k^{-1} \hat{\mathbf{Q}}_{G_k^0, \tilde{z}\tilde{z}})^{-1} \tilde{z}_{it} \right| |\tilde{\varrho}_{it}| \\
&\leq (N_k T)^{1/2} \left[\frac{M}{N_k T} \sum_{i \in G_k^0} \sum_{t=1}^T \left| \mathbf{b}'_c (M N_k^{-1} \hat{\mathbf{Q}}_{G_k^0, \tilde{z}\tilde{z}})^{-1} \tilde{z}_{it} \right|^2 \right]^{1/2} \left[\frac{1}{N_k T} \sum_{i \in G_k^0} \sum_{t=1}^T |\tilde{\varrho}_{it}|^2 \right]^{1/2},
\end{aligned} \tag{B.21}$$

where the first inequality holds by the triangle property and the second because of the Cauchy-Schwarz inequality. (B.19)-(B.20) provide the rate of the first term in squared brackets and (B.18) gives the rate of the second term in squared brackets of (B.21). Consequently, it is apparent that $|d_{12,G_k^0}| = (N_k T)^{1/2} O_p(1) O_p(M^{-\theta})$ and $O_p((N_k T)^{1/2} M^{-\theta}) = o_p(1)$ under Assumption 4(ii). Moreover, as $|s_{c,G_k^0}| = O_p(1)$ by Lemma B.6(ii), $|d_{12,G_k^0}|/s_{c,G_k^0} = o_p(1)$ and d_{12,G_k^0} is negligible in the limit.

As a result, it suffices to study the behavior of d_{11,G_k^0} in (B.17) to derive the limiting distribution of the *post-Lasso* estimator. To this end,

$$\begin{aligned}
d_{11,G_k^0} &= \sqrt{\frac{N_k T}{M}} \mathbf{b}'_c \hat{\mathbf{Q}}_{G_k^0, \tilde{z}\tilde{z}}^{-1} \hat{\mathbf{q}}_{G_k^0, \tilde{z}\tilde{\epsilon}} = \mathbf{b}'_c \left(\frac{M}{N_k} \hat{\mathbf{Q}}_{G_k^0, \tilde{z}\tilde{z}} \right)^{-1} \sqrt{\frac{M}{N_k T}} \sum_{i \in G_k^0} \sum_{t=1}^T \tilde{z}_{it} \tilde{\epsilon}_{it} \\
&= \left[\mathbf{b}'_c \left(\frac{M}{N_k} \hat{\mathbf{Q}}_{G_k^0, \tilde{z}\tilde{z}} \right)^{-1} \frac{M}{N_k T} \sum_{i \in G_k^0} \left(\tilde{\mathbf{Z}}'_i E(\boldsymbol{\epsilon}_i \boldsymbol{\epsilon}'_i) \tilde{\mathbf{Z}}_i \right) \left(\frac{M}{N_k} \hat{\mathbf{Q}}_{G_k^0, \tilde{z}\tilde{z}} \right)^{-1} \mathbf{b}_c \right]^{1/2} \zeta_i \\
&= \sum_{i \in G_k^0} a_i \zeta_i,
\end{aligned}$$

where $\boldsymbol{\epsilon}_i = (\epsilon_{i1}, \dots, \epsilon_{iT})'$, $\tilde{\mathbf{Z}}_i = (\tilde{\mathbf{z}}_{i1}, \dots, \tilde{\mathbf{z}}_{iT})'$, and

$$a_i = \left[\mathbf{b}'_c \left(\frac{M}{N_k} \hat{\mathbf{Q}}_{G_k^0, \tilde{z}\tilde{z}} \right)^{-1} \frac{M}{N_k T} \left(\tilde{\mathbf{Z}}'_i E(\boldsymbol{\epsilon}_i \boldsymbol{\epsilon}'_i) \tilde{\mathbf{Z}}_i \right) \left(\frac{M}{N_k} \hat{\mathbf{Q}}_{G_k^0, \tilde{z}\tilde{z}} \right)^{-1} \mathbf{b}_c \right]^{1/2}.$$

ζ_i is an independent random variable with variance one and mean $\mathbf{c}' \mathbf{q}_{G_k^0} = \mathbf{c}' \sqrt{M/(N_k T)} \sum_{i \in G_k^0} \sum_{t=1}^T E(\tilde{\mathbf{z}}_{it} \tilde{\epsilon}_{it})$, conditional on $\{\mathbf{z}_i\}_{i=1}^N$.

Subsequently, we prove

$$\frac{d_{11,G_k^0}}{\sqrt{\sum_{i \in G_k^0} a_i^2}} - \frac{\mathbf{c}' \mathbf{q}_{G_k^0}}{\sqrt{M/(N_k T) \mathbf{c}' \sum_{i \in G_k^0} (\tilde{\mathbf{Z}}_i' E(\boldsymbol{\epsilon}_i \boldsymbol{\epsilon}_i') \tilde{\mathbf{Z}}_i) \mathbf{c}}} \xrightarrow{D} N(0, 1),$$

by verifying the Lindeberg condition

$$\frac{\max_{i \in G_k^0} a_i^2}{\sum_{i \in G_k^0} a_i^2} = o_p(1).$$

Considering $\max_{i \in G_k^0} a_i^2$ first,

$$\begin{aligned} \max_{i \in G_k^0} a_i^2 &= \max_{i \in G_k^0} \left[\mathbf{b}_c' \left(\frac{M}{N_k} \hat{\mathbf{Q}}_{G_k^0, \tilde{z}\tilde{z}} \right)^{-1} \frac{M}{N_k T} (\tilde{\mathbf{Z}}_i' E(\boldsymbol{\epsilon}_i \boldsymbol{\epsilon}_i') \tilde{\mathbf{Z}}_i) \left(\frac{M}{N_k} \hat{\mathbf{Q}}_{G_k^0, \tilde{z}\tilde{z}} \right)^{-1} \mathbf{b}_c' \right] \\ &\leq \max_{i \in G_k^0} \left[\frac{M}{N_k T} \mu_{\max} (\tilde{\mathbf{Z}}_i' E(\boldsymbol{\epsilon}_i \boldsymbol{\epsilon}_i') \tilde{\mathbf{Z}}_i) \mathbf{b}_c' \left(\frac{M}{N_k} \hat{\mathbf{Q}}_{G_k^0, \tilde{z}\tilde{z}} \right)^{-1} \left(\frac{M}{N_k} \hat{\mathbf{Q}}_{G_k^0, \tilde{z}\tilde{z}} \right)^{-1} \mathbf{b}_c \right] \\ &\leq \frac{1}{N_k} \max_{i \in G_k^0} [\mu_{\max} (E(\boldsymbol{\epsilon}_i \boldsymbol{\epsilon}_i'))] \max_{i \in G_k^0} \left[\mu_{\max} \left(\frac{M}{T} \tilde{\mathbf{Z}}_i' \tilde{\mathbf{Z}}_i \right) \right] \left[\mu_{\min} \left(\frac{M}{N_k} \hat{\mathbf{Q}}_{G_k^0, \tilde{z}\tilde{z}} \right) \right]^{-2} \|\mathbf{b}_c\|_2^2 \\ &= \frac{1}{N_k} \bar{c}_{\epsilon\epsilon} O_p(1) O_p(1) O_p(1) = o_p(1) \end{aligned}$$

by Assumptions 1(iv) and 4(i). Note that the inequalities hold by the property of a p.s.d. symmetric matrix A and a conformable vector a , $a' A a \leq \mu_{\max}(A) a'a$. Furthermore, $\mu_{\max}(E(\boldsymbol{\epsilon}_i \boldsymbol{\epsilon}_i'))$ is bounded from above by Assumption 4(i), while $\mu_{\max}(MT^{-1} \tilde{\mathbf{Z}}_i' \tilde{\mathbf{Z}}_i) = \mu_{\max}(MT^{-1} \sum_{t=1}^T \tilde{z}_{it} \tilde{z}_{it}')$ and $\mu_{\min}(MN_k^{-1} \hat{\mathbf{Q}}_{G_k^0, \tilde{z}\tilde{z}})$ are bounded by Lemma B.2. In addition, $\|\mathbf{b}_c\|_2 = 1$ following Lemma B.6(i).

In conclusion, it is straightforward to see that the whole term in (B.15) converges in distribution

$$\frac{\sqrt{N_k T / M} \mathbf{c}' [\hat{\boldsymbol{\alpha}}_{G_k}^p(v) - \boldsymbol{\alpha}_k^0(v)]}{\sqrt{\sum_{i \in G_k^0} a_i^2}} - \frac{\mathbf{c}' \mathbf{q}_{G_k^0}}{\sqrt{M/(N_k T) \mathbf{c}' \sum_{i \in G_k^0} (\tilde{\mathbf{Z}}_i' E(\boldsymbol{\epsilon}_i \boldsymbol{\epsilon}_i') \tilde{\mathbf{Z}}_i) \mathbf{c}}} \xrightarrow{D} N(0, 1),$$

for all $k = 1, \dots, K_0$. By defining $\sum_{i \in G_k^0} a_i^2 = \mathbf{c}' \hat{\mathbf{\Omega}}_{G_k^0} \mathbf{c}$ and making use of the Cramér-Wold Theorem, this generalizes to

$$\sqrt{\frac{N_k T}{M}} \hat{\mathbf{\Omega}}_{G_k^0}^{-1/2} [\hat{\boldsymbol{\alpha}}_{G_k}^p(v) - \boldsymbol{\alpha}_k^0(v)] - \hat{\mathbf{\mathcal{E}}}_{G_k^0}^{-1/2} \mathbf{q}_{G_k^0} \xrightarrow{D} N(0, \mathbf{I}_p), \text{ for } k = 1, \dots, K_0,$$

where $\hat{\mathbf{\Omega}}_{G_k^0}^{-1/2}$ is the symmetric square root of the inverse of $\hat{\mathbf{\Omega}}_{G_k^0} = \hat{\boldsymbol{\nu}}_{G_k^0}' \hat{\mathbf{\mathcal{E}}}_{G_k^0} \hat{\boldsymbol{\nu}}_{G_k^0}$, with

$$\hat{\mathbf{\mathcal{E}}}_{G_k^0} = \frac{M}{N_k T} \sum_{i \in G_k^0} \tilde{\mathbf{Z}}_i' E(\boldsymbol{\epsilon}_i \boldsymbol{\epsilon}_i') \tilde{\mathbf{Z}}_i \text{ and } \hat{\boldsymbol{\nu}}_{G_k^0} = \left(\frac{M}{N_k} \hat{\mathbf{Q}}_{G_k^0, \tilde{z}\tilde{z}} \right)^{-1} (\mathbf{I}_p \otimes \mathbf{b}(v)).$$

See [Qian and Su \(2016a, Theorem 3.5\)](#), [Mehrabani \(2023, Theorem 3.5\)](#), and [Su et al. \(2019, Theorem 4.5\)](#) for similar derivations. \square

Proof of Theorem 3.6. First, recall that $IC(\lambda) = \ln(\sigma_{\hat{\mathcal{G}}_{\hat{K},\lambda}}^2) + \rho_{NT} p M \hat{K}_\lambda$, where ρ_{NT} is a tuning parameter and $\sigma_{\hat{\mathcal{G}}_{\hat{K},\lambda}}^2$ reflects the *MSE* $\sigma_{\hat{\mathcal{G}}_{\hat{K},\lambda}}^2 = (NT)^{-1} \sum_{k=1}^{\hat{K}_\lambda} \sum_{i \in \hat{\mathcal{G}}_{k,\lambda}} \sum_{t=1}^T \left(\tilde{y}_{it} - \hat{\boldsymbol{\alpha}}_{\hat{\mathcal{G}}_{k,\lambda}}^{p'} (t/T) \tilde{\mathbf{x}}_{it} \right)^2$.

Let $\Lambda = [0, \lambda_{\max}]$ be an interval in \mathbb{R}^+ . Define three subsets Λ_0 , Λ_- and Λ_+ , such that

$$\Lambda_0 = \{\lambda \in \Lambda : \hat{K}_\lambda = K_0\}, \quad \Lambda_- = \{\lambda \in \Lambda : \hat{K}_\lambda < K_0\}, \quad \Lambda_+ = \{\lambda \in \Lambda : \hat{K}_\lambda > K_0\}.$$

Moreover, all $\lambda \in \Lambda_0$ comply with the regularity conditions in [Assumption 2](#), which allows the use of the oracle property by [Theorem 3.4](#). In addition, since the *post-Lasso* estimator converges to the true estimator by [Theorem 3.5](#), $\sigma_{\hat{\mathcal{G}}_{\hat{K},\lambda}}^2 = \sigma_{\mathcal{G}^0}^2$ w.p.a.1. Therefore, let $\inf_{\lambda \in \Lambda_{0,NT}} IC(\lambda) = IC(\lambda_0)$ and

$$IC(\lambda_0) = \ln(\sigma_{\mathcal{G}^0}^2) + \rho_{NT} p M \hat{K}_\lambda \xrightarrow{p} \ln(\sigma_0^2),$$

where σ_0^2 is the irreducible *MSE* $\sigma_0^2 = \lim_{(N,T) \rightarrow \infty} (NT)^{-1} \sum_{i=1}^N \sum_{t=1}^T \tilde{\epsilon}_{it}^2$ and [Assumption 6\(i\)](#) gives $\rho_{NT} M K_0 \rightarrow 0$ as $(N, T) \rightarrow \infty$.

The proof of [Theorem 3.6](#) works by showing that $IC(\lambda)$ converges in probability to some value strictly larger than $IC(\lambda_0)$, $\forall \lambda \in \Lambda_- \cup \Lambda_+$.

Case 1 Underfitting: $\lambda \in \Lambda_-$ such that $\hat{K}_\lambda < K_0$. Let \mathbb{G} denote the set of all possible partitions over N . Note that

$$\begin{aligned} \sigma_{\hat{\mathcal{G}}_{\hat{K},\lambda}}^2 &= (NT)^{-1} \sum_{k=1}^{\hat{K}_\lambda} \sum_{i \in \hat{\mathcal{G}}_{k,\lambda}} \sum_{t=1}^T \left(\tilde{y}_{it} - \hat{\boldsymbol{\xi}}_{\hat{\mathcal{G}}_{k,\lambda}}^{p'} \tilde{\mathbf{z}}_{it} \right)^2 \\ &\geq \min_{1 \leq K < K_0} \inf_{\mathcal{G}_K \in \mathbb{G}} \sum_{k=1}^K \sum_{i \in G_k} \sum_{t=1}^T \left(\tilde{y}_{it} - \hat{\boldsymbol{\xi}}_{G_k}^{p'} \tilde{\mathbf{z}}_{it} \right)^2 \\ &= \min_{1 \leq K < K_0} \inf_{\mathcal{G}_K \in \mathbb{G}} \hat{\sigma}_{\mathcal{G}_K}^2. \end{aligned}$$

[Assumption 5](#) states, $\lim_{(N,T) \rightarrow \infty} \min_{1 \leq K < K_0} \inf_{\mathcal{G}_K \in \mathbb{G}} \hat{\sigma}_{\mathcal{G}_K}^2 \xrightarrow{p} \underline{\sigma}^2 > \sigma_0^2$. Therefore, applying Slutsky,

$$\inf_{\lambda \in \Lambda_-} IC(\lambda) \geq \min_{1 \leq K < K_0} \inf_{\mathcal{G}_K \in \mathbb{G}} \ln(\sigma_{\mathcal{G}_K}^2) + \rho_{NT} p M K \xrightarrow{p} \ln(\underline{\sigma}^2) > \ln(\sigma_0^2)$$

and in consequence $\Pr(\inf_{\lambda \in \Lambda_-} IC(\lambda) \geq IC(\lambda_0)) \rightarrow 1$.

Case 2 Overfitting: $\lambda \in \Lambda_+$ such that $\hat{K}_\lambda > K_0$. Define the set $\bar{\mathbb{G}}_K = \{\bar{\mathcal{G}}_K = \{\bar{G}_k\}_{k=1}^K : \nexists i, j \in \bar{G}_K$ where $i \in G_l^0, j \notin G_l^0, 1 \leq l \leq K_0\}$ with $K > K_0$. That is, each $\bar{\mathcal{G}}_K \in \bar{\mathbb{G}}_K$ denotes a partition of $K > K_0$ over N , where no heterogeneous cross-sectional units are pooled together in any of the K groups. Recognize that such an over-fitted model yields a weakly lower *MSE* than when using the true group structure $\hat{\sigma}_{\bar{\mathcal{G}}_K}^2 \leq \hat{\sigma}_{\mathcal{G}^0}^2$.

Let

$$\begin{aligned} & \Pr \left(\inf_{\lambda \in \Lambda_+} IC(\lambda) > IC(\lambda_0) \right) \\ & \geq \Pr \left(\min_{K_0 < K \leq N} \inf_{\bar{\mathcal{G}}_K \in \bar{\mathbb{G}}_K} \left(\ln(\hat{\sigma}_{\bar{\mathcal{G}}_K}^2) + \rho_{NT} p M K \right) > \ln(\sigma_{\mathcal{G}^0}^2) + \rho_{NT} p M K_0 \right) \\ & \geq \Pr \left(\min_{K_0 < K \leq N} \inf_{\bar{\mathcal{G}}_K \in \bar{\mathbb{G}}_K} \left(\ln(\hat{\sigma}_{\bar{\mathcal{G}}_K}^2) + \rho_{NT} p M K \right) > \ln(\sigma_{\mathcal{G}^0}^2) + \rho_{NT} p M K_0 \right) \\ & = \Pr \left(\min_{K_0 < K \leq N} \inf_{\bar{\mathcal{G}}_K \in \bar{\mathbb{G}}_K} \left[\ln(\hat{\sigma}_{\bar{\mathcal{G}}_K}^2 / \sigma_{\mathcal{G}^0}^2) + \rho_{NT} p M (K - K_0) \right] > 0 \right) \\ & = \Pr \left(\min_{K_0 < K \leq N} \inf_{\bar{\mathcal{G}}_K \in \bar{\mathbb{G}}_K} \left[(\hat{\sigma}_{\bar{\mathcal{G}}_K}^2 - \sigma_{\mathcal{G}^0}^2) / \sigma_{\mathcal{G}^0}^2 + o_p(1) + \rho_{NT} p M (K - K_0) \right] > 0 \right). \end{aligned}$$

Employing Lemma B.7, $TM^{-1}(\hat{\sigma}_{\bar{\mathcal{G}}_K}^2 - \sigma_{\mathcal{G}^0}^2) = O_p(1)$ and $\sigma_{\mathcal{G}^0}^2 \rightarrow \sigma_0^2$ as shown above. Therefore, after expanding by TM^{-1} and using the fact that $T\rho_{NT} \rightarrow \infty$ by Assumption 6(ii),

$$\Pr \left(\min_{K_0 < K \leq N} \inf_{\bar{\mathcal{G}}_K \in \bar{\mathbb{G}}_K} [O_p(1) + o_p(1) + T\rho_{NT} p (K - K_0)] > 0 \right) \rightarrow 1,$$

as $(N, T) \rightarrow \infty$. □

Proof of Lemma B.1.

Part (i): $b_m(v) > 0$, $m = -d, \dots, M^*$, is a basis function of degree d (order $d+1$) and defined on the interval $[v_m, v_{m+d+1})$ (De Boor, 2001, ch. 9, eq. 21). Moreover, by property of B-splines, all spline basis functions sum up to one for each v : $\sum_{m=-d}^{M^*} b_m(v) = 1$ (De Boor, 2001, ch. 9, eq. 37). From here it follows that $\|\mathbf{b}(v)\|_2 = \left[\sum_{j=-d}^{M^*} b_m(v)^2 \right]^{1/2} \leq \left[\sum_{j=-d}^{M^*} b_m(v) \right]^{1/2} = 1$.

Part (ii): As stated above, $b_m(v)$ is uniformly bounded on the unit interval and $\sum_{m=-d}^{M^*} b_m(v) = 1$. As a consequence, $\int_0^1 b_m(v) dv = O(M^{-1})$ and

$$\int_0^1 \|\mathbf{b}(v)\|_2 dv = \int_0^1 \left[\sum_{m=-d}^{M^*} b_m(v)^2 \right]^{1/2} dv \leq \int_0^1 \left[\sum_{m=-d}^{M^*} b_m(v) \right]^2 dv = 1.$$

Part (iii): As shown in [De Boor \(2001, ch. 11, eq. 8\)](#), there exist two constants $0 < \underline{c}_b \leq \bar{c}_b < \infty$ such that $\underline{c}_b \|\mathbf{c}\|_2^2 \leq M \int (\mathbf{c}' \mathbf{b}(v))^2 dv \leq \bar{c}_b \|\mathbf{c}\|_2^2$ for all nonrandom $\mathbf{c} \in \mathbb{R}^M$. Using the Cramér-World device, $M \int_0^1 \mathbf{b}(v) \mathbf{b}(v)' dv = O(1)$ and the minimum and maximum eigenvalues are bounded $\underline{c}_b \leq \mu_{\min} \left(M \int_0^1 \mathbf{b}(v) \mathbf{b}(v)' dv \right) \leq \mu_{\max} \left(M \int_0^1 \mathbf{b}(v) \mathbf{b}(v)' dv \right) \leq \bar{c}_b$.

Part (iv): The proof is analogous to [De Boor \(2001, ch. 12, Theorem 6\)](#). \square

Proof of Lemma B.2.

Part (i): Consistent with [Su et al. \(2019, Lemma A.3\)](#), the proof exploits the inherent property that B-splines are bounded. Recall that $\hat{\mathbf{Q}}_{i,\tilde{z}\tilde{z}} = T^{-1} \sum_{t=1}^T \tilde{z}_{it} \tilde{z}'_{it}$ and $\hat{\mathbf{Q}}_{i,\tilde{z}\tilde{z}} = \sum_{i \in G_k^0} T^{-1} \sum_{t=1}^T \tilde{z}_{it} \tilde{z}'_{it}$. Define the $M \times p$ matrix $\mathbf{W} = (\boldsymbol{\varpi}_1, \dots, \boldsymbol{\varpi}_p)$ with $\boldsymbol{\varpi} = \text{vec}(\mathbf{W})$, $\boldsymbol{\varpi}_l = (\varpi_{l,1}, \dots, \varpi_{l,M})'$, and $\|\boldsymbol{\varpi}\|_2 \leq c_{\boldsymbol{\varpi}} < \infty$ for some positive constant $c_{\boldsymbol{\varpi}}$. Let $\mathbb{B}_{\mathbb{V},M}$ denote a linear space as defined in Subsection 2.2. The vector $\mathbf{g}_{\boldsymbol{\varpi}}(v) = \mathbf{W}' \mathbf{b}(v)$ collects spline basis functions $\mathbf{g}_{\boldsymbol{\varpi}}(v) = (g_1(v, \varpi_1), \dots, g_p(v, \varpi_p))'$, where $g_l(v, \varpi_l) = \boldsymbol{\varpi}'_l \mathbf{b}(v) \in \mathbb{B}_{\mathbb{V},M}$ for $l = 1, \dots, p$ and $\mathbf{g}_{\boldsymbol{\varpi}}(v) \in \mathbb{B}_{\mathbb{V},M}^{\otimes p}$. Recognize that $\hat{\mathbf{Q}}_{i,\tilde{z}\tilde{z}} = T^{-1} \sum_{t=1}^T \mathbf{z}_{it} \mathbf{z}'_{it} - T^{-1} \sum_{t=1}^T \mathbf{z}_{it} T^{-1} \sum_{t=1}^T \mathbf{z}'_{it} = \mathbf{A}_{1i} - \mathbf{A}_{2i}$.

Case 1: \mathbf{x}_{it} does not contain an intercept. Consider $\boldsymbol{\varpi}' \mathbf{A}_{1i} \boldsymbol{\varpi}$,

$$\begin{aligned} \boldsymbol{\varpi}' \frac{1}{T} \sum_{t=1}^T \mathbf{z}_{it} \mathbf{z}'_{it} \boldsymbol{\varpi} &= \boldsymbol{\varpi}' \frac{1}{T} \sum_{t=1}^T \left[\mathbf{x}_{it} \otimes \mathbf{b} \left(\frac{t}{T} \right) \right] \left[\mathbf{x}_{it} \otimes \mathbf{b} \left(\frac{t}{T} \right) \right]' \boldsymbol{\varpi} \\ &= \frac{1}{T} \sum_{t=1}^T \left[\mathbf{b} \left(\frac{t}{T} \right)' \mathbf{W} \mathbf{x}_{it} \right]^2 = \frac{1}{T} \sum_{t=1}^T \left[\mathbf{g}_{\boldsymbol{\varpi}} \left(\frac{t}{T} \right)' \mathbf{x}_{it} \right]^2 = \frac{1}{T} \sum_{t=1}^T \mathbf{g}_{\boldsymbol{\varpi}} \left(\frac{t}{T} \right)' \mathbf{x}_{it} \mathbf{x}'_{it} \mathbf{g}_{\boldsymbol{\varpi}} \left(\frac{t}{T} \right), \end{aligned} \quad (\text{B.22})$$

since $(\mathbf{x}_{it} \otimes \mathbf{b}(v)) \text{vec}(\mathbf{W})' = \text{vec}(\mathbf{b}'(v) \mathbf{W} \mathbf{x}_{it})$ by property of the Kronecker product (see [Bernstein, 2009, p. 249](#)).

Note that the maximum eigenvalue of $E(\mathbf{x}_{it} \mathbf{x}'_{it})$ is bounded away from infinity by Assumption 1(iv). Furthermore, as shown in Lemma [Huang et al. \(2004, A.2\)](#),

$$\frac{1}{T} \sum_{t=1}^T \mathbf{g}_{\boldsymbol{\varpi}} \left(\frac{t}{T} \right)' \mathbf{x}_{it} \mathbf{x}'_{it} \mathbf{g}_{\boldsymbol{\varpi}} \left(\frac{t}{T} \right) = \frac{1}{T} \sum_{t=1}^T \mathbf{g}_{\boldsymbol{\varpi}} \left(\frac{t}{T} \right)' E(\mathbf{x}_{it} \mathbf{x}'_{it}) \mathbf{g}_{\boldsymbol{\varpi}} \left(\frac{t}{T} \right) (1 + o_p(1)) \quad (\text{B.23})$$

for strong mixing processes and

$$\frac{1}{T} \sum_{t=1}^T \mathbf{g}_{\boldsymbol{\varpi}} \left(\frac{t}{T} \right)' E(\mathbf{x}_{it} \mathbf{x}'_{it}) \mathbf{g}_{\boldsymbol{\varpi}} \left(\frac{t}{T} \right) (1 + o_p(1)) \leq \bar{c}_{xx} \frac{1}{T} \sum_{t=1}^T \mathbf{g}_{\boldsymbol{\varpi}} \left(\frac{t}{T} \right)' \mathbf{g}_{\boldsymbol{\varpi}} \left(\frac{t}{T} \right) (1 + o_p(1)), \quad (\text{B.24})$$

where $T^{-1} \sum_{t=1}^T \mathbf{g}_{\boldsymbol{\varpi}}(t/T)' \mathbf{g}_{\boldsymbol{\varpi}}(t/T) = \int_0^1 \mathbf{g}_{\boldsymbol{\varpi}}(v)' \mathbf{g}_{\boldsymbol{\varpi}}(v) dv [1 + O(T^{-1})]$ by property of the Riemann

sum and $\int_0^1 \mathbf{g}_\varpi(v)' \mathbf{g}_\varpi(v) dv = \sum_{l=1}^p \varpi_l' \int_0^1 \mathbf{b}(v) \mathbf{b}(v)' dv \varpi_l = O_p(M^{-1})$ by Lemma B.1(iii), since $\|\varpi\|_2^2 < \infty$. As a consequence, after plugging into (B.24) it is apparent that the whole term in (B.22) $\varpi' \mathbf{A}_{1i} \varpi \leq O(M^{-1}) [1 + O(T^{-1})] (1 + o(1)) = O(M^{-1})$. Since $\mu_{\max}(\mathbf{B} - \mathbf{C}) \leq \mu_{\max}(\mathbf{B}) + \mu_{\max}(-\mathbf{C}) = \mu_{\max}(\mathbf{B}) - \mu_{\min}(\mathbf{C}) \leq \mu_{\max}(\mathbf{B})$ for two generic real matrices \mathbf{B}, \mathbf{C} , $\mu_{\max}(\hat{\mathbf{Q}}_{i,\tilde{z}\tilde{z}}) \leq \mu_{\max}(\mathbf{A}_{1i})$ and $\mu_{\max}(M \hat{\mathbf{Q}}_{i,\tilde{z}\tilde{z}})$ is bounded away from infinity in probability, uniformly in ϖ . This result also applies uniformly across the cross-section to $\max_i \mu_{\max}(M \hat{\mathbf{Q}}_{i,\tilde{z}\tilde{z}})$ with probability $1 - o(N^{-1})$.

To study the behavior of the minimum eigenvalue of $\hat{\mathbf{Q}}_{i,\tilde{z}\tilde{z}}$, one must also consider \mathbf{A}_{2i} . For this purpose, take

$$\begin{aligned} \varpi' \mathbf{A}_{2i} \varpi &= \varpi' \frac{1}{T} \sum_{t=1}^T \mathbf{z}_{it} \frac{1}{T} \sum_{t=1}^T \mathbf{z}'_{it} \varpi \\ &= \varpi' \frac{1}{T} \sum_{t=1}^T \left[\mathbf{x}_{it} \otimes \mathbf{b} \left(\frac{t}{T} \right) \right] \frac{1}{T} \sum_{t=1}^T \left[\mathbf{x}_{it} \otimes \mathbf{b} \left(\frac{t}{T} \right) \right]' \varpi \\ &= \left[\frac{1}{T} \sum_{t=1}^T \mathbf{b} \left(\frac{t}{T} \right)' \varpi \mathbf{x}_{it} \right]^2 = \left[\frac{1}{T} \sum_{t=1}^T \mathbf{g}_\varpi \left(\frac{t}{T} \right)' \mathbf{x}_{it} \right]^2 \\ &= E \left[\frac{1}{T} \sum_{t=1}^T \mathbf{g}_\varpi \left(\frac{t}{T} \right)' \mathbf{x}_{it} \right]^2 (1 + o_p(1)), \end{aligned} \tag{B.25}$$

where the last equality holds again by Lemma Huang et al. (2004, A.2). Using (B.25) and the result in (B.23),

$$\begin{aligned} \varpi' (\mathbf{A}_{1i} - \mathbf{A}_{2i}) \varpi &= \varpi' \left(\hat{\mathbf{Q}}_{i,zz} - T^{-1} \sum_{t=1}^T \mathbf{z}_{it} T^{-1} \sum_{t=1}^T \mathbf{z}'_{it} \right) \varpi \\ &= \frac{1}{T} \sum_{t=1}^T E \left[\left(\mathbf{g}_\varpi \left(\frac{t}{T} \right)' \mathbf{x}_{it} \right)^2 \right] - E \left[\frac{1}{T} \sum_{t=1}^T \mathbf{g}_\varpi \left(\frac{t}{T} \right)' \mathbf{x}_{it} \right]^2 + o(N^{-1}), \end{aligned} \tag{B.26}$$

uniformly in ϖ and i .

In order to show that the minimum eigenvalue of $M \hat{\mathbf{Q}}_{i,\tilde{z}\tilde{z}}$ is bounded away from 0, define

$$\boldsymbol{\mu}_i(v) = \begin{cases} \mathbf{0}_{p \times 1} & \text{if } v = 0 \\ E(\mathbf{x}_{it}) & \text{if } v \in (\frac{t-1}{T}, \frac{t}{T}] \end{cases} \quad \text{and} \quad \boldsymbol{\Sigma}_i(v) = \begin{cases} \mathbf{0}_{p \times p} & \text{if } v = 0 \\ E(\mathbf{x}_{it} \mathbf{x}'_{it}) & \text{if } v \in (\frac{t-1}{T}, \frac{t}{T}], \end{cases}$$

for $v \in [0, 1]$. Note that $\bar{\boldsymbol{\Sigma}}_i(t/T) = \boldsymbol{\Sigma}_i(t/T) - \boldsymbol{\mu}_i(t/T) \boldsymbol{\mu}_i(t/T)' = \text{Var}(\mathbf{x}_{it})$. Rewrite $T^{-1} \sum_{t=1}^T E \left[(\mathbf{g}_\varpi(t/T)' \mathbf{x}_{it})^2 \right] -$

$E \left[T^{-1} \sum_{t=1}^T \mathbf{g}_\varpi(t/T)' \mathbf{x}_{it} \right]^2$ in (B.26) to

$$\begin{aligned}
& \frac{1}{T} \sum_{t=1}^T \left[\mathbf{g}_\varpi \left(\frac{t}{T} \right)' \boldsymbol{\Sigma}_i \left(\frac{t}{T} \right) \mathbf{g}_\varpi \left(\frac{t}{T} \right) \right] - \left[\frac{1}{T} \sum_{t=1}^T \mathbf{g}_\varpi \left(\frac{t}{T} \right)' \boldsymbol{\mu}_i \left(\frac{t}{T} \right) \right]^2 \\
&= \int_0^1 \mathbf{g}_\varpi(v)' \boldsymbol{\Sigma}_i(v) \mathbf{g}_\varpi(v) dv [1 + O(T^{-1})] - \left[\int_0^1 \mathbf{g}_\varpi(v)' \boldsymbol{\mu}_i(v) dv [1 + O(T^{-1})] \right]^2 \\
&\geq \int_0^1 \mathbf{g}_\varpi(v)' \boldsymbol{\Sigma}_i(v) \mathbf{g}_\varpi(v) dv [1 + O(T^{-1})] - \int_0^1 \mathbf{g}_\varpi(v)' \boldsymbol{\mu}_i(v) \boldsymbol{\mu}_i(v)' \mathbf{g}_\varpi(v) dv [1 + O(T^{-1})] \\
&= \left[\int_0^1 \mathbf{g}_\varpi(v)' \boldsymbol{\Sigma}_i(v) \mathbf{g}_\varpi(v) dv - \int_0^1 \mathbf{g}_\varpi(v)' \boldsymbol{\mu}_i(v) \boldsymbol{\mu}_i(v)' \mathbf{g}_\varpi(v) dv \right] \\
&\quad - O(T^{-1}) \left[\int_0^1 \mathbf{g}_\varpi(v)' \boldsymbol{\Sigma}_i(v) \mathbf{g}_\varpi(v) dv - \int_0^1 \mathbf{g}_\varpi(v)' \boldsymbol{\mu}_i(v) \boldsymbol{\mu}_i(v)' \mathbf{g}_\varpi(v) dv \right] \\
&= d_{1i} - d_{2i},
\end{aligned}$$

where the inequality holds because of Jensen's inequality. Studying d_{1i} first,

$$\begin{aligned}
d_{1i} &= \int_0^1 \mathbf{g}_\varpi(v)' \boldsymbol{\Sigma}_i(v) \mathbf{g}_\varpi(v) dv - \int_0^1 \mathbf{g}_\varpi(v)' \boldsymbol{\mu}_i(v) \boldsymbol{\mu}_i(v)' \mathbf{g}_\varpi(v) dv \\
&= \int_0^1 \mathbf{g}_\varpi(v)' \bar{\boldsymbol{\Sigma}}_i(v) \mathbf{g}_\varpi(v) dv \geq \underline{c}_{zz} \sum_{l=1}^p \int_0^1 g_l(v, \varpi_l)' g_l(v, \varpi_l) dv \\
&= \underline{c}_{zz} \sum_{l=1}^p \varpi_{il}' \int_0^1 \mathbf{b}(v) \mathbf{b}(v)' dv \varpi_{il} = \|\varpi\|_2^2 O(M^{-1}) = O(M^{-1}),
\end{aligned}$$

where $\underline{c}_{zz} \leq \text{Var}(\mathbf{x}_{it}) = \bar{\boldsymbol{\Sigma}}_i(t/T)$ by Assumption 1(iv).

Since $D_{2i} = O(T^{-1})D_{1i} = O((MT)^{-1})$, the minimum eigenvalue $\min_i \mu_{\min}(M \hat{\mathbf{Q}}_{i,zz})$ is bounded away from 0 uniformly in \mathbf{W} and i with probability $1 - o(N^{-1})$.

Case 2: $\mathbf{x}_{it} = 1$. Then (B.22) collapses to

$$\varpi' \frac{1}{T} \sum_{t=1}^T \mathbf{z}_{it} \mathbf{z}_{it}' \varpi = \varpi' \frac{1}{T} \sum_{t=1}^T \mathbf{b} \left(\frac{t}{T} \right) \mathbf{b} \left(\frac{t}{T} \right)' \varpi \tag{B.27}$$

and (B.26) becomes

$$\begin{aligned}
& \varpi' \left(\hat{\mathbf{Q}}_{i,zz} - \frac{1}{T} \sum_{t=1}^T \mathbf{z}_{it} \frac{1}{T} \sum_{t=1}^T \mathbf{z}_{it}' \right) \varpi \\
&= \varpi' \left(\frac{1}{T} \sum_{t=1}^T \mathbf{b} \left(\frac{t}{T} \right) \mathbf{b} \left(\frac{t}{T} \right)' - \frac{1}{T} \sum_{t=1}^T \mathbf{b} \left(\frac{t}{T} \right) \frac{1}{T} \sum_{t=1}^T \mathbf{b} \left(\frac{t}{T} \right)' \right) \varpi.
\end{aligned} \tag{B.28}$$

It suffices to apply the basic properties of B-splines in order to study the minimum and maximum eigenvalues of $\hat{\mathbf{Q}}_{i,zz}$. To this end, Lemma B.1(iii) shows that $M \int_0^1 \mathbf{b}(t/T) \mathbf{b}(t/T)' dv$ has bounded

minimum and maximum eigenvalues, where $T^{-1} \sum_{t=1}^T \mathbf{b}(t/T) \mathbf{b}(t/T)' = \int_0^1 \mathbf{b}(t/T) \mathbf{b}(t/T)' dv [1 + O(T^{-1})]$ by the Riemann sum and $\|\mathbf{W}\|_F < \infty$ in (B.27). Furthermore, $T^{-1} \sum_{t=1}^T \mathbf{b}(t/T) \mathbf{b}(t/T)' - T^{-1} \sum_{t=1}^T \mathbf{b}(t/T) T^{-1} \sum_{t=1}^T$ in (B.28) can be considered as a vector product of standardized spline basis functions. Subsequently, the properties of B-splines, including the ones stated in Lemma B.1(iii) carry over. As a consequence, the results obtained under Case 1 hold by Lemma B.1(iii).

Case 3: \mathbf{x}_{it} contains an intercept and stochastic regressors. Reorder \mathbf{x}_{it} so that $\mathbf{x}_{it} = (1, \mathbf{x}_{it}^{(2) \prime})'$ and $\mathbf{x}_{it}^{(2)}$ is a $(p-1) \times 1$ vector of random variables. This instance presents a mix of the two previously considered cases, where Case 1 applies to $\mathbf{x}_{it}^{(2)}$ and Case 2 concerns the intercept in \mathbf{x}_{it} . Therefore, the results with respect to the minimum and maximum eigenvalues of $\hat{\mathbf{Q}}_{i,\tilde{z}\tilde{z}}$ also hold for $\mathbf{x}_{it} = (1, \mathbf{x}_{it}^{(2) \prime})$, see [Su et al. \(2019, Lemma A.3\(i\)\)](#) for more details.

Part (ii): Consider $\hat{\mathbf{Q}}_{i,\tilde{z}\tilde{z}} = \sum_{i \in G_k^0} \hat{\mathbf{Q}}_{i,\tilde{z}\tilde{z}}$. Since cross-sectional individuals are weakly dependent as given in [Assumption 1\(i\)](#), it holds that

$$\Pr \left(\underline{c}_{\tilde{z}\tilde{z}} \leq \mu_{\min} \left(\frac{M}{N_k} \hat{\mathbf{Q}}_{i,\tilde{z}\tilde{z}} \right) < \mu_{\max} \left(\frac{M}{N_k} \hat{\mathbf{Q}}_{i,\tilde{z}\tilde{z}} \right) \leq \bar{c}_{\tilde{z}\tilde{z}} \right) = 1 - o(N^{-1})$$

for $i = 1, \dots, N$ and two constants $0 < \underline{c}_{\tilde{z}\tilde{z}} \leq \bar{c}_{\tilde{z}\tilde{z}} < \infty$, as shown in [Lemma B.2\(i\)](#). \square

Proof of Lemma B.3. Recall $\hat{\mathbf{q}}_{i,\tilde{z}\tilde{u}} = T^{-1} \sum_{t=1}^T \tilde{z}_{it} \tilde{u}_{it}$, where $\tilde{u}_{it} = \tilde{\epsilon}_{it} + \tilde{\varrho}_{it}$, $\varrho_{it} = \boldsymbol{\eta}'_{it} \mathbf{x}_{it}$. Following [Su et al. \(2019, Lemma A.4\)](#), the proof of Lemma B.3 is constructed by decomposing the error u_{it} into the idiosyncratic and the sieve elements and analyzing both separately.

Part (i): As defined in [Section 2.2](#), the sieve-bias equals $\boldsymbol{\eta}_{it} = \boldsymbol{\beta}_i^0(t/T) - \boldsymbol{\Pi}_i^0 \mathbf{b}(t/T)$ and $\varrho_{it} = \boldsymbol{\eta}'_{it} \mathbf{x}_{it}$. By the identity $u_{it} = \epsilon_{it} + [\boldsymbol{\beta}_i^0(t/T) \mathbf{x}_{it} - \boldsymbol{\pi}_i^0 \mathbf{z}_{it}] = \epsilon_{it} + [\boldsymbol{\beta}_i^0(t/T) - \boldsymbol{\Pi}_i^0 \mathbf{b}(t/T)]' \mathbf{x}_{it} = \epsilon_{it} + \varrho_{it}$ we have $\tilde{u}_{it} = \tilde{\varrho}_{it} + \tilde{\epsilon}_{it}$, $\hat{\mathbf{q}}_{i,\tilde{z}\tilde{u}} = \hat{\mathbf{q}}_{i,\tilde{z}\tilde{\varrho}} + \hat{\mathbf{q}}_{i,\tilde{z}\tilde{\epsilon}}$, and $\|\hat{\mathbf{q}}_{i,\tilde{z}\tilde{u}}\|_2 \leq \|\hat{\mathbf{q}}_{i,\tilde{z}\tilde{\varrho}}\|_2 + \|\hat{\mathbf{q}}_{i,\tilde{z}\tilde{\epsilon}}\|_2$ by the Triangle inequality, where $\hat{\mathbf{q}}_{i,\tilde{z}a} = T^{-1} \sum_{t=1}^T \mathbf{z}_{it} a_{it}$ for $a_{it} = \{\tilde{\varrho}_{it}, \tilde{\epsilon}_{it}\}$. First we derive the rate of $\|\hat{\mathbf{q}}_{i,\tilde{z}\tilde{\varrho}}\|_2$, then the rate of $\|\hat{\mathbf{q}}_{i,\tilde{z}\tilde{\epsilon}}\|_2$.

By the triangle inequality and the sub-multiplicative property

$$\|\hat{\mathbf{q}}_{i,\tilde{z}\tilde{\varrho}}\|_2 = \left\| T^{-1} \sum_{t=1}^T \mathbf{z}_{it} \varrho_{it} - T^{-1} \sum_{t=1}^T \mathbf{z}_{it} T^{-1} \sum_{t=1}^T \varrho_{it} \right\|_2 \leq \left\| T^{-1} \sum_{t=1}^T \mathbf{z}_{it} \varrho_{it} \right\|_2 + \left\| T^{-1} \sum_{t=1}^T \mathbf{z}_{it} \right\|_2 \left| T^{-1} \sum_{t=1}^T \varrho_{it} \right|. \quad (\text{B.29})$$

Studying all these elements in isolation, consider

$$\left\| \frac{1}{T} \sum_{t=1}^T \varrho_{it} \right\|^2 = \left\| \frac{1}{T} \sum_{t=1}^T \mathbf{x}'_{it} \boldsymbol{\eta}_{it} \right\|^2 \leq \left\| \frac{1}{T} \sum_{t=1}^T \mathbf{x}_{it} \mathbf{x}'_{it} \right\|_F \left\| \frac{1}{T} \sum_{t=1}^T \boldsymbol{\eta}_{it} \boldsymbol{\eta}'_{it} \right\|_F, \quad (\text{B.30})$$

where the inequality holds because of the Chauchy-Schwarz property. Assumption 1(iv) ensures that

$\left\| T^{-1} \sum_{t=1}^T \mathbf{x}_{it} \mathbf{x}'_{it} \right\|_2 \leq \bar{c}_{xx}$ in probability. Furthermore, Lemma B.1(iv) gives $\sup_{v \in [0,1]} \|\boldsymbol{\beta}_i^0(t/T) - \boldsymbol{\Pi}_i^{0'} \mathbf{b}(t/T)\|_2 = O(M^{-\theta})$. As a consequence,

$$\begin{aligned} \left\| \frac{1}{T} \sum_{t=1}^T \boldsymbol{\eta}_{it} \boldsymbol{\eta}'_{it} \right\|_F &= \left\| \left[\boldsymbol{\beta}_i^0 \left(\frac{t}{T} \right) - \boldsymbol{\Pi}_i^{0'} \mathbf{b} \left(\frac{t}{T} \right) \right] \left[\boldsymbol{\beta}_i^0 \left(\frac{t}{T} \right) - \boldsymbol{\Pi}_i^{0'} \mathbf{b} \left(\frac{t}{T} \right) \right]' \right\|_F \\ &\leq \left[\sup_{v \in [0,1]} \|\boldsymbol{\beta}_i^0(v) - \boldsymbol{\Pi}_i^{0'} \mathbf{b}(v)\|_2 \right]^2 = O(M^{-2\theta}), \end{aligned} \quad (\text{B.31})$$

and $\left| T^{-1} \sum_{t=1}^T \varrho_{it} \right|^2 = \bar{c}_{xx} O_p(M^{-2\theta})$, from which follows $\left| T^{-1} \sum_{t=1}^T \varrho_{it} \right| = O_p(M^{-\theta})$.

Define the real $M \times p$ matrix \mathbf{W} with $\text{vec}(\mathbf{W}) = \boldsymbol{\varpi}$ and $\|\boldsymbol{\varpi}\|_2 < \infty$. Then

$$\begin{aligned} \boldsymbol{\varpi}' \left\| \frac{1}{T} \sum_{t=1}^T \mathbf{z}_{it} \right\|_2^2 \boldsymbol{\varpi} &= \left| \boldsymbol{\varpi}' \frac{1}{T} \sum_{t=1}^T \left[\mathbf{x}_{it} \otimes \mathbf{b} \left(\frac{t}{T} \right) \right] \right|^2 \\ &= \left\| \frac{1}{T} \sum_{t=1}^T \mathbf{b} \left(\frac{t}{T} \right)' \mathbf{W} \mathbf{x}_{it} \right\|^2 \leq \left\| \frac{1}{T} \sum_{t=1}^T \mathbf{W}' \mathbf{b} \left(\frac{t}{T} \right) \mathbf{b} \left(\frac{t}{T} \right)' \mathbf{W} \right\|_F \left\| \frac{1}{T} \sum_{t=1}^T \mathbf{x}_{it} \mathbf{x}'_{it} \right\|_F, \end{aligned}$$

where by Assumption 1(iv) $\left\| T^{-1} \sum_{t=1}^T \mathbf{x}_{it} \mathbf{x}'_{it} \right\|_F \leq \bar{c}_{xx}$ in probability. In addition, using the B-spline property in Lemma B.1(iii)

$$\begin{aligned} \left\| \frac{1}{T} \sum_{t=1}^T \mathbf{W}' \mathbf{b} \left(\frac{t}{T} \right) \mathbf{b} \left(\frac{t}{T} \right)' \mathbf{W} \right\|_F &= \left\| \mathbf{W}' \int_0^1 \mathbf{b}(v) \mathbf{b}(v)' dv \mathbf{W} (1 + O(T^{-1})) \right\|_F \\ &\leq \|\mathbf{W}\|_F^2 O(M^{-1}) (1 + O(T^{-1})) = O(M^{-1}), \end{aligned} \quad (\text{B.32})$$

since $\|\mathbf{W}\|_F^2$ is bounded. Subsequently, $\left\| T^{-1} \sum_{t=1}^T \mathbf{z}_{it} \right\|_2 = O_p(M^{-1/2})$.

Lastly, making use of the Cauchy-Schwarz inequality,

$$\|\hat{\mathbf{q}}_{i,z\varrho}\|_2^2 = \left\| \frac{1}{T} \sum_{t=1}^T \mathbf{z}_{it} \varrho_{it} \right\|^2 \leq \left\| \frac{1}{T} \sum_{t=1}^T \mathbf{z}_{it} \mathbf{z}'_{it} \right\|_F \left| \frac{1}{T} \sum_{t=1}^T \varrho_{it}^2 \right|, \quad (\text{B.33})$$

where $\left\| T^{-1} \sum_{t=1}^T \mathbf{z}_{it} \mathbf{z}'_{it} \right\|_F = O_p(M^{-1})$ by Lemma B.2(i) and

$$\begin{aligned} E \left| \frac{1}{T} \sum_{t=1}^T \varrho_{it}^2 \right| &= E \left| \frac{1}{T} \sum_{t=1}^T (\mathbf{x}'_{it} \boldsymbol{\eta}_{it})^2 \right| = \left[\sup_{v \in [0,1]} \left\| \boldsymbol{\alpha}_k^0(v) - \boldsymbol{\Pi}_i^{0\prime} \mathbf{b}(v) \right\|_2 \right]^2 \frac{1}{T} \sum_{t=1}^T E \|\mathbf{x}_{it}\|_2^2 \\ &\leq O(M^{-2\theta}) \bar{c}_x^{2/q} = O(M^{-2\theta}), \end{aligned} \quad (\text{B.34})$$

where $\sup_{v \in [0,1]} \left\| \boldsymbol{\alpha}_k^0(v) - \boldsymbol{\Pi}_i^{0\prime} \mathbf{b}(v) \right\|_2 = O(M^{-\theta})$ by Lemma B.1(iv) and $E \|\mathbf{x}_{it}\|_2^2 \leq \bar{c}_x^{2/q}$ by Assumption 1(iii). As a consequence, $\left| \frac{1}{T} \sum_{t=1}^T \varrho_{it}^2 \right| = O_p(M^{-2\theta})$ by Chebyshev's inequality and $\|\hat{\mathbf{q}}_{i,z\varrho}\|_2^2 = O_p(M^{-1})O_p(M^{-2\theta})$ with $\|\hat{\mathbf{q}}_{i,z\varrho}\|_2 = O_p(M^{-\theta-1/2})$.

Plugging the results of (B.31), (B.32), (B.33), and (B.34) into (B.29) yields

$$\|\hat{\mathbf{q}}_{i,\tilde{z}\varrho}\|_2 \leq \|\hat{\mathbf{q}}_{i,z\varrho}\|_2 + \left\| T^{-1} \sum_{t=1}^T \mathbf{z}_{it} \right\|_2 \left| T^{-1} \sum_{t=1}^T \varrho_{it} \right| = O_p(M^{-\theta-1/2}) + O_p(M^{-1/2})O_p(M^{-\theta}) = O_p(M^{-\theta-1/2}). \quad (\text{B.35})$$

Turning to $\hat{\mathbf{q}}_{i,\tilde{z}\tilde{\epsilon}}$, note that $\hat{\mathbf{q}}_{i,\tilde{z}\tilde{\epsilon}} = \hat{\mathbf{q}}_{i,z\epsilon} - T^{-1} \sum_{t=1}^T \mathbf{z}_{it} T^{-1} \sum_{t=1}^T \epsilon_{it}$. Studying $\hat{\mathbf{q}}_{i,z\epsilon}$ first,

$$\begin{aligned} E \|\hat{\mathbf{q}}_{i,z\epsilon}\|_2^2 &= E \left\| \frac{1}{T} \sum_{t=1}^T \mathbf{z}_{it} \epsilon_{it} \right\|_2^2 = E \left\| \frac{1}{T} \sum_{t=1}^T \left[\mathbf{x}_{it} \otimes \mathbf{b} \left(\frac{t}{T} \right) \right] \epsilon_{it} \right\|_2^2 = E \left\| \frac{1}{T} \sum_{t=1}^T (\mathbf{x}_{it} \epsilon_{it}) \otimes \mathbf{b} \left(\frac{t}{T} \right) \right\|_2^2 \\ &= \frac{1}{T^2} \sum_{t=1}^T \sum_{s=1}^T E(\mathbf{x}'_{it} \mathbf{x}_{is} \epsilon_{it} \epsilon_{is}) \mathbf{b} \left(\frac{t}{T} \right)' \mathbf{b} \left(\frac{s}{T} \right) \\ &= \frac{1}{T^2} \sum_{t=1}^T E(\mathbf{x}'_{it} \mathbf{x}_{it} \epsilon_{it}^2) \left\| \mathbf{b} \left(\frac{t}{T} \right) \right\|_2^2 \\ &\quad + \frac{2}{T^2} \sum_{t=1}^{T-1} \sum_{s=t+1}^T E(\mathbf{x}'_{it} \mathbf{x}_{is} \epsilon_{it} \epsilon_{is}) \mathbf{b} \left(\frac{t}{T} \right)' \mathbf{b} \left(\frac{s}{T} \right) = d_{1i} + d_{2i}. \end{aligned}$$

Employing Assumption 1(iii) gives $E(\mathbf{x}'_{it} \mathbf{x}_{it} \epsilon_{it}^2) \leq E(\|\mathbf{x}_{it}\|_2^2 \|\epsilon_{it}\|_2^2) \leq (\bar{c}_x \bar{c}_\epsilon)^{2/q}$. In addition, $T^{-1} \sum_{t=1}^T \|\mathbf{b}(t/T)\|_2^2 = \int_0^1 \|\mathbf{b}(v)\|_2^2 dv (1 + O(T^{-1})) \leq (1 + O(T^{-1}))$ by Lemma B.1(ii) and the Riemann sum. Therefore,

$$d_{1i} \leq T^{-1} (\bar{c}_x \bar{c}_\epsilon)^{2/q} (1 + O(T^{-1})) = O(T^{-1}).$$

Similarly,

$$\begin{aligned} |d_{2i}| &= \left| \frac{2}{T^2} \sum_{t=1}^{T-1} \sum_{s=t+1}^T E(\mathbf{x}'_{it} \mathbf{x}_{is} \epsilon_{it} \epsilon_{is}) \mathbf{b} \left(\frac{t}{T} \right)' \mathbf{b} \left(\frac{s}{T} \right) \right| \\ &\leq \frac{2}{T^2} \sum_{l=1}^p \sum_{t=1}^{T-1} \sum_{s=t+1}^T \left| E(\mathbf{x}_{it,l} \epsilon_{it} \mathbf{x}_{is,l} \epsilon_{is}) \mathbf{b} \left(\frac{t}{T} \right) \right| \\ &\leq \frac{16}{T^2} \sum_{l=1}^p \max_{i,t} \left\{ E |x_{it,l} \epsilon_{it}|^{2/q} \right\}^{4/q} \sum_{t=1}^{T-1} \sum_{j=1}^{\infty} \phi(j)^{q-4/q}, \end{aligned}$$

where the last inequality holds by the Davydov inequality for strong mixing processes in combination with the moment conditions in Assumption 1(iii), qualified by the strong mixing condition on $\{(\mathbf{x}_{it}^{(2)}, \epsilon_{it}, t = 1, \dots, T)\}$ in Assumption 1(ii). Subsequently,

$$\begin{aligned} & \frac{16}{T^2} \sum_{l=1}^p \max_{i,t} \left\{ E |x_{it,l} \epsilon_{it}|^{2/q} \right\}^{4/q} \sum_{t=1}^{T-1} \sum_{j=1}^{\infty} \phi(j)^{q-4/q} \\ & \leq \frac{16}{T} \sum_{l=1}^p \max_{i,t} \{E |x_{it,l} \epsilon_{it}|\}^{6/q} c_{\phi} = O_p(T^{-1}). \end{aligned}$$

As a result, $E \|\hat{\mathbf{q}}_{i,z\epsilon}\|_2^2 = O(T^{-1})$ and, using Chebyshev's inequality, $\|\hat{\mathbf{q}}_{i,z\epsilon}\|_2 = O_p(T^{-1/2})$. Furthermore, $\|T^{-1} \sum_{t=1}^T \mathbf{z}_{it}\|_2 = O_p(M^{-1/2})$ as shown in (B.32) and $|T^{-1} \sum_{t=1}^T \epsilon_{it}| = O_p(T^{-1/2})$ by Assumption 1(ii). Using these intermediary steps, the triangle inequality, and the sub-multiplicative property,

$$\|\hat{\mathbf{q}}_{i,\tilde{z}\tilde{\epsilon}}\|_2 \leq \|\hat{\mathbf{q}}_{i,z\epsilon}\|_2 + \|T^{-1} \sum_{t=1}^T \mathbf{z}_{it}\|_2 |T^{-1} \sum_{t=1}^T \epsilon_{it}| = O_p(T^{-1/2}) + O_p(M^{-1/2}) O_p(T^{-1/2}) = O_p(T^{-1/2}). \quad (\text{B.36})$$

Combining the results in (B.35) and (B.36) yields

$$\|\hat{\mathbf{q}}_{i,\tilde{z}\tilde{u}}\|_2 = \|\hat{\mathbf{q}}_{i,\tilde{z}\tilde{\epsilon}} + \hat{\mathbf{q}}_{i,\tilde{z}\tilde{\rho}}\|_2 \leq \|\hat{\mathbf{q}}_{i,\tilde{z}\tilde{\epsilon}}\|_2 + \|\hat{\mathbf{q}}_{i,\tilde{z}\tilde{\rho}}\|_2 = O_p(T^{-1/2}) + O_p(M^{-\theta-1/2}) = O_p(T^{-1/2} + M^{-\theta-1/2})$$

by the triangle inequality.

Part (ii): Since the cross-sectional dependence is bounded according to Assumption 1(i), it follows readily that

$$\frac{1}{N} \sum_{i=1}^N \|\hat{\mathbf{q}}_{i,\tilde{z}\tilde{\epsilon}}\|_2^2 = O_p(T^{-1} + M^{-2\theta-1}),$$

using Lemma B.3(i). \square

Proof of Lemma B.4. Consider the un-penalized criterion function $\mathcal{F}_{NT,i}^*(\boldsymbol{\pi}_i) = T^{-1} \sum_{t=1}^T [\tilde{y}_{it} - \tilde{\mathbf{z}}_{it}' \boldsymbol{\pi}_i]^2$. Define $\mathbf{a}_i = \boldsymbol{\pi}_i - \boldsymbol{\pi}_i^0$ and recognize that $\mathcal{F}_{NT,i}^*(\boldsymbol{\pi}_i) - \mathcal{F}_{NT,i}^*(\boldsymbol{\pi}_i^0) = -2\mathbf{a}_i' \hat{\mathbf{q}}_{i,\tilde{z}\tilde{u}} + \mathbf{a}_i' \hat{\mathbf{Q}}_{i,\tilde{z}\tilde{z}} \mathbf{a}_i$ as shown in (B.1). The inequality $\mathcal{F}_{NT,i}^*(\dot{\boldsymbol{\pi}}_i, \lambda) \leq \mathcal{F}_{NT,i}^*(\boldsymbol{\pi}_i^0, \lambda)$ holds trivially since $\dot{\boldsymbol{\pi}}_i = \arg \min_{\boldsymbol{\pi}_i} \mathcal{F}_{NT,i}^*(\boldsymbol{\pi}_i, \lambda)$. Plugging the decomposition into this inequality gives

$$\begin{aligned} 0 & \geq \mathcal{F}_{NT,i}^*(\dot{\boldsymbol{\pi}}_i, \lambda) - \mathcal{F}_{NT,i}^*(\boldsymbol{\pi}_i^0, \lambda) = -2\dot{\mathbf{a}}_i' \hat{\mathbf{q}}_{i,\tilde{z}\tilde{u}} + \dot{\mathbf{a}}_i' \hat{\mathbf{Q}}_{i,\tilde{z}\tilde{z}} \dot{\mathbf{a}}_i \\ & \geq -2\|\dot{\mathbf{a}}_i\|_2 \|\hat{\mathbf{q}}_{i,\tilde{z}\tilde{u}}\|_2 + \|\dot{\mathbf{a}}_i\|_2^2 M^{-1} \underline{c}_{\tilde{z}\tilde{z}} = 2\|\dot{\mathbf{a}}_i\|_2 O_p(T^{-1/2} + M^{-\theta-1/2}) + \|\dot{\mathbf{a}}_i\|_2^2 M^{-1} \underline{c}_{\tilde{z}\tilde{z}}, \end{aligned}$$

where Lemma B.3(i) provides the rate of $\|\hat{\mathbf{q}}_{i,\tilde{z}\tilde{u}}\|_2$ and the predictor variance-covariance matrix is substituted with its lower bound $\underline{c}_{\tilde{z}\tilde{z}}$ according to Lemma B.2(i), similar to the argument in the proof of Theorem 3.1.

Averaging over all $i = 1, \dots, N$ and rearranging yields

$$\frac{2}{\underline{c}_{\tilde{z}\tilde{z}}} O_p(MT^{-1/2} + M^{-\theta+1/2}) \frac{1}{N} \sum_{i=1}^N \|\dot{\mathbf{a}}_i\|_2 \geq \sum_{i=1}^N \|\dot{\mathbf{a}}_i\|_2^2. \quad (\text{B.37})$$

As in Theorem 3.1, $\|\dot{\mathbf{a}}_i\|_2 = \|\dot{\boldsymbol{\pi}}_i - \boldsymbol{\pi}_i^0\|_2 = O_p(T^{-1/2}M + M^{-\theta+1/2})$ to ensure that the inequality in (B.37) holds for an arbitrarily large $\|\dot{\mathbf{a}}_i\|_2$. Assumption 2(i) ensures that $T^{-1/2}M$ is not explosive and $-\theta + 1/2 < 0$ by Assumption 1(vi). \square

Proof of Lemma B.5. Recall that $\dot{\boldsymbol{\pi}} = (\dot{\boldsymbol{\pi}}_1', \dots, \dot{\boldsymbol{\pi}}_N')'$ represents an initial least squares estimate, which, given Lemma B.4, is $(MT^{-1/2} + M^{-\theta+1/2})^{-1}$ consistent. Define $\dot{\boldsymbol{\pi}}_i - \boldsymbol{\pi}_i^0 = (MT^{-1/2} + M^{-\theta+1/2})\dot{\mathbf{v}}_i$ and recognize that $\|\dot{\mathbf{v}}_i\|_2 = O_p(1)$. Along the lines of Qian and Su (2016a, Lemma B.2), rewrite

$$\begin{aligned} \dot{\omega}_{ij} &= \|\dot{\boldsymbol{\pi}}_i - \dot{\boldsymbol{\pi}}_j\|_2^{-\kappa} = \left\| \left[(MT^{-1/2} + M^{-\theta+1/2})\dot{\mathbf{v}}_i + \boldsymbol{\pi}_i^0 \right] - \left[(MT^{-1/2} + M^{-\theta+1/2})\dot{\mathbf{v}}_j + \boldsymbol{\pi}_j^0 \right] \right\|_2^{-\kappa} \\ &= \left\| \boldsymbol{\pi}_i^0 - \boldsymbol{\pi}_j^0 + (MT^{-1/2} + M^{-\theta+1/2})(\dot{\mathbf{v}}_i - \dot{\mathbf{v}}_j) \right\|_2^{-\kappa} = \left\| \boldsymbol{\pi}_i^0 - \boldsymbol{\pi}_j^0 + (MT^{-1/2} + M^{-\theta+1/2}) \right\|_2^{-\kappa}. \end{aligned}$$

Part (i): Let $i, j \in G_k^0$ and subsequently $\boldsymbol{\pi}_i^0 = \boldsymbol{\pi}_j^0 = \boldsymbol{\xi}_k^0$. Considering the minimum adaptive weight,

$$\begin{aligned} \min_{i,j \in G_k^0} \dot{\omega}_{ij} &= \min_{i,j \in G_k^0} \left\| \boldsymbol{\pi}_i^0 - \boldsymbol{\pi}_j^0 + O_p(MT^{-1/2} + M^{-\theta+1/2}) \right\|_2^{-\kappa} \\ &= \min_{i,j \in G_k^0} \left\| O_p(MT^{-1/2} + M^{-\theta+1/2}) \right\|_2^{-\kappa} = O_p((MT^{-1/2} + M^{-\theta+1/2})^{-\kappa}). \end{aligned}$$

Part (ii): Let $i \in G_k^0, j \notin G_k^0$ and as a result $\boldsymbol{\pi}_i^0 \neq \boldsymbol{\pi}_j^0$. Now, analyzing the maximum weight,

$$\begin{aligned} \max_{i \in G_k^0, j \notin G_k^0} \dot{\omega}_{ij} &= \max_{i \in G_k^0, j \notin G_k^0} \left\| \boldsymbol{\pi}_i^0 - \boldsymbol{\pi}_j^0 + O_p(MT^{-1/2} + M^{-\theta+1/2}) \right\|_2^{-\kappa} \\ &= \left\| \min_{i \in G_k^0, j \notin G_k^0} (\boldsymbol{\pi}_i^0 - \boldsymbol{\pi}_j^0) + O_p(MT^{-1/2} + M^{-\theta+1/2}) \right\|_2^{-\kappa} \\ &= O_p(J_{\min}^{-\kappa}), \end{aligned}$$

where $J_{\min} = \min_{i \in G_k^0, j \notin G_k^0} \|\boldsymbol{\pi}_i^0 - \boldsymbol{\pi}_j^0\|_2$ and Assumption 2(ii) ensures that J_{\min} dominates an $O_p(MT^{-1/2} + M^{-\theta+1/2})$ term in the limit. \square

Proof of Lemma B.6.

Part (i): Recognize that $\|\mathbf{b}_c\|_2 = \|\mathbf{c} \otimes \mathbf{b}(v)\|_2 = \|\mathbf{c}\|_2 \|\mathbf{b}(v)\|_2$ by property of the Kronecker product and a nonrandom $p \times 1$ vector \mathbf{c} with $\|\mathbf{c}\|_2 = 1$ (see the proof of Theorem 3.5(ii)) and, following Lemma B.1(i), $\|\mathbf{b}(v)\|_2 = 1$. Subsequently, $\|\mathbf{b}_c\|_2 = O_p(1)$.

Part (ii): Consider

$$\begin{aligned} s_{c,\hat{G}_k}^2 &= \frac{M}{N_k T} \mathbf{b}_c' \left(M N_k^{-1} \hat{\mathbf{Q}}_{G_k^0, \tilde{z}\tilde{z}} \right)^{-1} \sum_{i \in G_k^0} \left[\tilde{\mathbf{Z}}_i' E(\boldsymbol{\epsilon}_i \boldsymbol{\epsilon}_i') \tilde{\mathbf{Z}}_i \right] \left(M N_k^{-1} \hat{\mathbf{Q}}_{G_k^0, \tilde{z}\tilde{z}} \right)^{-1} \mathbf{b}_c \\ &\leq \|\mathbf{b}_c\|_2^2 \left[\mu_{\min} \left(M N_k^{-1} \hat{\mathbf{Q}}_{G_k^0, \tilde{z}\tilde{z}} \right) \right]^{-2} \frac{M}{N_k T} \sum_{i \in G_k^0} \left[\tilde{\mathbf{Z}}_i' E(\boldsymbol{\epsilon}_i \boldsymbol{\epsilon}_i') \tilde{\mathbf{Z}}_i \right] \\ &\leq \|\mathbf{b}_c\|_2^2 \left[\mu_{\min} \left(M N_k^{-1} \hat{\mathbf{Q}}_{G_k^0, \tilde{z}\tilde{z}} \right) \right]^{-2} \max_{i \in G_k^0} [\mu_{\max}(E(\boldsymbol{\epsilon}_i \boldsymbol{\epsilon}_i'))] \mu_{\max} \left(\frac{M}{N_k} \hat{\mathbf{Q}}_{G_k^0, \tilde{z}\tilde{z}} \right) \\ &\leq \frac{\|\mathbf{b}_c\|_2^2 \bar{c}_{\epsilon\epsilon} \bar{c}_{\tilde{z}\tilde{z}}}{\underline{c}_{\tilde{z}\tilde{z}}^2}, \end{aligned}$$

by the Triangle property and $\mathbf{a}' \mathbf{A} \mathbf{a} \geq \mu_{\min}(\mathbf{A}) \mathbf{a}' \mathbf{a}$ for a conformable vector \mathbf{a} and matrix \mathbf{A} . Furthermore, notice that $\|\mathbf{b}_c\|_2^2 = O_p(1)$ as shown in Lemma B.6(i), $\max_{1 \leq i \leq N} \mu_{\max} \left(M N_k^{-1} \hat{\mathbf{Q}}_{G_k^0, \tilde{z}\tilde{z}} \right) \leq \bar{c}_{\tilde{z}\tilde{z}}$ and $\min_{1 \leq i \leq N} \mu_{\min} \left(M N_k^{-1} \hat{\mathbf{Q}}_{G_k^0, \tilde{z}\tilde{z}} \right) \geq \underline{c}_{\tilde{z}\tilde{z}}$ by Lemma B.2(ii), and $\max_{i \in G_k^0} \mu_{\max}(E(\boldsymbol{\epsilon}_i \boldsymbol{\epsilon}_i')) \leq \bar{c}_{\epsilon\epsilon}$ by Assumption 4(i). In consequence, $s_{c,\hat{G}_k}^2 = O_p(1)$ (see Su et al., 2019, Lemma A.8). \square

Proof of Lemma B.7. The proof of (B.41) works by demonstrating that the *MSE* of an overfitted model and the *MSE* of a model with the true grouping structure both converge towards the non-reducible residual error variance in the limit. The different converge rates give the result in (B.41).

$$\begin{aligned} \hat{\sigma}_{G^0}^2 &= \frac{1}{NT} \sum_{k=1}^{K_0} \sum_{i \in G_k^0} \sum_{t=1}^T \hat{u}_{it}^2 = \frac{1}{NT} \sum_{k=1}^{K_0} \sum_{i \in G_k^0} \sum_{t=1}^T \left[\tilde{y}_{it} - \hat{\boldsymbol{\alpha}}_{G_k^0}^{p'} \left(\frac{t}{T} \right) \tilde{\mathbf{x}}_{it} \right]^2 \\ &= \frac{1}{NT} \sum_{k=1}^{K_0} \sum_{i \in G_k^0} \sum_{t=1}^T \left[\tilde{\epsilon}_{it} - \left(\hat{\boldsymbol{\alpha}}_{G_k^0}^p \left(\frac{t}{T} \right) - \boldsymbol{\alpha}_{G_k^0}^0 \left(\frac{t}{T} \right) \right)' \tilde{\mathbf{x}}_{it} \right]^2 \\ &= \frac{1}{NT} \sum_{i=1}^N \sum_{t=1}^T \tilde{\epsilon}_{it}^2 - \frac{1}{NT} \sum_{k=1}^{K_0} \sum_{i \in G_k^0} \sum_{t=1}^T \left[\left(\hat{\boldsymbol{\alpha}}_{G_k^0}^p \left(\frac{t}{T} \right) - \boldsymbol{\alpha}_{G_k^0}^0 \left(\frac{t}{T} \right) \right)' \tilde{\mathbf{x}}_{it} \tilde{\epsilon}_{it} \right] \\ &\quad + \frac{1}{NT} \sum_{k=1}^{K_0} \sum_{i \in G_k^0} \sum_{t=1}^T \left[\left(\hat{\boldsymbol{\alpha}}_{G_k^0}^p \left(\frac{t}{T} \right) - \boldsymbol{\alpha}_{G_k^0}^0 \left(\frac{t}{T} \right) \right)' \tilde{\mathbf{x}}_{it} \right]^2 \end{aligned} \tag{B.38}$$

Denote the irreducible sample *MSE* as $\bar{\sigma}_{NT}^2 = (NT)^{-1} \sum_{i=1}^N \sum_{t=1}^T \tilde{\epsilon}_{it}^2$. Moreover, given Theo-

rem 3.5(ii), $\hat{\alpha}_{\tilde{G}_k}^p(t/T)$ is $((N_{k,\min}T)^{1/2}M^{1/2})$ -consistent, where $N_{k,\min} = \min_{k=1,\dots,K_0} N_k$. Due to Assumption 1(ii), $\|T^{-1} \sum_{t=1}^T \tilde{\mathbf{x}}_{it} \tilde{\epsilon}_{it}\|_2 = O_p(T^{1/2})$. In addition, note that $N^{-1} \sum_{k=1}^{K_0} \sum_{i \in G_k^0} \|\hat{\mathbf{q}}_{i,\tilde{x}\tilde{\epsilon}}\|_2 = N^{1/2} O_p(T^{1/2})$ as a function of weak cross-sectional dependence (see Assumption 1(i)). Plugging these results into (B.38) yields the rates

$$\begin{aligned} \hat{\sigma}_{\mathcal{G}^0}^2 &= \bar{\sigma}_{NT}^2 + O_p\left((NT)^{1/2}M^{1/2}\right) O_p((NT)^{1/2}) + O_p\left((NT)^{-1}M\right) O_p(1) \\ &= \bar{\sigma}_{NT}^2 + O_p\left((TN)^{-1}M\right). \end{aligned} \quad (\text{B.39})$$

Define the set $\bar{\mathbb{G}}_K = \{\bar{\mathcal{G}}_K = \{\bar{G}_k\}_{k=1}^K : \nexists i, j \in \bar{G}_K \text{ where } i \in G_l^0, j \notin G_l^0, 1 \leq l \leq K_0\}$ with $K_0 < K \leq K_{\max} = N$. That is, each $\bar{\mathcal{G}}_K \in \bar{\mathbb{G}}_K$ denotes a partition of $K > K_0$ over N where no heterogeneous cross-sectional units are pooled together in any group. Hence, it is trivial that $\hat{\sigma}_{\bar{\mathcal{G}}_K}^2 \leq \hat{\sigma}_{\mathcal{G}^0}^2$. Given the result in (B.39), we can expand this inequality to

$$0 \leq \hat{\sigma}_{\mathcal{G}^0}^2 - \hat{\sigma}_{\bar{\mathcal{G}}_K}^2 = \bar{\sigma}_{NT}^2 - \hat{\sigma}_{\bar{\mathcal{G}}_K}^2 + O_p((NT)^{-1}M). \quad (\text{B.40})$$

Let \mathcal{J}_{NT} be the largest distance between the estimated and irreducible mean squared error for any of the $K_0 < K \leq K_{\max}$ groups

$$\mathcal{J}_{NT} = \max_{K_0 < k \leq K} \inf_{\alpha} \left\{ \frac{1}{N_k T} \sum_{i \in \bar{G}_k} \sum_{t=1}^T \left[\tilde{\epsilon}_{it}^2 - \left(\tilde{y}_{it} - \tilde{\mathbf{x}}_{it}' \alpha_k \left(\frac{t}{T} \right) \right)^2 \right] \right\},$$

such that $\bar{\sigma}_{NT}^2 - \hat{\sigma}_{\bar{\mathcal{G}}_K}^2 \leq K \mathcal{J}_{NT}$. Then

$$\check{\alpha}_k \left(\frac{t}{T} \right) = \check{\boldsymbol{\Xi}}_k' B \left(\frac{t}{T} \right) = \arg \min_{\xi_k} \frac{1}{N_k T} \sum_{i \in \bar{G}_k} \sum_{t=1}^T \left[\tilde{\epsilon}_{it}^2 - \left(\tilde{y}_{it} - \tilde{\mathbf{z}}_{it}' \check{\boldsymbol{\xi}}_k \left(\frac{t}{T} \right) \right)^2 \right],$$

with $\check{\boldsymbol{\xi}}_k = (\sum_{i \in \bar{G}_k} \sum_{t=1}^T \tilde{\mathbf{z}}_{it} \tilde{\mathbf{z}}_{it}')^{-1} \sum_{i \in \bar{G}_k} \sum_{t=1}^T \tilde{\mathbf{z}}_{it} \tilde{y}_{it}$. Since $K_0 < K \leq K_{\max} = N$, the minimum group cardinality is 1 and $\check{\alpha}_k(t/T)$ is, in line with section B.2, only $\sqrt{M/T}$ -consistent. As a consequence, $\mathcal{J}_{NT} = O_p(T^{-1}M)$.

Plugging $\bar{\sigma}_{NT}^2 - \hat{\sigma}_{\bar{\mathcal{G}}_K}^2 \leq K \mathcal{J}_{NT} = O_p(T^{-1}M)$ into (B.40), it becomes apparent that $0 \leq \hat{\sigma}_{\mathcal{G}^0}^2 - \hat{\sigma}_{\bar{\mathcal{G}}_K}^2 \leq O_p(T^{-1}M) + O_p((NT)^{-1}M) = O_p(T^{-1}M)$. Then, by construction of \mathcal{J}_{NT} ,

$$\max_{K_0 < K \leq K_{\max}} \sup_{\bar{\mathcal{G}}_K \in \bar{\mathbb{G}}_K} |\hat{\sigma}_{\bar{\mathcal{G}}_K}^2 - \hat{\sigma}_{\mathcal{G}^0}^2| = O_p(T^{-1}M). \quad (\text{B.41})$$

□

C Numerical Implementation

We minimize the criterion (2.6) using an iterative *ADMM* algorithm, adapted from [Ma and Huang \(2017, sec. 3.1\)](#) and [Mehrabani \(2023, sec. 5.1\)](#). Let $\mathbf{a}_{ij} = \boldsymbol{\pi}_i - \boldsymbol{\pi}_j$. Then minimizing

$$\mathcal{F}_{NT}(\boldsymbol{\pi}, \mathbf{a}, \lambda) = \frac{1}{T} \sum_{i=1}^N \sum_{t=1}^T (\tilde{y}_{it} - \boldsymbol{\pi}'_i \tilde{\mathbf{z}}_{it})^2 + \frac{\lambda}{N} \sum_{i=1}^{N-1} \sum_{j=i+1}^N \omega_{ij} \|\mathbf{a}_{ij}\|_2 \text{ subject to } \mathbf{a}_{ij} = \boldsymbol{\pi}_i - \boldsymbol{\pi}_j, \quad (\text{C.1})$$

is equivalent to optimizing the objective in (2.6). We can rewrite this constraint optimization as an Augmented Lagrangian problem

$$\begin{aligned} \mathcal{L}_{NT,\vartheta}(\boldsymbol{\pi}, \mathbf{a}, \lambda, \mathbf{v}) &= \frac{T}{2} \mathcal{F}_{NT}(\boldsymbol{\pi}, \mathbf{a}, \lambda) + \sum_{i=1}^{N-1} \sum_{j=i+1}^N \mathbf{v}'_{ij} (\boldsymbol{\pi}_i - \boldsymbol{\pi}_j - \mathbf{a}_{ij}) + \frac{\vartheta}{2} \sum_{i=1}^{N-1} \sum_{j=i+1}^N \|\boldsymbol{\pi}_i - \boldsymbol{\pi}_j - \mathbf{a}_{ij}\|_2^2 \\ &= \mathcal{F}_{NT}^*(\boldsymbol{\pi}) + \mathcal{P}_{NT}^*(\mathbf{a}, \lambda) + \sum_{i=1}^{N-1} \sum_{j=i+1}^N \mathbf{v}'_{ij} (\boldsymbol{\pi}_i - \boldsymbol{\pi}_j - \mathbf{a}_{ij}) \\ &\quad + \frac{\vartheta}{2} \sum_{i=1}^{N-1} \sum_{j=i+1}^N \|\boldsymbol{\pi}_i - \boldsymbol{\pi}_j - \mathbf{a}_{ij}\|_2^2, \end{aligned} \quad (\text{C.2})$$

where \mathcal{F}_{NT}^* reflects the goodness-of-fit term and $\mathcal{P}_{NT}^*(\mathbf{a}, \lambda)$ the *PAGFL* penalty in (C.1), \mathbf{v}_{ij} denotes the dual variable and $\vartheta > 0$ the *ADMM* penalty parameter controlling the trade-off between feasibility and optimization.

The *ADMM* algorithm 1 iteratively minimizes (C.2) until convergence or until a maximum number of iterations l_{\max} is reached. We set the $l_{\max} = 50,000$ and the convergence tolerance $\varepsilon_{\text{tol}}^{\text{ADMM}}$ to $\varepsilon_{\text{tol}}^{\text{ADMM}} = 1 \times 10^{-10}$ for the simulation study and empirical illustration. Define $\tilde{\mathbf{y}} = (\tilde{y}'_1, \dots, \tilde{y}'_N)'$, $\tilde{\mathbf{y}}_i = (\tilde{y}_{i1}, \dots, \tilde{y}_{iT})'$; the $NT \times NMp$ regressor block-matrix $\tilde{\mathbf{Z}} = \text{diag}(\tilde{\mathbf{Z}}_1, \dots, \tilde{\mathbf{Z}}_N)$ with $\tilde{\mathbf{Z}}_i = (\tilde{\mathbf{z}}_{i1}, \dots, \tilde{\mathbf{z}}_{iT})'$; the $NMp \times 1$ coefficient vector $\boldsymbol{\pi} = (\boldsymbol{\pi}'_1, \dots, \boldsymbol{\pi}'_N)'$; the $MpN(N-1)/2 \times NMp$ differencing matrix $\boldsymbol{\Delta} = \boldsymbol{\varsigma} \otimes \mathbf{I}_{Mp}$ with $\boldsymbol{\varsigma} = \{\zeta_i - \zeta_j, 1 \leq i < j \leq N\}'$, and the $N \times 1$ indicator vector $\boldsymbol{\zeta}_i$ with a one as its i^{th} element and zeros elsewhere; the $MpN(N-1)/2 \times 1$ vectors $\mathbf{a} = \{\mathbf{a}'_{ij}, 1 \leq i < j \leq N\}'$ and $\mathbf{v} = \{\mathbf{v}'_{ij}, 1 \leq i < j \leq N\}'$. The primal steps of the *ADMM* are proximal updates of $\hat{\boldsymbol{\pi}}$ and $\hat{\mathbf{a}}$ and take the form

$$\begin{aligned} \boldsymbol{\pi}^{(l+1)} &= \arg \min_{\boldsymbol{\pi}} \left\{ \mathcal{F}_{NT}^*(\boldsymbol{\pi}) + \frac{\vartheta}{2} \left\| \boldsymbol{\Delta} \boldsymbol{\pi} - \mathbf{a}^{(l)} + \vartheta^{-1} \mathbf{v}^{(l)} \right\|_2^2 \right\} \\ \mathbf{a}^{(l+1)} &= \arg \min_{\mathbf{a}} \left\{ \mathcal{P}_{NT}^*(\mathbf{a}, \lambda) + \frac{\vartheta}{2} \left\| \boldsymbol{\Delta} \boldsymbol{\pi}^{(l)} - \mathbf{a} + \vartheta^{-1} \mathbf{v}^{(l)} \right\|_2^2 \right\}. \end{aligned}$$

Algorithm 1: *ADMM* algorithm to minimize the *FUSE-TIME* criterion (2.6).

Result: $\hat{\boldsymbol{\pi}}_i = \boldsymbol{\pi}_i^{(l)}$

$l \leftarrow 0;$

$\boldsymbol{\pi}^{(l)} \leftarrow \dot{\boldsymbol{\pi}};$

$\mathbf{a}^{(l)} \leftarrow \Delta\boldsymbol{\pi}^{(l)};$

$\mathbf{v}^{(l)} \leftarrow 0;$

while $\|\Delta\boldsymbol{\pi}^{(l)} - \mathbf{a}^{(l)}\|_2 > \varepsilon_{tol}^{ADMM}$ & $l < l_{\max}$ **do**

$l \leftarrow l + 1;$

Primal step 1: $\boldsymbol{\pi}^{(l)} \leftarrow \left(\tilde{\mathbf{Z}}' \tilde{\mathbf{Z}} + \vartheta \Delta' \Delta \right)^{-1} \left(\tilde{\mathbf{Z}}' \tilde{\mathbf{y}} + \vartheta \Delta' \mathbf{a}^{(l-1)} - \Delta' \mathbf{v}^{(l-1)} \right);$

Primal step 2: $\boldsymbol{\psi}_{ij}^{(l)} \leftarrow \boldsymbol{\pi}_i^{(l)} - \boldsymbol{\pi}_j^{(l)} - \vartheta^{-1} \mathbf{v}_{ij}^{(l-1)},$

$\mathbf{a}_{ij}^{(l)} \leftarrow \max \left\{ 1 - \dot{\boldsymbol{\omega}}_{ij} T \lambda / \left(2N \vartheta \|\boldsymbol{\psi}_{ij}^{(l)}\|_2 \right), 0 \right\} \boldsymbol{\psi}_{ij}^{(l)}$ for each $1 \leq i < j \leq N,$

$\mathbf{a}^{(l)} \leftarrow \left\{ \mathbf{a}_{ij}^{(l)}, 1 \leq i < j \leq N \right\}';$

Dual step: $\mathbf{v}^{(l)} \leftarrow \mathbf{v}^{(l-1)} + \vartheta (\Delta\boldsymbol{\pi}^{(l)} - \mathbf{a}^{(l)});$

end

In particular, we obtain $\boldsymbol{\pi}^{(l+1)}$ by solving

$$\frac{\partial}{\partial \boldsymbol{\pi}} \left[\mathcal{F}_{NT}^*(\boldsymbol{\pi}) + \vartheta/2 \left\| \Delta\boldsymbol{\pi} - \mathbf{a}^{(l)} + \vartheta^{-1} \mathbf{v}^{(l)} \right\|_2^2 \right] = 0,$$

where $\mathcal{F}_{NT}^*(\boldsymbol{\pi}) = 1/2 \|\tilde{\mathbf{y}} - \tilde{\mathbf{Z}}\boldsymbol{\pi}\|_2^2$.

The *PAGFL* penalty is applied to each pair of cross-sectional units separately. Subsequently, $\mathbf{a}^{(l+1)}$ must be derived individually for each i, j . Therefore, we take

$$\mathbf{a}_{ij}^{(l+1)} = \arg \min_{\mathbf{a}_{ij}} \left\{ \frac{T\lambda}{2N} \sum_{i=1}^{N-1} \sum_{j=i+1}^N \dot{\boldsymbol{\omega}}_{ij} \|\mathbf{a}_{ij}\|_2 + \frac{\vartheta}{2} \sum_{i=1}^{N-1} \sum_{j=i+1}^N \|\boldsymbol{\pi}_i^{(l)} - \boldsymbol{\pi}_j^{(l)} - \mathbf{a}_{ij} - \vartheta^{-1} \mathbf{v}_{ij}\|_2^2 \right\},$$

the closed-form solution of which is the typical soft-thresholding rule

$$\mathbf{a}_{ij}^{(l+1)} = \max \left\{ 1 - \frac{T\lambda}{2N} \frac{\dot{\boldsymbol{\omega}}_{ij}/\vartheta}{\|\boldsymbol{\pi}_i^{(l)} - \boldsymbol{\pi}_j^{(l)} - \mathbf{a}_{ij} - \vartheta^{-1} \mathbf{v}_{ij}\|_2}, 0 \right\} \left(\boldsymbol{\pi}_i^{(l)} - \boldsymbol{\pi}_j^{(l)} - \mathbf{a}_{ij} - \vartheta^{-1} \mathbf{v}_{ij} \right),$$

which appears in Algorithm 1. The dual step of the *ADMM* algorithm enforces feasibility by updating the Lagrange multipliers to drive the constraint $\boldsymbol{\pi}_i - \boldsymbol{\pi}_j = \mathbf{a}_{ij}$, moderated by the *ADMM* penalty ϑ .

Since the objective function of *FUSE-TIME* (2.6) is convex, Algorithm 1 achieves convergence to the optimal point as $l \rightarrow \infty$. Furthermore, given that the primal residual $\mathbf{r}_1^{(l)} = \Delta\boldsymbol{\pi}^{(l)} - \mathbf{a}^{(l)}$ and

dual residual $\mathbf{r}_2^{(l)} = \vartheta \Delta(\boldsymbol{\pi}^{(l)} - \boldsymbol{\pi}^{(l-1)})$ tend to zero asymptotically

$$\lim_{l \rightarrow \infty} \|\mathbf{r}_d^{(l)}\|_2^2 = 0, \quad d = \{1, 2\},$$

the algorithm achieves both primal and dual feasibility. The proof of these properties is identical to [Mehrabani \(2023, Supplement, Appendix C\)](#) and thus omitted.

In theory, two individuals i, j are only fused together if $\|\hat{\boldsymbol{\pi}}_i - \hat{\boldsymbol{\pi}}_j\|_2 = 0$. However, employing the *ADMM* algorithm, it is not always computationally feasible for normed coefficient vector differences to equal zero exactly. As a consequence, we relax this condition and group two individuals if $\|\hat{\boldsymbol{\pi}}_i - \hat{\boldsymbol{\pi}}_j\|_2 < \varepsilon_{\text{tol}}^{\mathcal{G}}$, where $\varepsilon_{\text{tol}}^{\mathcal{G}}$ is set to a machine inaccuracy value. The smaller $\varepsilon_{\text{tol}}^{\mathcal{G}}$, the more *ADMM* algorithm iterations are required to obtain suitable results. As a consequence, there is an efficiency-accuracy trade-off when selecting $\varepsilon_{\text{tol}}^{\mathcal{G}}$. We find that $\varepsilon_{\text{tol}}^{\mathcal{G}} = 0.001$ yields good computational efficiency while still providing sharp between-group distinction. Similarly, it may occur that $\|\hat{\boldsymbol{\pi}}_i - \hat{\boldsymbol{\pi}}_j\|_2 < \varepsilon_{\text{tol}}^{\mathcal{G}}$ and $\|\hat{\boldsymbol{\pi}}_i - \hat{\boldsymbol{\pi}}_l\|_2 < \varepsilon_{\text{tol}}^{\mathcal{G}}$, but $\|\hat{\boldsymbol{\pi}}_j - \hat{\boldsymbol{\pi}}_l\|_2 \geq \varepsilon_{\text{tol}}^{\mathcal{G}}$. Since the group structure must be transitive, we nonetheless assign such triplets (i, j, l) to the same group in our numerical implementation.

Furthermore, splinter groups with only one or a few members may emerge in empirical or simulation settings. This characteristic also has been previously documented for similar models (see [Su et al., 2016, 2019; Mehrabani, 2023; Dzemski and Okui, 2024](#)). Such trivial groups can be precluded by either increasing $\varepsilon_{\text{tol}}^{\mathcal{G}}$ or by increasing the number of iterations of the *ADMM* algorithm. However, another solution is to specify a floor on the group cardinalities, e.g., 5% of N , and place individuals of groups that fall short of this threshold into remaining groups of sufficient size according to the lowest *MSE*. We impose such a $N_k/N \geq 5\%$ rule for the simulation study in Section 4 and the empirical illustration in Section 5. Note that in the subsequent simulation study, the preliminary coefficient vector differences $\|\hat{\boldsymbol{\pi}}_i - \hat{\boldsymbol{\pi}}_j\|_2$ exceed $\varepsilon_{\text{tol}}^{\mathcal{G}} = 0.001$ in all but a negligible amount of instances. Subsequently, this simple *MSE*-based classifier in combination with $\varepsilon_{\text{tol}}^{\mathcal{G}}$ leads to almost no groupings and the clustering procedure is driven by the penalization routine.

The function `fuse_time()` of our companion R-package `PAGFL` ([Haimerl et al., 2025](#)) provides an user-friendly and efficient open-source software implementation of the numerical algorithm presented in this section, along with a plethora of other functions and extensions.

D Extensions

In the following, we provide details on several extensions to broaden the scope of *FUSE-TIME*.

D.1 Panels with Coefficient-specific Groups or Breaks in the Group Structure

Consider a panel data model where each coefficient function follows a distinct group structure. This a setup reflects, for example, heterogeneous responses of economies to commodity price shocks: a specific country may be equally exposed to fluctuations in oil prices than one set of peers but form a group with a different set of countries regarding the effect of coal prices (Cashin et al., 2014).

We extend the DGP in (2.1) to allow each of the p functional coefficients in $\beta_i^0(t/T)$ to follow a unique unobserved group pattern

$$\beta_{il}^0\left(\frac{t}{T}\right) = \sum_{k=1}^{K_{0l}} \alpha_{kl}^0\left(\frac{t}{T}\right) \mathbf{1}\{i \in G_{kl}^0\}, \quad l = 1, \dots, p. \quad (\text{D.1})$$

Note that both the group adherence G_{kl}^0 and the total number of groups K_{0l} may vary for each of the p coefficient functions. To identify the coefficient-specific groups in (D.1), we adjust the penalty in the *FUSE-TIME* criterion (2.6) such that the group-Lasso operates on the M control points associated with each functional coefficient, as opposed to the entire $M \times p$ matrix Π_i . Let π_{il} denote the l^{th} column of Π_i and specify the criterion

$$\mathcal{F}_{NT}(\pi, \lambda) = \frac{1}{T} \sum_{i=1}^N \sum_{t=1}^T (\tilde{y}_{it} - \pi_i' \tilde{z}_{it})^2 + \frac{\lambda}{N} \sum_{l=1}^p \sum_{i=1}^{N-1} \sum_{j=i+1}^N \dot{\omega}_{ijl} \|\pi_{il} - \pi_{jl}\|_2,$$

where the adaptive weight is defined as $\dot{\omega}_{ijl} = \|\dot{\pi}_{il} - \dot{\pi}_{jl}\|_2^{-\kappa}$ and $\dot{\pi}_i$ is identical to the base-case in Section 2.

Having obtained the p distinct group structures, the *post-Lasso* estimator follows as

$$\hat{\xi}^p = (\check{\mathbf{Z}}' \check{\mathbf{Z}})^{-1} \check{\mathbf{Z}}' \tilde{y},$$

where the $M \times \sum_{l=1}^p \hat{K}_l$ matrix $\hat{\Xi}^p = (\hat{\Xi}_1^p, \dots, \hat{\Xi}_p^p)$, $\text{vec}(\hat{\Xi}^p) = \hat{\xi}^p$, stacks coefficient-wise with $\hat{\Xi}_l^p = (\hat{\xi}_{l1}^p, \dots, \hat{\xi}_{l\hat{K}_l}^p)$ and $\hat{\xi}_{lk}^p$ holds the M control points shaping the time-varying function l of group k , with $k = 1, \dots, \hat{K}_l$ and $l = 1, \dots, p$. Moreover, let $\tilde{y} = (\tilde{y}_1', \dots, \tilde{y}_N')'$, $\tilde{y}_i = (\tilde{y}_{i1}, \dots, \tilde{y}_{iT})'$, and $\check{\mathbf{Z}} = (\check{\mathbf{Z}}_1, \dots, \check{\mathbf{Z}}_p)$, where $\check{\mathbf{Z}}_l$ is a $NT \times \hat{K}_l M$ regressor matrix $\check{\mathbf{Z}}_l = (\mathbf{D}_{l1}, \dots, \mathbf{D}_{l\hat{K}_l})(\mathbf{I}_{\hat{K}_l} \otimes \tilde{\mathbf{z}}_l)$. \mathbf{D}_{kl} indicates a $NT \times NT$ matrix selecting observations pertaining to group k of the l^{th} coefficient function $\mathbf{D}_{kl} = \text{diag}(\mathbf{d}_{kl}) \otimes \mathbf{I}_T$, where \mathbf{d}_{kl} is a vector of length N with ones for all $\{i \in \hat{G}_{kl}, 1 \leq i \leq N\}$ and zeros elsewhere. $\tilde{\mathbf{z}}_l$ is a $NT \times M$ matrix that collects all basis functions corresponding to the l^{th} coefficient function $\tilde{\mathbf{z}}_l = (\tilde{z}_{1l}', \dots, \tilde{z}_{Nl}')'$, $\tilde{z}_{il} = (\tilde{z}_{i1l}, \dots, \tilde{z}_{iTl})'$, with $\tilde{z}_{itl} = (\mathbf{r}_l \tilde{\mathbf{x}}_{it}) \otimes \mathbf{b}(t/T)$ and the $1 \times p$ selection vector \mathbf{r}_l featuring a one at position l and zeros for all remaining elements. The

time-varying functional coefficients for individual i are given by $\hat{\alpha}_i^p(t/T) = \mathbf{W}_i \hat{\Xi}^{p'} \mathbf{b}(t/T)$, where \mathbf{W}_i represents a $p \times \sum_{l=1}^p \hat{K}_l$ selection matrix $\mathbf{W}_i = \{(\mathbf{0}'_{1\{\{l\neq 1\}\sum_{s=1}^{l-1} \hat{K}_s}, \mathbf{w}'_l, \mathbf{0}'_{1\{\{l\neq p\}\sum_{s=l+1}^p \hat{K}_s})', 1 \leq l \leq p)\}'$ and \mathbf{w}_l is a vector of length \hat{K}_l with a one on position $k = \{k : i \in \hat{G}_{kl}, 1 \leq k \leq \hat{K}_l\}$ and zeros elsewhere.

Based on the derivations in Section 3, we conjecture that the preliminary convergence rates extend naturally to coefficient-wise groups. Moreover, the same applies to the limiting distribution of each coefficient function in Theorem 3 after replacing the global N_k with the coefficient-specific group size N_{kl} and inserting the coefficient group equivalents of $\hat{\Omega}_{G_k^0}$, $\hat{\mathcal{E}}_{G_k^0}$, and $\mathbf{q}_{G_k^0}$.

Analogous to defining the group-Lasso over the columns of $\hat{\Pi}_i$, it is also straightforward to penalize $\hat{\Pi}_i$ row-wise. In that case, the groupings do not vary among the p functional coefficients but among each of the M basis functions in $\mathbf{b}(t/T)$. Since the basis functions vanish outside their respective interval $\{V_m\}_{m=-d}^{M^*}$ (cf. (A.1)), the groups change over time. Furthermore, as $d+1$ basis functions overlap at any point along the domain (see Figure A.1, left panel), such a specification produces up to $\prod_{j=0}^d \hat{K}_{-d+j+\varphi}$ functional coefficient vectors unique to each interval $[v_\varphi, v_{\varphi+1})$ for $\varphi = 0, \dots, M^* - 1$ and $[v_{M^*}, v_{M^*+1}]$, where $\hat{K}_{-d+j+\varphi} = \hat{K}_m$ denotes the estimated number of groups of basis function m and v_φ indicates the respective knot (cf. Appendix A). Each interior knot reflects a break-point at which the group adherence may change, allowing for a total of $M^* + 1$ distinct groupings with a potential switch every $T/(M^* + 1)$ time periods. This significantly complicates the interpretation of the group structure but allows the coefficient functions of different cross-sectional individuals to coincide only for specific periods.

In addition, models with a mix of global, group-specific, and individual coefficients have found ample empirical use, mirroring models with both common, group-level, and idiosyncratic factors (see Diebold et al., 2008; Ando and Bai, 2016; Freyaldenhoven, 2022, among others). Such a structure is nested within coefficient-specific groups as introduced above. This becomes evident by reordering $\beta_i(t/T)$ such that $\beta_i(t/T) = (\beta_i^{(1)'}(t/T), \beta_i^{(2)'}(t/T), \beta^{(3)'}(t/T))'$, where only the $p^{(1)} \times 1$ functional vector $\beta_i^{(1)}(t/T)$ follows a latent group structure as described in (2.3), that is $\hat{\mathcal{G}}_l$ is identical for all $l = 1, \dots, p^{(1)}$. The $p^{(2)} \times 1$ vector $\beta_i^{(2)}(t/T)$ is idiosyncratic, $K_l = N$ for all $l = p^{(1)} + 1, \dots, p^{(2)}$. The $p^{(3)} \times 1$ vector $\beta^{(3)}(t/T)$ is common across all cross-sectional units such that $K_l = 1$ for all $l = p^{(2)} + 1, \dots, p^{(3)}$. Estimation then follows readily from the derivations above, where $\hat{\omega}_{ijl}$ is set to zero for all $l \in (p^{(1)}, p^{(2)})$ —inducing groups of cardinality one—and to an arbitrarily large value for all $l \in (p^{(2)}, p^{(3)})$ —inducing groups of cardinality N . The limiting distributions in Theorem 3.5 now hold for $\hat{\alpha}_{\hat{G}_k}^{(1)p}(t/T)$ when replacing p with $p^{(1)}$ and for $\hat{\alpha}_i^{(2)p}(t/T)$ when setting $p = p^{(2)}$ and $N_k = 1$. The global coefficients are subject to quicker convergence rates since all N individuals

are pooled. Subsequently, $\hat{\boldsymbol{\pi}}_i^{(3)}$ converges pointwise with a rate of $O_p(M(NT)^{-\frac{1}{2}} + M^{-\theta+\frac{1}{2}})$ and in mean-squares with $O_p(M^2(NT)^{-1} + M^{-2\theta+1})$. Likewise, to obtain the limiting distributions of the global coefficients in $\hat{\boldsymbol{\alpha}}_i^{(3)p}(t/T)$, one only needs to replace p with $p^{(3)}$ and substitute N_k with N in Theorem 3.5.

D.2 Panels with Time-Varying and Time-Constant Coefficients

Despite the frequent occurrence of time-variant functional relationships in applied settings, some coefficients may nonetheless remain constant. To accommodate this, reorder $\boldsymbol{\beta}_i(t/T)$ such that $\boldsymbol{\beta}_i(t/T) = (\boldsymbol{\beta}_i^{(1)'}(t/T), \boldsymbol{\beta}_i^{(2)'}')'$, where the $p^{(1)} \times 1$ vector $\boldsymbol{\beta}_i^{(1)}(t/T)$ varies smoothly over time and the $p^{(2)} \times 1$ vector $\boldsymbol{\beta}^{(2)}$ is constant. After partitioning $\mathbf{x}_{it} = (\mathbf{x}_{it}^{(1)'}, \mathbf{x}_{it}^{(2)'})'$ to conform with $\boldsymbol{\beta}_i(t/T)$, extend the criterion (2.6) to

$$\begin{aligned} \mathcal{F}_{NT}(\boldsymbol{\pi}^{(1)}, \boldsymbol{\beta}^{(2)}, \lambda) = & \frac{1}{T} \sum_{i=1}^N \sum_{t=1}^T \left(\tilde{y}_{it} - \boldsymbol{\pi}_i^{(1)'} \tilde{\mathbf{z}}_{it}^{(1)} - \boldsymbol{\beta}_i^{(2)'} \tilde{\mathbf{x}}_{it}^{(2)} \right)^2 \\ & + \frac{\lambda}{N} \sum_{i=1}^{N-1} \sum_{j=i+1}^N \dot{\omega}_{ij} \|\boldsymbol{\varpi}_i - \boldsymbol{\varpi}_j\|_2, \end{aligned}$$

where $\boldsymbol{\beta}^{(2)} = (\boldsymbol{\beta}_1^{(2)'}, \dots, \boldsymbol{\beta}_N^{(2)'})'$ and $\boldsymbol{\varpi}_i = (\boldsymbol{\pi}_i^{(1)'}, \boldsymbol{\beta}_i^{(2)'})'$. Furthermore, we now estimate the adaptive penalty weight $\dot{\omega}_{ij} = \|\dot{\boldsymbol{\varpi}}_i - \dot{\boldsymbol{\varpi}}_j\|_2^{-\kappa}$ as

$$\dot{\boldsymbol{\varpi}}_i = \arg \min_{\boldsymbol{\varpi}_i} \frac{1}{T} \sum_{t=1}^T \left(\tilde{y}_{it} - \boldsymbol{\pi}_i^{(1)'} \tilde{\mathbf{z}}_{it}^{(1)} - \boldsymbol{\beta}_i^{(2)'} \tilde{\mathbf{x}}_{it}^{(2)} \right)^2.$$

The *post-Lasso* estimator is defined as

$$\hat{\boldsymbol{\varpi}}^p = \arg \min_{\boldsymbol{\varpi}} \frac{1}{T} \sum_{t=1}^T \left(\tilde{y}_t - \text{diag}(\tilde{\mathbf{Z}}_{\hat{G}_1 t}^{(1)}, \dots, \tilde{\mathbf{Z}}_{\hat{G}_{\hat{K}} t}^{(1)})' \boldsymbol{\xi}^{(1)} - \text{diag}(\tilde{\mathbf{X}}_{\hat{G}_1 t}^{(2)}, \dots, \tilde{\mathbf{X}}_{\hat{G}_{\hat{K}} t}^{(2)})' \boldsymbol{\alpha}^{(2)} \right)^2,$$

where $\tilde{\mathbf{Z}}_{\hat{G}_k t}^{(1)} = \{\tilde{\mathbf{z}}_{it}^{(1)} : i \in \hat{G}_k, 1 \leq i \leq N\}$ and $\tilde{\mathbf{X}}_{\hat{G}_k t}^{(2)} = \{\tilde{\mathbf{x}}_{it}^{(2)} : i \in \hat{G}_k, 1 \leq i \leq N\}$, $\hat{\boldsymbol{\varpi}}^p = (\hat{\boldsymbol{\varpi}}_{\hat{G}_1}^{p'}, \dots, \hat{\boldsymbol{\varpi}}_{\hat{G}_{\hat{K}}}^{p'})'$ are $Mp^{(1)} \times \hat{K}$ and $Mp^{(2)} \times \hat{K}$ matrices collecting all observations pertaining to group k , respectively. Furthermore, $\hat{\boldsymbol{\varpi}}_{\hat{G}_k}^p = (\hat{\boldsymbol{\xi}}_{\hat{G}_k}^{(1)p}, \hat{\boldsymbol{\alpha}}_{\hat{G}_k}^{(2)p})'$, $\hat{\boldsymbol{\xi}}^{(1)p} = (\hat{\boldsymbol{\xi}}_{\hat{G}_1}^{(1)p}, \dots, \hat{\boldsymbol{\xi}}_{\hat{G}_{\hat{K}}}^{(1)p})$, $\hat{\boldsymbol{\alpha}}_{\hat{G}_k}^{(2)p} = (\hat{\boldsymbol{\alpha}}_{\hat{G}_1}^{(2)p}, \dots, \hat{\boldsymbol{\alpha}}_{\hat{G}_{\hat{K}}}^{(2)p})'$, and $\hat{\boldsymbol{\alpha}}_{\hat{G}_k}^{(1)p}(t/T) = \hat{\boldsymbol{\Xi}}_{\hat{G}_k}^{(1)p} \mathbf{b}(t/T)$. The remaining terms are as introduced in Section 2 and above.

It is straightforward to see that the asymptotic properties of $\boldsymbol{\pi}_i^{(1)}$ remain unchanged from Section 3 when substituting p with $p^{(1)}$. The same holds for $\hat{\boldsymbol{\beta}}_i^{(2)}$ when taking $M = 1$, $p = p^{(2)}$, and treating M as constant. The limiting distributions in Theorem 3.5 apply, when replacing p with

$p^{(l)}$, $l = \{1, 2\}$, respectively, and when fixing $M = 1$ for the vector of time-invariant coefficients.

D.3 Unbalanced Panels

Panel datasets with varying numbers of observations among individuals are ubiquitous in empirical applications. We accommodate such unbalanced panels in the *FUSE-TIME* framework by adjusting the DGP in (2.5) to

$$y_{it} = \gamma_i + \boldsymbol{\pi}_i^0 \mathbf{z}_{it} + u_{it}, \quad i = 1, \dots, N, \quad t = t_i, \dots, T_i,$$

where t_i indicates the individual start of the observational period for each cross-sectional unit, T_i the end, and $\mathcal{T}_i = T_i - t_i - 1$ the number of observed time periods per unit. It is straightforward to extend the objective function (2.6) to this scenario by rewriting

$$\mathcal{F}_{NT}(\boldsymbol{\pi}, \lambda) = \frac{1}{\mathcal{T}_i} \sum_{i=1}^N \sum_{t=t_i}^{T_i} (\tilde{y}_{it} - \boldsymbol{\pi}_i' \tilde{\mathbf{z}}_{it})^2 + \frac{\lambda}{N} \sum_{i=1}^{N-1} \sum_{j=i+1}^N \dot{\omega}_{ij} \|\boldsymbol{\pi}_i - \boldsymbol{\pi}_j\|_2,$$

with $\tilde{a}_{it} = a_{it} - \mathcal{T}_i^{-1} \sum_{t=t_i}^{T_i} a_{it}$ for $a_{it} = \{y_{it}, \mathbf{z}_{it}\}$. The remaining notation is left unchanged.

Similarly, the *post-Lasso* is given by

$$\hat{\boldsymbol{\xi}}_{\hat{G}_k}^p = \left(\sum_{i \in \hat{G}_k} \sum_{t=t_i}^{T_i} \tilde{\mathbf{z}}_{it} \tilde{\mathbf{z}}_{it}' \right)^{-1} \sum_{i \in \hat{G}_k} \sum_{t=t_i}^{T_i} \tilde{\mathbf{z}}_{it} \tilde{y}_{it}.$$

In order to study the asymptotic behavior, let $T_{\min} = \min_i \mathcal{T}_i$ and assume $T_{\min} \rightarrow \infty$. When substituting T with T_{\min} , all proofs and assumptions carry seamlessly over to unbalanced panel datasets (see [Su et al., 2019](#), sec. 5.2). Notice that this extension also applies to missing observations in the middle of the panel, i.e. $t = t_i, \dots, t_{i+j}, t_{i+j+l}, \dots, T_i$, for some integers $0 < j < T_i - 2$ and $1 < l < T_i - i - j$, since nonparametric splines implicitly interpolate missing values. Furthermore, the *post-Lasso* pools homogeneous cross-sectional units. In consequence, remaining group members compensate for a missing observation in individual series. These two aspects make our methodology particularly powerful in empirical applications with unbalanced panel datasets.

E Additional Simulation Studies and Details

Subsections [E.1](#) and [E.2](#) present the simulation study results when the errors are serially correlated and when 30% of observations are randomly discarded, respectively. Subsection [E.3](#) provides details on the implementation of the *time-varying C-Lasso* benchmark model.

Table E.1 reports the tuning parameter candidate values employed in the Monte Carlo experiments.

Table E.1: λ tuning parameter candidate values in the simulation studies

DGP 1		Section 4.3		AR(1) errors (E.1)		30% of the sample discarded (E.2)	
N	T	$\underline{\lambda}$	$\bar{\lambda}$	$\underline{\lambda}$	$\bar{\lambda}$	$\underline{\lambda}$	$\bar{\lambda}$
50	50	0.1	50	0.1	20	0.1	10
100	50	0.1	50	0.1	20	0.1	10
50	100	0.1	50	0.1	20	0.1	10
100	100	0.1	50	0.1	20	0.1	10
DGP 2		Section 4.3		AR(1) errors (E.1)		30% of the sample discarded (E.2)	
N	T	$\underline{\lambda}$	$\bar{\lambda}$	$\underline{\lambda}$	$\bar{\lambda}$	$\underline{\lambda}$	$\bar{\lambda}$
50	50	10	35	30	75	15	47
100	50	10	35	25	65	10	30
50	100	1	20	8	25	10	60
100	100	1	20	18	37	10	60
DGP 3		Section 4.3		AR(1) errors (E.1)		30% of the sample discarded (E.2)	
N	T	$\underline{\lambda}$	$\bar{\lambda}$	$\underline{\lambda}$	$\bar{\lambda}$	$\underline{\lambda}$	$\bar{\lambda}$
50	50	0.01	15	0.1	20	0.1	20
100	50	0.01	15	4	20	5	25
50	100	0.01	15	0.1	20	0.1	20
100	100	0.01	15	0.1	8	0.1	9

Notes: Upper and lower limits for the sequences of candidate λ penalty tuning parameter values. The sequences are of length 50 and run from $\underline{\lambda}$ to $\bar{\lambda}$.

E.1 DGPs with Serially Correlated Errors

Tables E.2 and E.3 report the Monte Carlo simulation study results of *FUSE-TIME* when the innovations are constructed as $\epsilon_{it} = 0.3\epsilon_{it-1} + e_{it}$, where $e_{it} \sim i.i.d.N(0, 1)$. Serial correlation in the errors to such an extent does not infringe on Assumption 1(ii), as the process still remains stationary. However, as serial correlation introduces additional estimation uncertainty and previous simulation studies in Section 4 show that such uncertainty complicates the clustering mechanism, we choose to reduce the number of interior knots M^* for this exercise. We select $M^* = 2$ for DGP 1 and $M^* = 1$ for DGPs 2 and 3.

When $T = 100$, the simulation results mirror largely the ones reported in Section 4.3. However, as serially correlated errors effectively reduce the informational value contained in a time series, the performance in small samples is notably reduced. This does not just concern the grouping mechanism and the resulting estimation inaccuracy, but also the *RMSE* of the infeasible oracle estimator.

Table E.2: Clustering accuracy with serially correlated errors

	N	T	Freq. $\hat{K} = K_0$	Freq. $\hat{\mathcal{G}}_{\hat{K}} = \mathcal{G}_{K_0}^0$	ARI	\bar{K}
DGP 1	50	50	0.680	0.190	0.855	3.270
	50	100	0.927	0.753	0.978	3.080
	100	50	0.680	0.077	0.809	2.753
	100	100	1.000	0.720	0.990	3.000
DGP 2	50	50	0.140	0.027	0.577	2.130
	50	100	0.757	0.647	0.878	2.760
	100	50	0.073	0.007	0.501	1.940
	100	100	0.512	0.383	0.768	2.510
DGP 3	50	50	0.567	0.030	0.708	2.680
	50	100	0.903	0.560	0.937	2.990
	100	50	0.160	0.007	0.550	2.130
	100	100	0.933	0.433	0.951	2.970

Notes: Frequency of *FUSE-TIME* obtaining the correct number of groups $\hat{K} = K_0$ and the correct grouping $\hat{\mathcal{G}}_{\hat{K}} = \mathcal{G}_{K_0}^0$, the ARI, and the average estimated number of total groups \bar{K} based on a Monte Carlo study with 300 replications. The errors are serially correlated with an autoregressive coefficient of 0.3.

Table E.3: *RMSE* of coefficient estimates with serially correlated errors

		N	T	<i>PSE</i>	<i>post-Lasso</i>	oracle
DGP 1	$\hat{\alpha}_{k,0}(t/T)$	50	50	0.426	0.282	0.188
		50	100	0.346	0.226	0.165
		100	50	0.470	0.290	0.163
		100	100	0.339	0.212	0.15
DGP 2	$\hat{\alpha}_{k,1}(t/T)$	50	50	0.357	0.225	0.161
		50	100	0.275	0.158	0.137
		100	50	0.359	0.238	0.135
		100	100	0.309	0.149	0.095
	$\hat{\alpha}_{k,2}(t/T)$	50	50	0.454	0.279	0.161
		50	100	0.314	0.162	0.120
		100	50	0.465	0.315	0.121
		100	100	0.385	0.184	0.088
DGP 3	$\hat{\alpha}_{k,3}(t/T)$	50	50	0.419	0.269	0.216
		50	100	0.339	0.230	0.222
		100	50	0.498	0.321	0.212
		100	100	0.364	0.226	0.219

Notes: *RMSE* of the *FUSE-TIME PSE*, the *FUSE-TIME post-Lasso*, and an infeasible oracle estimator based on a Monte Carlo study with 300 replication. The errors are serially correlated with an autoregressive coefficient of 0.3.

Table E.4: Clustering metrics in an unbalanced panel

	N	T	Freq. $\hat{K} = K_0$	Freq. $\hat{\mathcal{G}}_{\hat{K}} = \mathcal{G}_{K_0}^0$	ARI	\bar{K}
DGP 1	50	50	0.907	0.620	0.961	3.093
	50	100	1.000	0.973	0.998	3.000
	100	50	0.990	0.543	0.976	2.990
	100	100	1.000	0.980	0.999	3.000
DGP 2	50	50	0.477	0.090	0.713	2.530
	50	100	0.983	0.887	0.985	2.997
	100	50	0.337	0.050	0.620	2.260
	100	100	0.990	0.810	0.988	2.990
DGP 3	50	50	0.700	0.030	0.734	3.060
	50	100	0.910	0.467	0.939	3.057
	100	50	0.200	0.003	0.522	2.170
	100	100	0.853	0.277	0.906	2.873

Notes: Frequency of *FUSE-TIME* obtaining the correct number of groups $\hat{K} = K_0$ and the correct grouping $\hat{\mathcal{G}}_{\hat{K}} = \mathcal{G}_{K_0}^0$, the ARI, and the average estimated number of total groups \bar{K} based on a Monte Carlo study with 300 replications. 30% of observations randomly discarded to create an unbalanced panel dataset.

E.2 DGPs with Unbalanced Panels

Unbalanced panel datasets are a frequent occurrence in empirical work. Subsequently, we re-run our simulation study after discarding a randomly drawn 30% subset of each time series. This exercise gives an understanding how the clustering performance and the estimation of the functional coefficients behave when some observations have to be interpolated. Furthermore, in line with the decreased informational value of an unbalanced panel dataset, we again deviate from the heuristic for the number of internal knots M^* provided in section 4 and set $M^* = 2$ for DGP 1 and $M^* = 1$ for the remaining two DGPs. Table E.4 displays the clustering performance and Table E.5 the *RMSE* values.

In large samples both the clustering performance and the *RMSE* are very similar to the ones reported in Section 4.3. However, just like the in the previous subsection, small samples suffer from the reduced number of observations. This dynamic is particularly apparent in DGP 2. Omitting observations, even on the interior of time series, seems akin to reducing T with respect to the clustering performance and estimation accuracy of *FUSE-TIME*.

E.3 Implementation of the *Time-Varying C-Lasso*

In Section 4 we employ the *time-varying C-Lasso* by [Su et al. \(2019\)](#) as a benchmark, using Matlab replication files kindly provided by the authors. The *time-varying C-Lasso* and our methodology are exposed to the same simulated data, the DGPs following [Su et al. \(2019, sec. 6\)](#). The settings of the

Table E.5: *RMSE* of coefficient estimates in an unbalanced panel

		N	T	<i>PSE</i>	<i>post-Lasso</i>	oracle
DGP 1	$\hat{\alpha}_{k,0}(t/T)$	50	50	0.370	0.235	0.226
		50	100	0.276	0.212	0.152
		100	50	0.371	0.218	0.153
		100	100	0.259	0.203	0.142
DGP 2	$\hat{\alpha}_{k,1}(t/T)$	50	50	0.316	0.201	0.142
		50	100	0.233	0.145	0.123
		100	50	0.334	0.225	0.124
		100	100	0.241	0.138	0.112
DGP 3	$\hat{\alpha}_{k,2}(t/T)$	50	50	0.403	0.240	0.149
		50	100	0.267	0.138	0.124
		100	50	0.413	0.278	0.127
		100	100	0.273	0.127	0.112
DGP 3	$\hat{\alpha}_{k,3}(t/T)$	50	50	0.304	0.162	0.109
		50	100	0.207	0.076	0.064
		100	50	0.402	0.228	0.068
		100	100	0.236	0.076	0.053

Notes: *RMSE* of the *FUSE-TIME PSE*, the *FUSE-TIME post-Lasso*, and an infeasible oracle estimator based on a Monte Carlo study with 300 replication. 30% of observations randomly discarded to create an unbalanced panel dataset.

time-varying C-Lasso are specified as documented in [Su et al. \(2019, sec. 6\)](#): We set the polynomial degree to $d = 3$, the number of interior spline knots according to the heuristic $M^* = \lfloor (NT)^{1/6} \rfloor$ and the *C-Lasso* penalty tuning parameter to $\lambda = (NT)^{-(2K+3)/24}$. Furthermore, as the *C-Lasso* requires an explicit specification of the number of groups, we evaluate their IC for $K = \{2, 3, 4\}$, with ρ in the IC equaling $\rho = M^* \log(NT)/(NT)$ (cf. [Su et al., 2019, eq. 4.9](#)).

E.4 Benchmarking the *FUSE-TIME* and *C-Lasso* Implementation Speed

To provide a feel of the computational load, we benchmark the computational speed of both the *time-varying C-Lasso* and our *FUSE-TIME* routines on the first 100 out of the 300 simulated sample paths of DGP 1 with $N = 50$ and $T = 50$ (see Section 4.1).

The settings for each model are identical to Section 4. The *FUSE-TIME* is specified as in Section C, using the function `fuse_time()` of our companion R-package `PAGFL` ([Haimerl et al., 2025](#)) and searching over the 50 λ tuning parameter values given in Table E.1. We refer to the replication files available at github.com/Paul-Haimerl/replication-tv-pagfl for the exact implementation. The *time-varying C-Lasso* implementation is detailed in Section E.3.

Table E.6 presents summary statistics of the computing time of each software routine in seconds on a Lenovo Thinkpad T14 (64-bit Windows 11 E) with a quad-core AMD Ryzen 7 Pro 7840U CPU

Table E.6: Implementation speed benchmark

	Min	Q25	Median	Q75	Max	Freq. converged
<i>FUSE-TIME</i>	4.606s	9.600s	15.240s	39.345s	259.493s	1.000
<i>Time-varying C-Lasso</i>	77.769s	116.855s	141.435s	187.787s	387.950s	0.060

Notes: Computing time for each software routine for the first 100 simulated sample paths with $N = 50$ and $T = 50$ and the percentage amount of sample paths for which numerical convergence of the optimization routines was achieved.

and 16 GB of memory. Since the computational speed depends on whether a convergence criterion is met or the maximum number of iterations is reached, we also report the proportion of sample paths for which convergence was achieved.

The *FUSE-TIME* implementation is approximately nine times faster than the *time-varying C-Lasso*. This is, although *FUSE-TIME* satisfies the convergence criterion for every sample path, whereas the maximum number of iterations, set by the original authors in [Su et al. \(2019\)](#), is exceeded in 94% of cases. If we were to allow the numerical algorithm of the *time-varying C-Lasso* to fully converge, the computational load would increase significantly. In addition, the 50 considered λ values of *FUSE-TIME* lead to groupings ranging from a homogeneous panel ($\hat{K} = 1$) to an entirely heterogenous one ($\hat{K} = N$), whereas the *time-varying C-Lasso* considers only $K = \{2, 3, 4\}$.

F Details on the Empirical Illustration

The empirical illustration focuses on the 100 largest economies by GDP in 2022. The Global Carbon Budget provides CO₂ emission data for 99 of these economies, not tracking Puerto Rico. Additionally, we omit Azerbaijan (AZE), Iraq (IRQ), Kuwait (KWT), Luxembourg (LUX), Qatar (QAT), Turkmenistan (TKM), and the United Arab Emirates (ARE) from our study. These countries exhibit severe outliers and pronounced idiosyncratic volatility in their CO₂ intensity time series, predominantly attributable to extraordinary geopolitical events, such as conflicts and oil shocks, or unique economic structure, such as tax havens or petro-economies. Figure F.1 makes it apparent that the CO₂ intensity trajectories of these discarded economies diverge markedly from one another and from the estimated trend functions, further justifying their exclusion.

Table F.1 presents descriptive statistics for the final sample of CO₂ emission intensities. Table F.2 provides a detailed report of the estimated group structure, along with the group compositions in terms of the 92 countries included in the sample.

When estimating the empirical model, we consider the following candidate values of d , M^* , and λ : $d = \{2, 3, 4, 5\}$, $M^* = \{1, 2, \dots, 5\}$, $\lambda \in [0.01, 1.5]$ in increments of 0.01.

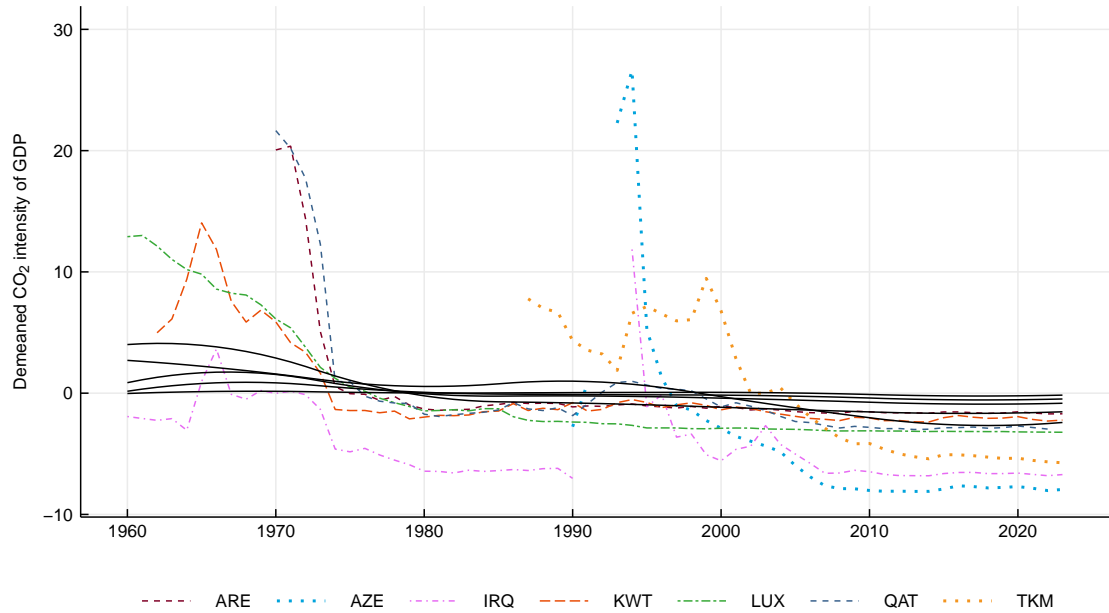


Figure F.1: Demeaned CO₂ intensity of countries excluded from the analysis (colored) and the estimated group-specific trend functions (black, solid) based on the remaining panel dataset. The 1991 and 1992 observations for Iraq (1991: 103.51, 1992: 117.79) in addition to the 1992 and 1993 observations for Azerbaijan (1992: 99.06, 1993: 53.88) are omitted from the figure for ease of exposition.

Table F.1: Descriptive statistics of the CO₂ intensity panel dataset

	Mean	Std.	Min	Q25	Median	Q75	Max
CO ₂	249.916	849.137	0.026	10.414	42.67	152.551	11953.218
GDP	395.621	1521.375	0.063	11.349	49.997	217.156	27360.935
CO ₂ intensity	1.381	1.696	0.037	0.358	0.784	1.675	13.685
Observational horizon	56.511	12.48	29	55.5	64	64	64

Notes: Summary statistics on the panel dataset employed in the empirical illustration. CO₂ is measured in million tonnes, GDP in billion 2024 U.S. dollars, and the observational horizon in years.

Table F.2: Group structure in the CO₂ emission intensity of GDP

	Angola	China	Kazakhstan	Serbia	Uruguay
Group 1 (18)	Belarus	Czechia	Poland	Slovakia	Uzbekistan
	Bulgaria	Estonia	Romania	Sweden	
	Chile	Italy	Russia	Ukraine	
	Algeria	Greece	Libya	Panama	Switzerland
	Argentina	Hong Kong	Malaysia	Philippines	Tunisia
Group 2 (28)	Bolivia	India	Mexico	Portugal	Turkey
	Dem. Rep. Congo	Indonesia	New Zealand	Saudi Arabia	Vietnam
	Egypt	Israel	Norway	Singapore	
	Finland	Kenya	Pakistan	Spain	
	Australia	Colombia	Hungary	Lithuania	South Africa
	Austria	Croatia	Iran	Myanmar	South Korea
Group 3 (24)	Bahrain	Denmark	Ireland	Netherlands	USA
	Belgium	France	Japan	Peru	United Kingdom
	Canada	Germany	Latvia	Slovenia	
Group 4 (8)	Bangladesh	Cameroon	Ethiopia	Nepal	
	Brazil	Ecuador	Ghana	Tanzania	
	Costa Rica	El Salvador	Morocco	Paraguay	Thailand
Group 5 (14)	Côte d'Ivoire	Guatemala	Nigeria	Sri Lanka	Uganda
	Dominican Republic	Jordan	Oman	Sudan	

Notes: Estimated group structure $\hat{\mathcal{G}}_K$ in the trends of the CO₂ emission intensity. Group cardinalities are in parenthesis.